NASA Technical Memorandum 85790

Installation Noise Measurements of Model SR and CR Propellers

P.J.W.Block

May 1984

NASA
National Aeronautics and
Space Administration

Langley Research Center
Hampton, Virginia 23665

INTRODUCTION

Recent studies have shown that turboprop-powered aircraft may offer significant fuel savings over turbofan-powered aircraft (ref. 1). Thus, new aircraft propulsion systems are being studied which incorporate new and advanced propeller concepts such as highly swept and tapered blades, pusher configurations, and counter-rotating propellers. The noise impact of these propellers and the effect of their installation on the noise radiation pattern is of concern from the standpoint of cabin or interior noise as well as from the community noise impact. To assess the magnitude of the noise impact, propeller noise measurements are needed on these advanced propeller concepts. However, the measurement of propeller noise is complicated by the fact that the installed configuration has a non-uniform directivity pattern (ref. 2). That is, the radiation pattern of a free propeller is modified or distorted when it is installed on the aircraft and the amount of additional noise from the installed propeller is dependent on the location of the observer (or microphone). Thus, a comprehensive experimental study of the noise from an installed propeller requires many microphone measurements. These measurements can then be used to validate available prediction methods and to supplement the data base on advanced propeller installation effects.

This paper summarizes noise measurements on a 0.1 scale SR-2 propeller in a single and counter rotation mode, in a pusher and tractor configuration, and operating at non-zero angles of attack. A measurement scheme which permitted 143 measurements of each of these configurations is also described.

SYMBOLS AND ABBREVIATIONS

a_n, b_n, c_n	Fourier coefficients
B	number of blades per row or per propeller disk
C_p	power coefficient = $P/\rho n^3 d^5$

C_T	thrust coefficient = $T/\rho n^2 d^4$
d	propeller diameter
f	frequency
J	propeller advance ratio, U/nd
M	Mach number
n	number of revolutions per second
P	power absorbed by the propeller
Q	free stream dynamic pressure
T	propeller thrust
T_A	air temperature
U	tunnel velocity
α	angle of attack or pitch angle of the propeller nacelle with respect to the airstream
$\beta_{.75}$	propeller pitch setting at .75 radial station with respect to the plane of rotation
ρ_A	air density

Abbreviations

BPF	blade passage frequency = nB
CR	counter rotation propeller
CRT	CR tractor
ips	inches per second
mic	microphone
OTS	open test section
rpm	revolutions per minute
SPL	sound pressure level
SR	single rotation propeller
SRP	SR pusher
SRT	SR tractor

DESCRIPTION OF THE EXPERIMENT

Propellers.- The SR2 propeller design was employed in this study. The coordinates of this design are documented (ref. 2) and are displayed in 3-D form in figure 1. The blades were fabricated on a numerically controlled milling machine to a tolerance of ± .003 inches (.076 mm) on the airfoil contour and ± .005 inches (.127 mm) on span warpage. When placed in the hub, the radial position tolerance was ± .0025 inches (.064 mm).

The hubs for the single rotation propeller (SR) and counter rotation propellers (CR) permitted 2, 4, or 8 blade operation over a blade pitch range from -2° to 60°. The blades were set into a collective pitch angle gear and clamped in the hub such that when assembled the blades did not wobble. The spinner, hub, and blades were dynamically balanced to 4000 rpm, not to exceed .01 ounce-inches (7.06×10^{-5} n-m) of imbalance*, and tested for failure at 10500 rpm for 30 seconds in a partial vacuum. Both the SR and CR systems were driven by a single 29 hp (10000 rpm) electric motor.

The SR and CR systems differed in the following ways. The SR was 16.9 inches (.429 m) in diameter, and the blade pitch angles were adjustable in one degree increments. To set the angle a pin was placed in a labeled hole in the hub. With this arrangement the collective blade angle was exactly repeatable. The actual blade pitch angle setting at the 75 percent radial station ($\beta_{.75}$) is obtained from the labeled hole or nominal setting by $\beta_{.75}$ (degrees) = .98522 x (nominal setting) + .89°. The SR rotated clockwise looking upstream.

The CR coordinates were obtained by scaling the SR coordinates down by a factor of 0.88757 to a diameter of 15 inches (.381 m). The blades were then

*At 4000 rpm the rotating system appeared to have a resonance. This imbalance was never exceeded throughout the rpm range tested.

shifted out radially .552 inches (.014 m). The resultant diameter of the CR was 16.104 inches (.409 m). The hub for the CR permitted a continuous range of blade angle settings. The collective blade angle for one row of blades was set using a blade mould fixture and protractor which resulted in an accuracy of ± .25 degrees. The reference chord for the CR was at the 79.1 percent radial station. To obtain the pitch angle at the standard 75 percent station the following relationship is used:

$$\beta_{.75} = \beta_{.79} + 1.34°$$

For the tests described herein, each disk of the CR had the same pitch setting. The pitch change axis of the two rows of blades was separated by 2.31 inches (.0587 m). The front row of blades was driven clockwise looking upstream; the back row was driven counterclockwise. A spider gear system consisting of two gears and two pinions drove the back row of blades in the opposite direction and at the same rpm.

Nacelle, Strut, and Sting.- The nacelle was a body of revolution with a maximum outside diameter of 6 inches (.152 m). It housed a 29 hp, 10000 rpm, water-cooled electric motor. All the test hardware configurations are described in figure 2.

There were two front ends for the nacelle - one for the SR and another for the CR, which included a gearbox. There were two mounts for the nacelle - the sting mount, where the nacelle was an aerodynamic extension of the straight sting, and the pylon or strut mount, where the nacelle was attached to a scaled horizontal tail surface which hung down from the sting via an adapter. There were also two configurations for the nacelle in the pylon mount - tractor (propeller precedes nacelle) and pusher (propeller follows nacelle). Photos of the SR in a tractor and pusher configuration on the pylon mount are shown in figure 3.

The strut was a tapered NACA 0012 airfoil. The chord length above the nacelle was 12.5 inches (.318 m) and below it was 10 inches (.254 m).

The location of the propeller disk plane for the sting mounted SR at zero angle of attack defines the reference plane for this test (see fig. 2). This location is the 0-stop for the microphone carriage which will be described next. In other hardware configurations the propeller disk plane was displaced from this reference line as shown in figure 2. These displacements are given for the zero angle-of-attack case in figure 2. At non-zero angles of attack the location of the disk plane was moved slightly forward (upstream) or backward from this position. The actual location of the propeller disk plane for all configurations and angles of attack is given in the test configurations table.

The straight sting was used to change the propeller pitch while keeping the height of the propeller axis 35 inches (.889 m) above the microphone carriage. The adapter, which connected the pylon or horizontal tail surface to the sting permitted the nacelle to be yawed in ± 5° increments, with the position of the centerline of the propeller disk kept constant.

Microphone Carriage.- The microphone carriage was a streamlined rectangular flat plate holding an array of eleven flush mounted microphones (see figure 4). It was designed to circumvent the complexity of reflections from the floor while providing the capability of making numerous streamwise noise measurements of all the propeller configurations.

The carriage was 72 inches (1.83 m) wide (streamwise dimension), 168 inches (4.27 m) long (cross stream dimension), and 2.3 inches (.0584 m) thick. Its construction included an aluminum frame, a rigid foam core, and an aluminum skin all sandwiched and bonded together using an epoxy adhesive with a wooden beam running spanwise down the center of the chord for microphone mounting. The microphones were slip fit into phenolic holders which were secured to the wooden beam. A three-view drawing of the carriage showing the microphone locations is given in figure 5 along with a description of the microphone mount.

The microphones, labeled 1 through 11, were positioned at nominally 12.5° increments in the cross stream direction (azimuthally) from the propeller axis, which was 35 inches (.889 m) above the carriage.

The carriage was moved in the streamwise direction on Thompson bearings and a set of one inch stainless steel rods (see figure 4). The drive system consisted of an electric motor, gearbox, sprocket, and continuous cable, which moved the carriage at a velocity of 4.4 inches/sec (.112 m/sec). The carriage was stopped at 13 to 15 fixed streamwise positions which corresponded to nominal 10° increments from the propeller disk plane, beginning at 60° in front of the disk plane and ending 60° behind for the reference condition. These stops, which were indicated by a microswitch, were labeled 6,5,...1,0,-1,...-5,-6, respectively. Two more stops, labeled 7 and 8, were added, which measured the noise at 72° and 78° in front of the disk plane. When at the stop labeled 0, the microphone array was in the disk plane of the reference configuration, namely the sting mounted SRT at zero angle of attack (see fig. 2). At stop 0 the noise at 0° from the disk plane was recorded, and at stop +4 the noise 40° in front of the disk plane was recorded, etc. For configurations other than this reference condition, the stop label does not correspond to the measurement angle with respect to the disk plane. The actual angles of the microphone with respect to the disk plane for all the carriage stops and test configurations (which will be discussed in a later section) are given in Table 1.

Thus, the noise radiation pattern for each of the propeller configurations was measured at a minimum of 143 locations covering the range from 60° upstream to 60° downstream and about 58° on both sides of the propeller axis. Figure 6 shows the coordinate system defining the microphone locations. This system is fixed, with respect to the tunnel, with its origin on the axis of the disk plane for the sting mounted SR at 0° pitch and 0° yaw (reference configuration). The microphone coordinates are given in Table 2 for all 15 carriage stops.

Since a microphone that is flush mounted in a large rigid surface will record a pressure doubling, a correction to all the data is made to obtain free field levels. This correction (6 dB) has been subtracted from all the acoustic data presented herein. The data have not been normalized to a reference distance from the propeller axis.

Facility.- The tests were conducted in the Langley 4- x 7-Meter Tunnel. This is a closed single-return atmospheric wind tunnel allowing open or closed test section operation. A more detailed description of this facility and an acoustic evaluation of the open test section (OTS) are given in reference 2. Figure 7 is a plan view of the OTS showing two of the extreme microphone carriage stops (+6 and -6), propeller plane location, and locations of the acoustic treatment. Unlike the previous test, described in reference 2, open cell foam bats 6 inches (.152 m) thick were applied to the raised ceiling, sidewalls, and control room wall. A reevaluation of the reflection characteristics of the OTS showed that within the dynamic range of the recording instrumentation the microphone systems were not able to detect reflections from these surfaces.

A typical background noise spectrum is given in figure 8. This was measured with no propeller on the sting-mounted nacelle. The results are from microphone 6 (tunnel centerline) with the microphone carriage at stop +4. The frequency bandwidth for this analysis is 9.765 Hz. To adjust for the difference in analysis bandwidth between these levels and the propeller data, the quantity

$$\Delta dB = 10 \log \frac{BPF}{9.765}$$

is added to the band levels in figure 8 to obtain the level of the corresponding background noise in the figures which give the propeller noise (figs. 9-14). Here BPF is the blade passage frequency of the propeller, which may change for each propeller noise run. The nominal flow velocity for this and all the propeller noise runs was 101 fps (30.5 m/s).

TEST CONDITIONS

Table 3 gives the conditions examined in this test. All data were obtained at a tunnel Q of 12 psf (575 n/m^2), which gave a nominal tunnel speed of 101 fps (30.5 m/s).

The first column gives the tunnel run number. This run number is given on the data plots. The next two columns describe the hardware and correspond to those configurations shown in figure 2. The next five columns describe the test conditions, namely the number of blades, nominal $\beta_{.75}$, propeller rps, and nacelle pitch (angle-of-attack) and yaw angles. The next seven columns give the measured values of parameters which may be appropriate for prediction purposes.

The axial location of the center of the propeller disk is given in terms of the coordinate x_3 shown in figure 6. A positive value (Δx_3) represents a position which is farther upstream than the reference position. The reference position is the sting-mounted SR at 0° pitch and 0° yaw. At this reference point the microphones are directly under the propeller disk at the stop labeled 0. For example, in runs 132 through 135 the pylon was rotated to the pusher position, making the disk of the SRP 40 inches (1.016 m) behind the plane of microphones at stop 0. In the case of counterrotating propellers, the location of the aft disk is given. For example, in runs 82 through 85 the aft disk of the sting mounted CRT was 2.61 inches (.0663 m) in front of the microphones at stop 0 because of the extra room required for the gearbox. This information is also found in figure 2.

The SR and CR propellers were each tested with 4 blades per disk or per row. The noise from SRT was measured on a sting mount (runs 52-55) as well as a pylon or strut mount (runs 136-139) to examine the change due to this installation. An 8-bladed SR was also tested (Runs 140-142) to provide a comparison with the 4 + 4 CR (runs 82-87) where the total number of blades is the same.

Two blade pitch angles, $\beta_{.75}$, were tested (nominally 12° and 20°). These were chosen to provide efficient propeller operation at the relatively low tunnel speed (100 fps) and high rotational tip speed (800 fps) being considered for full scale operation. The actual $\beta_{.75}$ is also given in the table. At each angle, $\beta_{.75}$, two rotational speeds (rps) were examined - one at the predicted peak efficiency and one slightly higher - to increase the loading of the propeller without stalling it. The abbreviation "perf" in the rps column (runs 136, 139, 140, 143, 146, and 149) indicates that an aerodynamic performance run was made over a range of rotational speeds.

To examine the effect of simply changing the pitch of the propeller shaft or axis, the noise of the sting mounted SRT and CRT was mapped at -8°, 0°, and + 8° (runs 52-55, 63-70, and 82-87). For these runs the height of the propeller was held at 35 inches (.889 m) above the microphone carriage; however, the axial location did shift slightly. The propeller disk was also yawed 10° (runs 146-151), with the axis of the disk kept at the same location as the no-yaw (yaw = 0°) propeller cases.

A representative sample of the data will be given in this report since the total number of measurements and conditions would comprise over 4500 figures. The conditions for which data are presented in this report are given in the last column of Table 3. The microphone stop for which the data will be given corresponds to an angle between 35° and 40° in front of the propeller disk plane.

MEASUREMENTS AND DATA REDUCTION

Propeller Force Data

To provide a correlation for various noise prediction schemes the propeller thrust and torque were measured. The torque data remained in question at the time this report was prepared and thus are not included. The propeller thrust for each configuration is given in Table 3.

Noise Data

The microphone data were high-pass filtered at 80 Hz and FM recorded on one-inch magnetic tape at 60 ips. A once-per-revolution pulse which was generated by a magnetic pick-up on the shaft was also recorded. A triple redundancy system was employed for recording the attenuator settings. The recorded data were digitized using the once-per-revolution pulse to obtain 512 points of data for each revolution of the shaft. A minimum of 120 revolutions of data were stored for each microphone (61440 points).

The data were analyzed in the time domain and the frequency domain and are presented in the time domain as pressure time histories and in the frequency domain as sound pressure levels for each of the first 25 harmonics of the blade passage frequency. In the time domain an average time history or mean signal was computed by averaging the sampled pressure signal over the 120 revolutions of the shaft. This resulted in a mean value of the signal and standard deviation (σ) for each of the 512 points. These results are presented as a function of the shaft rotation angle and labeled "mean signal + and - σ" on the data plots. These results show how much data scatter exists at a particular microphone location and for a given propeller configuration. The mean signal is Fourier analyzed and presented in the frequency domain as a function of the harmonics of the blade passage frequency (BPF).

In the frequency domain two methods of analysis were used. In the first method each revolution of data was Fourier analyzed to produce the sine and cosine coefficients for the first 25 harmonics of the BPF (a_n and b_n; n = 1-25, respectively). These coefficients are averaged over the 120 revolutions of data yielding $\bar{a}_n$ and $\bar{b}_n$. The root mean square (rms) amplitude of the noise contribution for each of the harmonics is computed from these using

$$c_n = \sqrt{\bar{a}_n^2 + \bar{b}_n^2} / \sqrt{2}$$

and converted to decibels using

$$SPL_n = 20 \log_{10} (c_n/.00002) \qquad (1)$$

Equation (1) gives the sound pressure level (SPL) in dB for each of the 25 harmonics. The result is labeled "Method 1" on the data plots. In principle, Method 1 should give the same results as the spectrum of the mean signal. Differences which arise are due to artifacts introduced by the computation and do not usually occur until the harmonic level is more than 30 dB down from the peak.

In the second method of analysis in the frequency domain, the sine and cosine coefficients are obtained for each revolution (as in method 1), and then the mean square is computed for each revolution using $c_n'^2 = (a_n^2 + b_n^2) / 2$. The values $c_n'^2$ are averaged over the 120 revolutions yielding $\bar{c}_n$ where

$$\bar{c}_n = \left\{ \frac{1}{120} \sum_{i=1}^{120} c'^2_{ni} \right\}^{1/2}$$

Equation (1) is used to compute the SPL's of each of the n harmonics. This method is labeled "Method 2" and is analagous to narrowband power spectral analysis with bandwidth equal to the BPF. For comparison purposes the BPF is given on the data plots (figs. 9-14) in the figure label with the rpm and rotational tip speed of the propeller (U_{Tip}). Typically, the results from Method 1 and Method 2 agree for the first few harmonics, which are above the background noise of the tunnel (SR). As the harmonic number increases, Method 2 gives the levels of the background noise (compare with figure 8), whereas Method 1 gives levels below the background noise which appear to follow the trends expected for propeller noise. Because some propeller configurations do not generate levels above the background noise in the higher harmonics, Method 1 is a valuable method of picking out the levels of a few more harmonics.

Finally, the results from method 1, namely $\bar{a}_n$ and $\bar{b}_n$ are used to reproduce the pressure time history for one revolution of the shaft. This time history, which is truly periodic, is plotted with the mean signal. Comparison of these time history results reveals differences in the noise generated by differences in the blades themselves or in their pitch setting. The above calculations are presented for each of the eleven microphones at a carriage stop corresponding to angles between 36.4 and 40.8 degrees upstream of the propeller disk plane (refer to Table 1). The data for the eleven microphones are followed by a summary of that stop. This summary consists of the OASPL, calculated all three ways, plotted against the microphone location.

DATA RESULTS

The data which are presented were obtained at angles corresponding to between 36.4° and 40.8° forward (upstream) of the propeller disk plane (refer to Table 1). These angles were chosen because they tend to show the effect of the unsteady loading of the propeller. The data have not been corrected for differences in distances in order to release the data in a timely manner.

The data obtained from the sting-mounted SR at $\beta_{.75} = 12°$ with 4 blades is shown in figure 9. Figures 9(a) through 9(k) give the results for each of the individual microphones (1 through 11) respectively. Figure 9(l) is a summary of the OASPL's for the particular carriage stop - in this case stop 4. Figure 10 shows the results from the same condition, except the angle of attack is +8°. The format of presentation is the same. Figure 11 shows the CR results. Figures 12, 13, and 14 show the SR pusher, SR tractor with 8 blades, and SR tractor with 4 blades, espectively.

Finally, since the number of points per revolution was held constant while the BPF increased by a factor of 2 on the data for run 141 (SR tractor with 8-blades), harmonics above 20 are affected by aliasing.

REFERENCES

1. Mitchell, G. A.; Mikkelson, D. C.: Summary and Recent Results from the NASA Advanced High-Speed Propeller Research Program. NASA TM 82891, 1983.

2. Block, P. J. W. and Gentry, G. L.: Evaluation of the 4- x 7-Meter Tunnel for Propeller Noise Measurements. NASA TM 85721, 1984.

Table 1.- Angles of the microphone array with respect to the propeller disk plane for all configurations, in degrees.

Runs	Configuration	Δx_3	Microphone carriage stop label														
		in.	8	7	6	5	4	3	2	1	0	-1	-2	-3	-4	-5	-6
52-54	SRT/sting	0	77.8	72.6	60.7	50.8	40.8	30.7	20.5	10.2	0	-10.2	-20.5	-30.7	-40.8	-50.8	-60.7
63,64,67,68	SRT " +8°	3.75	77.5	72.1	59.1	48.2	37.1	26.0	15.0	4.2	- 6.1	-16.0	-25.7	-35.0	-44.1	-53.1	-62.1
65,66,69,70	SRT " -8°	-.75	77.9	72.7	61.0	51.3	41.5	31.6	21.6	11.4	1.2	- 9.0	-19.4	-29.8	-40.1	-50.3	-60.4
82-85	CRT 0°	2.61	77.6	72.3	59.6	49.0	38.3	27.5	16.7	6.0	- 4.3	-14.3	-24.2	-33.8	-43.2	-52.4	-61.7
86	" +8°	6.36	77.3	71.7	58.0	46.2	34.3	22.4	10.9	.1	-10.3	-19.9	-29.1	-37.8	-46.6	-54.6	-63.0
87	" -8°	1.86	77.7	72.4	59.9	49.5	39.0	28.4	17.8	7.2	- 3.0	-13.1	-23.1	32.9	-42.5	-52.0	-61.4
132-135	SRP (pylon)	-40.	80.2	77.0	71.1	67.1	63.5	60.1	56.6	52.9	48.8	43.9	37.5	28.8	15.6	-4.74	-32.5
136-151	SRT (pylon)	- 5.	78.2	73.4	62.5	53.8	45.2	36.4	27.4	17.9	8.1	- 2.1	-13.0	-24.3	-35.7	-47.3	-58.6

Table 2.- List of microphone locations and distances for all microphone carriage stops in inches (m).

Stop	Mic	Coordinates of the Microphone Positions x_1	x_2	x_3	Distance R
8	1	-35.0(-0.89)	57.2(1.45)	162.0(4.11)	175.3(4.45)
8	2	-35.0(-0.89)	40.3(1.02)	162.0(4.11)	170.6(4.33)
8	3	-35.0(-0.89)	27.7(0.70)	162.0(4.11)	168.0(4.27)
8	4	-35.0(-0.89)	17.5(0.44)	162.0(4.11)	166.7(4.23)
8	5	-35.0(-0.89)	8.5(0.21)	162.0(4.11)	166.0(4.22)
8	6	-35.0(-0.89)	0.0(0.00)	162.0(4.11)	165.7(4.21)
8	7	-35.0(-0.89)	-8.5(-0.21)	162.0(4.11)	166.0(4.22)
8	8	-35.0(-0.89)	-17.5(-0.44)	162.0(4.11)	166.7(4.23)
8	9	-35.0(-0.89)	-27.7(-0.70)	162.0(4.11)	168.0(4.27)
8	10	-35.0(-0.89)	-40.3(-1.02)	162.0(4.11)	170.6(4.33)
8	11	-35.0(-0.89)	-57.2(-1.45)	162.0(4.11)	175.3(4.45)
7	1	-35.0(-0.89)	57.2(1.45)	112.0(2.84)	130.5(3.32)
7	2	-35.0(-0.89)	40.3(1.02)	112.0(2.84)	124.1(3.15)
7	3	-35.0(-0.89)	27.7(0.70)	112.0(2.84)	120.6(3.06)
7	4	-35.0(-0.89)	17.5(0.44)	112.0(2.84)	118.6(3.01)
7	5	-35.0(-0.89)	8.5(0.21)	112.0(2.84)	117.6(2.99)
7	6	-35.0(-0.89)	0.0(0.00)	112.0(2.84)	117.3(2.98)
7	7	-35.0(-0.89)	-8.5(-0.21)	112.0(2.84)	117.6(2.99)
7	8	-35.0(-0.89)	-17.5(-0.44)	112.0(2.84)	118.6(3.01)
7	9	-35.0(-0.89)	-27.7(-0.70)	112.0(2.84)	120.6(3.06)
7	10	-35.0(-0.89)	-40.3(-1.02)	112.0(2.84)	124.1(3.15)
7	11	-35.0(-0.89)	-57.2(-1.45)	112.0(2.84)	130.5(3.32)
6	1	-35.0(-0.89)	57.2(1.45)	62.3(1.58)	91.5(2.33)
6	2	-35.0(-0.89)	40.3(1.02)	62.3(1.58)	82.0(2.08)
6	3	-35.0(-0.89)	27.7(0.70)	62.3(1.58)	76.7(1.95)
6	4	-35.0(-0.89)	17.5(0.44)	62.3(1.58)	73.6(1.87)
6	5	-35.0(-0.89)	8.5(0.21)	62.3(1.58)	72.0(1.83)
6	6	-35.0(-0.89)	0.0(0.00)	62.3(1.58)	71.5(1.82)
6	7	-35.0(-0.89)	-8.5(-0.21)	62.3(1.58)	72.0(1.83)
6	8	-35.0(-0.89)	-17.5(-0.44)	62.3(1.58)	73.6(1.87)
6	9	-35.0(-0.89)	-27.7(-0.70)	62.3(1.58)	76.7(1.95)
6	10	-35.0(-0.89)	-40.3(-1.02)	62.3(1.58)	82.0(2.08)
6	11	-35.0(-0.89)	-57.2(-1.45)	62.3(1.58)	91.5(2.33)
5	1	-35.0(-0.89)	57.2(1.45)	42.9(1.09)	79.6(2.02)
5	2	-35.0(-0.89)	40.3(1.02)	42.9(1.09)	68.5(1.74)
5	3	-35.0(-0.89)	27.7(0.70)	42.9(1.09)	61.9(1.57)
5	4	-35.0(-0.89)	17.5(0.44)	42.9(1.09)	58.0(1.47)
5	5	-35.0(-0.89)	8.5(0.21)	42.9(1.09)	56.0(1.42)
5	6	-35.0(-0.89)	0.0(0.00)	42.9(1.09)	55.4(1.41)
5	7	-35.0(-0.89)	-8.5(-0.21)	42.9(1.09)	56.0(1.42)
5	8	-35.0(-0.89)	-17.5(-0.44)	42.9(1.09)	58.0(1.47)
5	9	-35.0(-0.89)	-27.7(-0.70)	42.9(1.09)	61.9(1.57)
5	10	-35.0(-0.89)	-40.3(-1.02)	42.9(1.09)	68.5(1.74)
5	11	-35.0(-0.89)	-57.2(-1.45)	42.9(1.09)	79.6(2.02)
4	1	-35.0(-0.89)	57.2(1.45)	30.2(0.77)	73.5(1.87)
4	2	-35.0(-0.89)	40.3(1.02)	30.2(0.77)	61.3(1.56)
4	3	-35.0(-0.89)	27.7(0.70)	30.2(0.77)	53.9(1.37)
4	4	-35.0(-0.89)	17.5(0.44)	30.2(0.77)	49.4(1.26)

Table 2.- Continued.

Stop	Mic	Coordinates of the Microphone Positions x_1	x_2	x_3	Distance R
4	5	-35.0(-0.89)	8.5(0.21)	30.2(0.77)	47.0(1.19)
4	6	-35.0(-0.89)	0.0(0.00)	30.2(0.77)	46.2(1.17)
4	7	-35.0(-0.89)	-8.5(-0.21)	30.2(0.77)	47.0(1.19)
4	8	-35.0(-0.89)	-17.5(-0.44)	30.2(0.77)	49.4(1.26)
4	9	-35.0(-0.89)	-27.7(-0.70)	30.2(0.77)	53.9(1.37)
4	10	-35.0(-0.89)	-40.3(-1.02)	30.2(0.77)	61.3(1.56)
4	11	-35.0(-0.89)	-57.2(-1.45)	30.2(0.77)	73.5(1.87)
3	1	-35.0(-0.89)	57.2(1.45)	20.8(0.53)	70.2(1.78)
3	2	-35.0(-0.89)	40.3(1.02)	20.8(0.53)	57.3(1.45)
3	3	-35.0(-0.89)	27.7(0.70)	20.8(0.53)	49.2(1.25)
3	4	-35.0(-0.89)	17.5(0.44)	20.8(0.53)	44.3(1.13)
3	5	-35.0(-0.89)	8.5(0.21)	20.8(0.53)	41.6(1.06)
3	6	-35.0(-0.89)	0.0(0.00)	20.8(0.53)	40.7(1.03)
3	7	-35.0(-0.89)	-8.5(-0.21)	20.8(0.53)	41.6(1.06)
3	8	-35.0(-0.89)	-17.5(-0.44)	20.8(0.53)	44.3(1.13)
3	9	-35.0(-0.89)	-27.7(-0.70)	20.8(0.53)	49.2(1.25)
3	10	-35.0(-0.89)	-40.3(-1.02)	20.8(0.53)	57.3(1.45)
3	11	-35.0(-0.89)	-57.2(-1.45)	20.8(0.53)	70.2(1.78)
2	1	-35.0(-0.89)	57.2(1.45)	13.1(0.33)	68.3(1.74)
2	2	-35.0(-0.89)	40.3(1.02)	13.1(0.33)	54.9(1.40)
2	3	-35.0(-0.89)	27.7(0.70)	13.1(0.33)	46.5(1.18)
2	4	-35.0(-0.89)	17.5(0.44)	13.1(0.33)	41.3(1.05)
2	5	-35.0(-0.89)	8.5(0.21)	13.1(0.33)	38.3(0.97)
2	6	-35.0(-0.89)	0.0(0.00)	13.1(0.33)	37.4(0.95)
2	7	-35.0(-0.89)	-8.5(-0.21)	13.1(0.33)	38.3(0.97)
2	8	-35.0(-0.89)	-17.5(-0.44)	13.1(0.33)	41.3(1.05)
2	9	-35.0(-0.89)	-27.7(-0.70)	13.1(0.33)	46.5(1.18)
2	10	-35.0(-0.89)	-40.3(-1.02)	13.1(0.33)	54.9(1.40)
2	11	-35.0(-0.89)	-57.2(-1.45)	13.1(0.33)	68.3(1.74)
1	1	-35.0(-0.89)	57.2(1.45)	6.3(0.16)	67.3(1.71)
1	2	-35.0(-0.89)	40.3(1.02)	6.3(0.16)	53.7(1.36)
1	3	-35.0(-0.89)	27.7(0.70)	6.3(0.16)	45.1(1.15)
1	4	-35.0(-0.89)	17.5(0.44)	6.3(0.16)	39.6(1.01)
1	5	-35.0(-0.89)	8.5(0.21)	6.3(0.16)	36.6(0.93)
1	6	-35.0(-0.89)	0.0(0.00)	6.3(0.16)	35.6(0.90)
1	7	-35.0(-0.89)	-8.5(-0.21)	6.3(0.16)	36.6(0.93)
1	8	-35.0(-0.89)	-17.5(-0.44)	6.3(0.16)	39.6(1.01)
1	9	-35.0(-0.89)	-27.7(-0.70)	6.3(0.16)	45.1(1.15)
1	10	-35.0(-0.89)	-40.3(-1.02)	6.3(0.16)	53.7(1.36)
1	11	-35.0(-0.89)	-57.2(-1.45)	6.3(0.16)	67.3(1.71)
0	1	-35.0(-0.89)	57.2(1.45)	0.0(0.00)	67.0(1.70)
0	2	-35.0(-0.89)	40.3(1.02)	0.0(0.00)	53.4(1.36)
0	3	-35.0(-0.89)	27.7(0.70)	0.0(0.00)	44.6(1.13)
0	4	-35.0(-0.89)	17.5(0.44)	0.0(0.00)	39.1(0.99)
0	5	-35.0(-0.89)	8.5(0.21)	0.0(0.00)	36.0(0.91)
0	6	-35.0(-0.89)	0.0(0.00)	0.0(0.00)	35.0(0.89)
0	7	-35.0(-0.89)	-8.5(-0.21)	0.0(0.00)	36.0(0.91)
0	8	-35.0(-0.89)	-17.5(-0.44)	0.0(0.00)	39.1(0.99)

Table 2.- Continued.

Stop	Mic	Coordinates of the Microphone Positions x_1	x_2	x_3	Distance R
0	9	-35.0(-0.89)	-27.7(-0.70)	0.0(0.00)	44.6(1.13)
0	10	-35.0(-0.89)	-40.3(-1.02)	0.0(0.00)	53.4(1.36)
0	11	-35.0(-0.89)	-57.2(-1.45)	0.0(0.00)	67.0(1.70)
-1	1	-35.0(-0.89)	57.2(1.45)	-6.3(-0.16)	67.3(1.71)
-1	2	-35.0(-0.89)	40.3(1.02)	-6.3(-0.16)	53.7(1.36)
-1	3	-35.0(-0.89)	27.7(0.70)	-6.3(-0.16)	45.1(1.15)
-1	4	-35.0(-0.89)	17.5(0.44)	-6.3(-0.16)	39.6(1.01)
-1	5	-35.0(-0.89)	8.5(0.21)	-6.3(-0.16)	36.6(0.93)
-1	6	-35.0(-0.89)	0.0(0.00)	-6.3(-0.16)	35.6(0.90)
-1	7	-35.0(-0.89)	-8.5(-0.21)	-6.3(-0.16)	36.6(0.93)
-1	8	-35.0(-0.89)	-17.5(-0.44)	-6.3(-0.16)	39.6(1.01)
-1	9	-35.0(-0.89)	-27.7(-0.70)	-6.3(-0.16)	45.1(1.15)
-1	10	-35.0(-0.89)	-40.3(-1.02)	-6.3(-0.16)	53.7(1.36)
-1	11	-35.0(-0.89)	-57.2(-1.45)	-6.3(-0.16)	67.3(1.71)
-2	1	-35.0(-0.89)	57.2(1.45)	-13.1(-0.33)	68.3(1.74)
-2	2	-35.0(-0.89)	40.3(1.02)	-13.1(-0.33)	54.9(1.40)
-2	3	-35.0(-0.89)	27.7(0.70)	-13.1(-0.33)	46.5(1.18)
-2	4	-35.0(-0.89)	17.5(0.44)	-13.1(-0.33)	41.3(1.05)
-2	5	-35.0(-0.89)	8.5(0.21)	-13.1(-0.33)	38.3(0.97)
-2	6	-35.0(-0.89)	0.0(0.00)	-13.1(-0.33)	37.4(0.95)
-2	7	-35.0(-0.89)	-8.5(-0.21)	-13.1(-0.33)	38.3(0.97)
-2	8	-35.0(-0.89)	-17.5(-0.44)	-13.1(-0.33)	41.3(1.05)
-2	9	-35.0(-0.89)	-27.7(-0.70)	-13.1(-0.33)	46.5(1.18)
-2	10	-35.0(-0.89)	-40.3(-1.02)	-13.1(-0.33)	54.9(1.40)
-2	11	-35.0(-0.89)	-57.2(-1.45)	-13.1(-0.33)	68.3(1.74)
-3	1	-35.0(-0.89)	57.2(1.45)	-20.8(-0.53)	70.2(1.78)
-3	2	-35.0(-0.89)	40.3(1.02)	-20.8(-0.53)	57.3(1.45)
-3	3	-35.0(-0.89)	27.7(0.70)	-20.8(-0.53)	49.2(1.25)
-3	4	-35.0(-0.89)	17.5(0.44)	-20.8(-0.53)	44.3(1.13)
-3	5	-35.0(-0.89)	8.5(0.21)	-20.8(-0.53)	41.6(1.06)
-3	6	-35.0(-0.89)	0.0(0.00)	-20.8(-0.53)	40.7(1.03)
-3	7	-35.0(-0.89)	-8.5(-0.21)	-20.8(-0.53)	41.6(1.06)
-3	8	-35.0(-0.89)	-17.5(-0.44)	-20.8(-0.53)	44.3(1.13)
-3	9	-35.0(-0.89)	-27.7(-0.70)	-20.8(-0.53)	49.2(1.25)
-3	10	-35.0(-0.89)	-40.3(-1.02)	-20.8(-0.53)	57.3(1.45)
-3	11	-35.0(-0.89)	-57.2(-1.45)	-20.8(-0.53)	70.2(1.78)
-4	1	-35.0(-0.89)	57.2(1.45)	-30.2(-0.77)	73.5(1.87)
-4	2	-35.0(-0.89)	40.3(1.02)	-30.2(-0.77)	61.3(1.56)
-4	3	-35.0(-0.89)	27.7(0.70)	-30.2(-0.77)	53.9(1.37)
-4	4	-35.0(-0.89)	17.5(0.44)	-30.2(-0.77)	49.4(1.26)
-4	5	-35.0(-0.89)	8.5(0.21)	-30.2(-0.77)	47.0(1.19)
-4	6	-35.0(-0.89)	0.0(0.00)	-30.2(-0.77)	46.2(1.17)
-4	7	-35.0(-0.89)	-8.5(-0.21)	-30.2(-0.77)	47.0(1.19)
-4	8	-35.0(-0.89)	-17.5(-0.44)	-30.2(-0.77)	49.4(1.26)
-4	9	-35.0(-0.89)	-27.7(-0.70)	-30.2(-0.77)	53.9(1.37)
-4	10	-35.0(-0.89)	-40.3(-1.02)	-30.2(-0.77)	61.3(1.56)
-4	11	-35.0(-0.89)	-57.2(-1.45)	-30.2(-0.77)	73.5(1.87)
-5	1	-35.0(-0.89)	57.2(1.45)	-42.9(-1.09)	79.6(2.02)

Table 2.- Concluded.

Stop	Mic	Coordinates of the Microphone Positions x_1	x_2	x_3	Distance R
-5	2	-35.0(-0.89)	40.3(1.02)	-42.9(-1.09)	68.5(1.74)
-5	3	-35.0(-0.89)	27.7(0.70)	-42.9(-1.09)	61.9(1.57)
-5	4	-35.0(-0.89)	17.5(0.44)	-42.9(-1.09)	58.0(1.47)
-5	5	-35.0(-0.89)	8.5(0.21)	-42.9(-1.09)	56.0(1.42)
-5	6	-35.0(-0.89)	0.0(0.00)	-42.9(-1.09)	55.4(1.41)
-5	7	-35.0(-0.89)	-8.5(-0.21)	-42.9(-1.09)	56.0(1.42)
-5	8	-35.0(-0.89)	-17.5(-0.44)	-42.9(-1.09)	58.0(1.47)
-5	9	-35.0(-0.89)	-27.7(-0.70)	-42.9(-1.09)	61.9(1.57)
-5	10	-35.0(-0.89)	-40.3(-1.02)	-42.9(-1.09)	68.5(1.74)
-5	11	-35.0(-0.89)	-57.2(-1.45)	-42.9(-1.09)	79.6(2.02)
-6	1	-35.0(-0.89)	57.2(1.45)	-62.3(-1.58)	91.5(2.33)
-6	2	-35.0(-0.89)	40.3(1.02)	-62.3(-1.58)	82.0(2.08)
-6	3	-35.0(-0.89)	27.7(0.70)	-62.3(-1.58)	76.7(1.95)
-6	4	-35.0(-0.89)	17.5(0.44)	-62.3(-1.58)	73.6(1.87)
-6	5	-35.0(-0.89)	8.5(0.21)	-62.3(-1.58)	72.0(1.83)
-6	6	-35.0(-0.89)	0.0(0.00)	-62.3(-1.58)	71.5(1.82)
-6	7	-35.0(-0.89)	-8.5(-0.21)	-62.3(-1.58)	72.0(1.83)
-6	8	-35.0(-0.89)	-17.5(-0.44)	-62.3(-1.58)	73.6(1.87)
-6	9	-35.0(-0.89)	-27.7(-0.70)	-62.3(-1.58)	76.7(1.95)
-6	10	-35.0(-0.89)	-40.3(-1.02)	-62.3(-1.58)	82.0(2.08)
-6	11	-35.0(-0.89)	-57.2(-1.45)	-62.3(-1.58)	91.5(2.33)

Table 3.- Test conditions.

HARDWARE				CONDITIONS			
Run #	Mount/ Configuration	Type Propeller	Number of Blades	Nominal $\beta_{.75}$, deg.	Nominal rps	Pitch, deg.	Yaw, deg.
52	Sting/tractor	SR	4	20	100	0	0
53	" "	"	"	20	120	"	"
54	" "	"	"	12	168	"	"
55	" "	"	"	12	190	"	"
63	Sting/tractor	SR	4	20	100	8	0
64	" "	"	"	"	120	8	"
65	" "	"	"	"	100	-8	"
66	" "	"	"	"	120	-8	"
67	" "	"	"	12	168	8	"
68	" "	"	"	"	190	8	"
69	" "	"	"	"	190	-8	"
70	" "	"	"	"	168	-8	"
82	Sting/tractor	CR	4+4	20	100	0	0
83	" "	"	"	"	120	"	"
84	" "	"	"	12	168	"	"
85	" "	"	"	"	190	"	"
86	" "	"	"	"	168	+8	"
87	" "	"	"	"	168	-8	"
132	Pylon/pusher	SR	4	12	168	0	0
133	" "	"	"	"	190	"	"
134	" "	"	"	20	100	"	"
135	" "	"	"	"	120	"	"
136	Pylon/tractor	SR	4	16	perf	0	0
137	" "	"	"	"	168	"	"
138	" "	"	"	"	190	"	"
139	" "	"	"	20	perf	"	"
140	" "	SR	8	12	perf	"	"
141	" "	"	"	"	168	"	"
142	" "	"	"	"	190	"	"
143	" "	SR	4	"	perf	"	"
144	" "	"	"	"	168	"	"
145	" "	"	"	"	190	"	"
146	" "	"	"	"	perf	"	10
147	" "	"	"	"	168	"	"
148	" "	"	"	"	190	"	"
149	" "	"	"	20	perf	"	"
150	" "	"	"	"	100	"	"
151	" "	"	"	"	120	"	"

Table 3 (cont'd)

Measured Values						
Actual $\beta_{.75}$, deg.	Position of disk plane with respect to reference,* inches (Δx_3)	T_A, °F	ρ_A, slugs/ft^3	U, fps	T, lbf	Figure No.
20.6	0.	43.0	.00243	99.6	17.7	
20.6	"	43.0	"	99.6	26.4	
12.7	"	43.7	"	99.7	X **	9
12.7	"	43.9	"	99.8	X **	
20.6	3.75	62.5	.00235	101.0	6.0	
"	3.75		"		15.5	
"	- 0.75	62.6	"	101.4	6.3	
"	- 0.75	62.7	"	101.4	16.1	
12.7	3.75	60.0	.00236	100.5	16.8	10
"	3.75	59.0	.00237	100.5	27.5	
"	- 0.75	57.0			28.6	
"	- 0.75	56.7	.00238	100.4	17.8	
21.3	2.61	67.5	.00228	102.4	9.8	
21.3	"	65.6	.00229		21.9	
13.3	"	52.6	.00239	100.5	25.5	11
"	"	55.0	.00238	100.8	39.3	
"	6.36	55.1	.00238	101.2	25.2	
"	1.86	55.1			26.5	
12.7	-40.	56.8	.00237	100.4	15.0	12
12.7	"	59.0	.00237	100.5	26.2	
20.6	"	65.0	.00233	101.7	14.1	
20.6	"	67.1	.00232	102.2	25.8	
17.5	- 5.	69.1	.00231	101.0	—	
"	"	69.0	.00232	102.2	34.1	
"	"	66.5	.00232	102.7	50.6	
20.6	"	62.7	.00234	101.5	—	
12.7	"	59.6	.00236	102.0	—	
"	"	58.7	.00236	101.2	20.6	13
"	"	58.2	.00237	101.1	34.8	
"	"	57.4	"	101.1	—	
"	"	58.0	"	101.5	15.4	14
"	"	58.0	"	101.5	26.3	
"	"	56.7	"	101.1	—	
"	"	56.7	"	101.4	12.9	
"	"	56.4	"	101.4	23.0	
20.6	"	55.3	.00238	101.5	—	
"	"	55.3	"	101.3	4.4	
"	"	54.8	"	101.2	13.2	

*Reference position is the sting mounted SR at 0° angle of attack.
**Balance data in question.

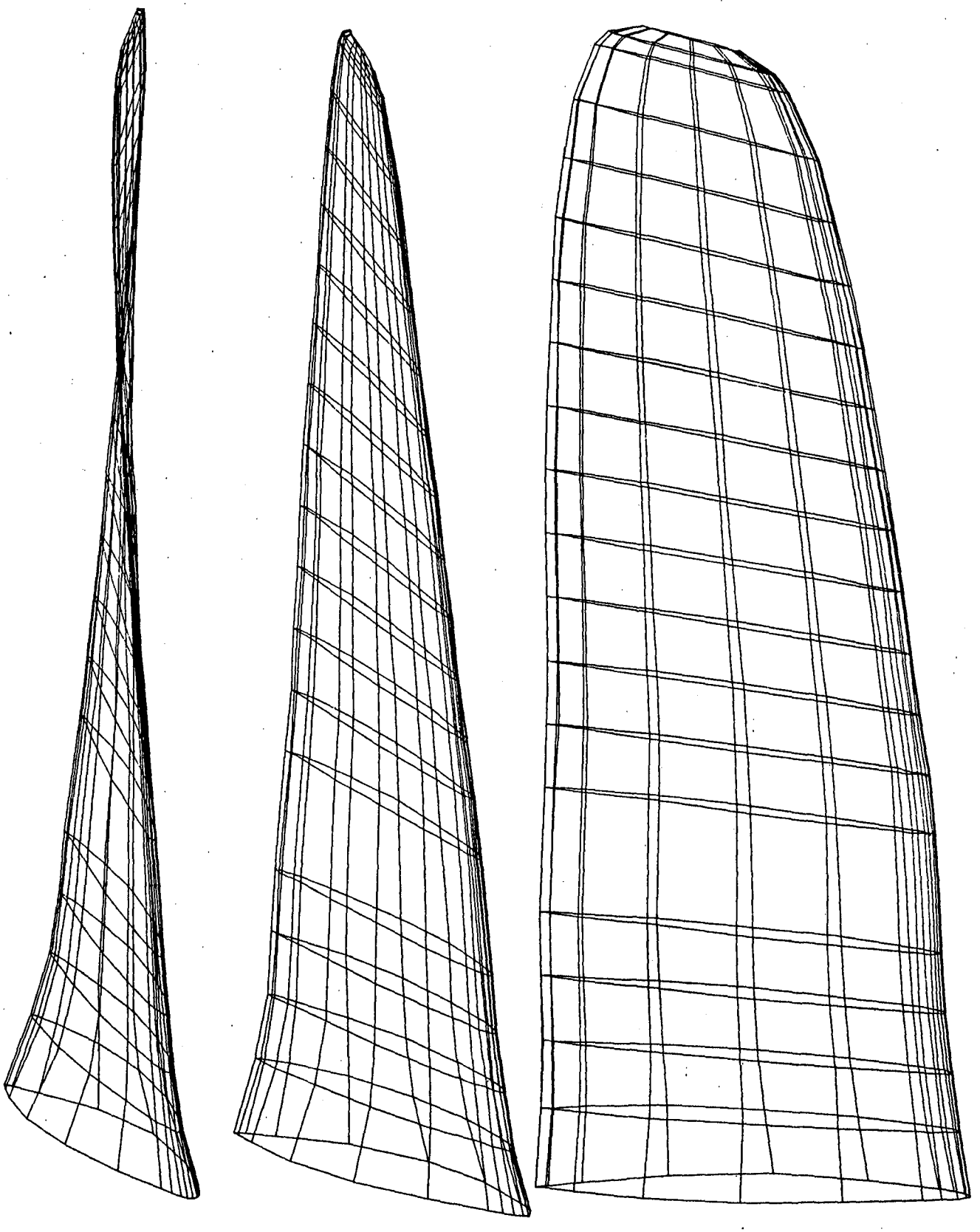

Figure 1.- Three dimensional display of SR2 propeller design which was used in this study.

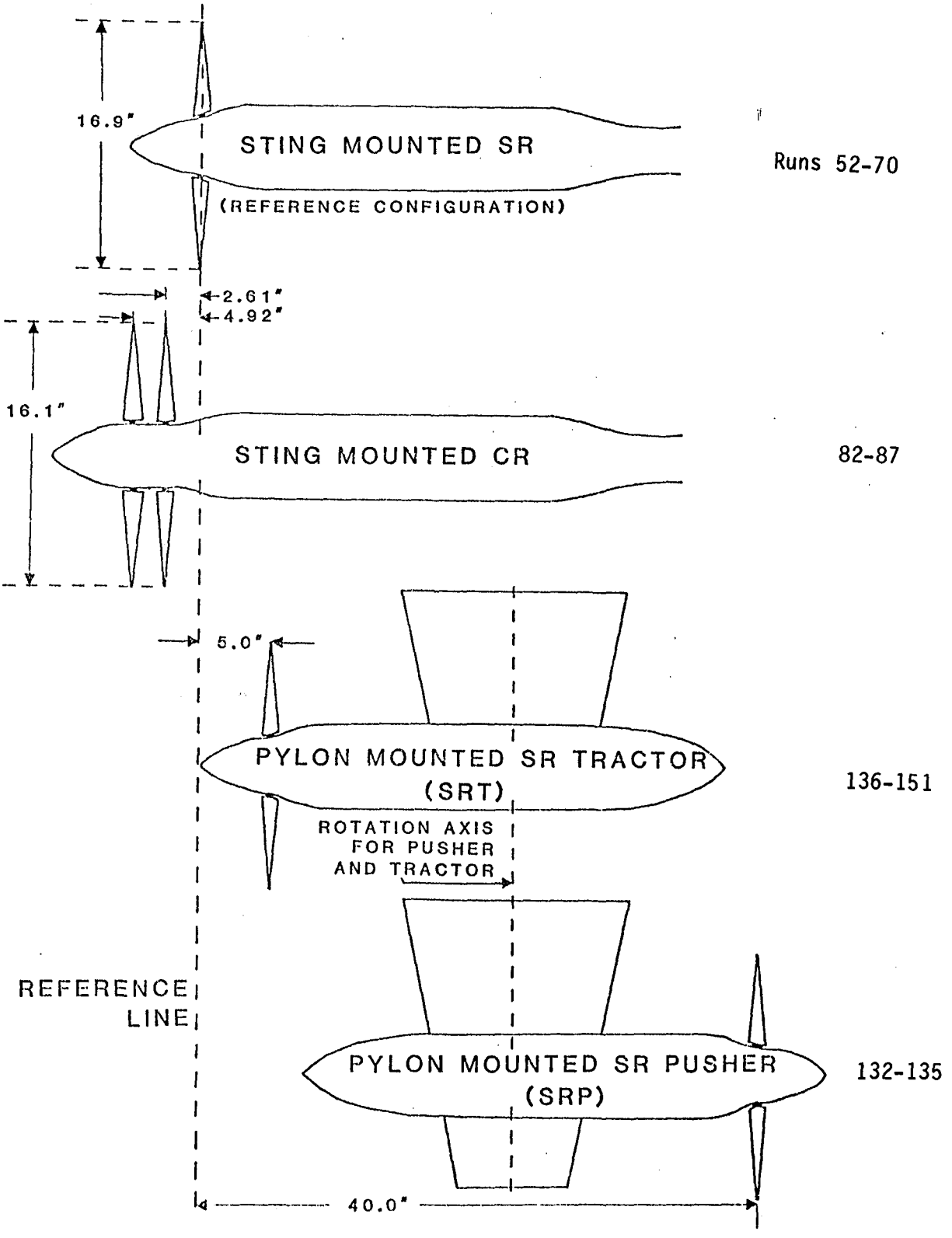

Figure 2.- Drawing of the propeller/nacelle configurations.

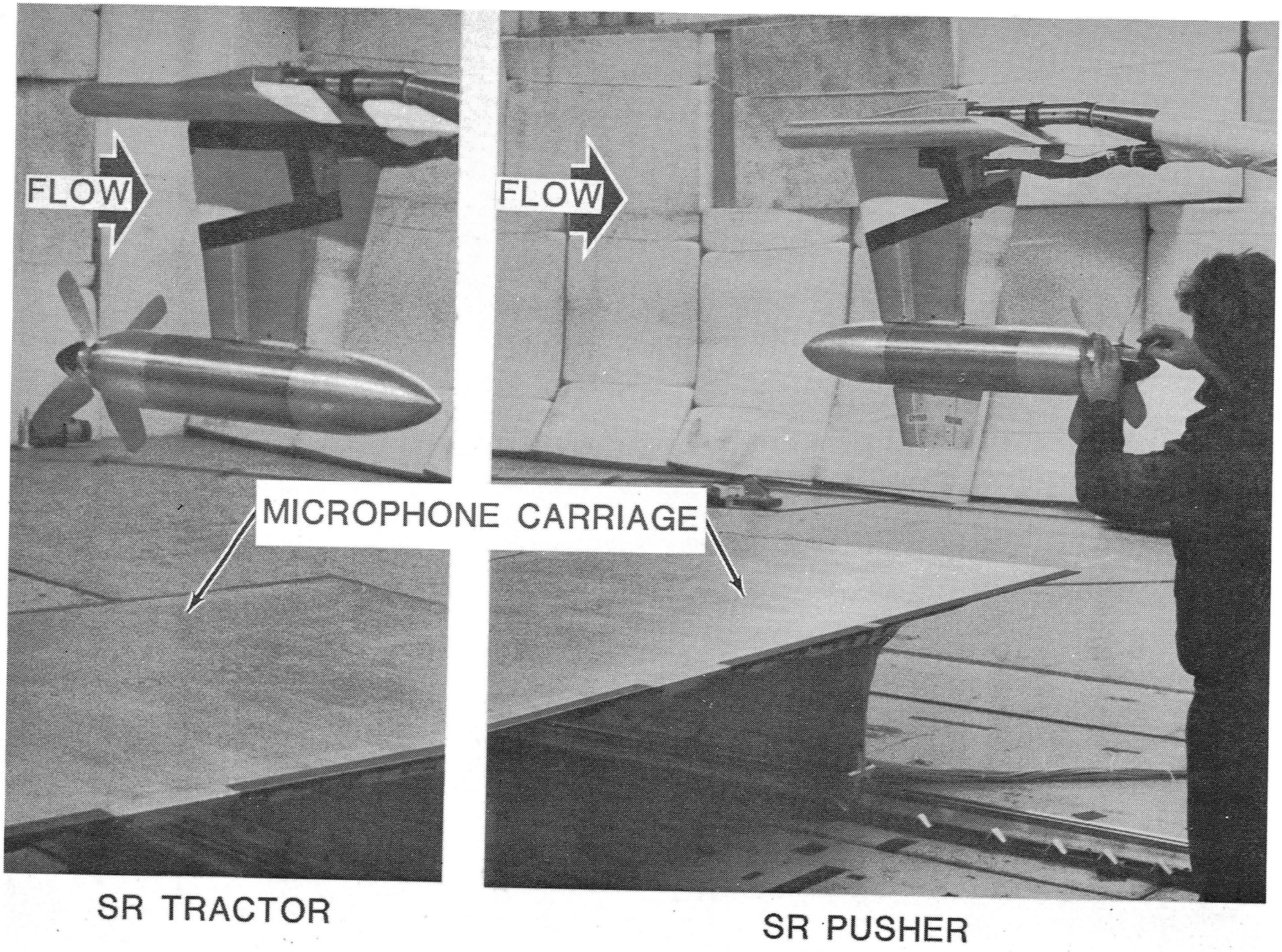

Figure 3.- Photo showing pylon mounted tractor and pusher configurations.

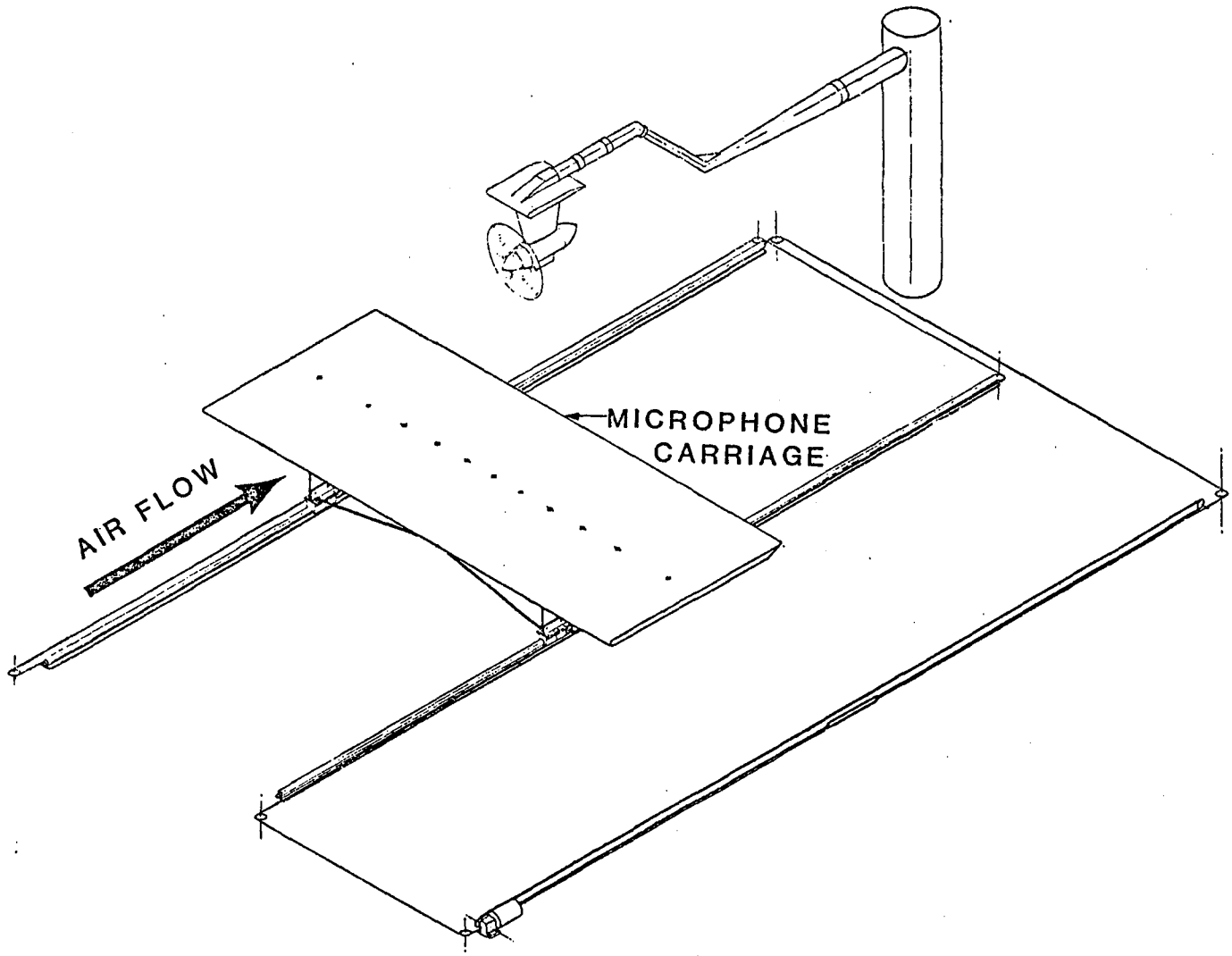

-Figure 4.- Isometric sketch of the microphone carriage in the Langley 4- x 7-Meter Tunnel.

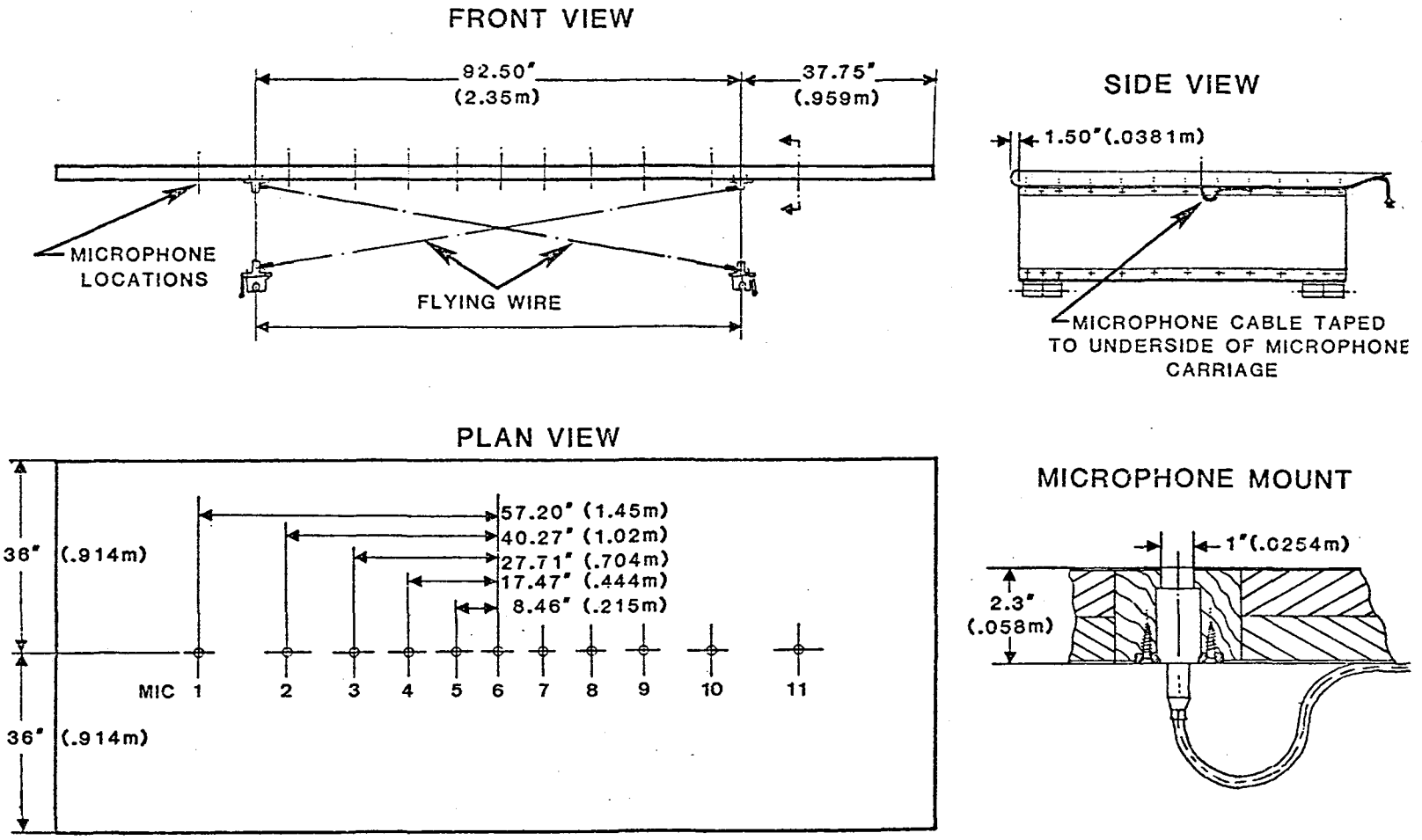

Figure 5.- Sketch of microphone carriage showing dimensions and microphone locations.

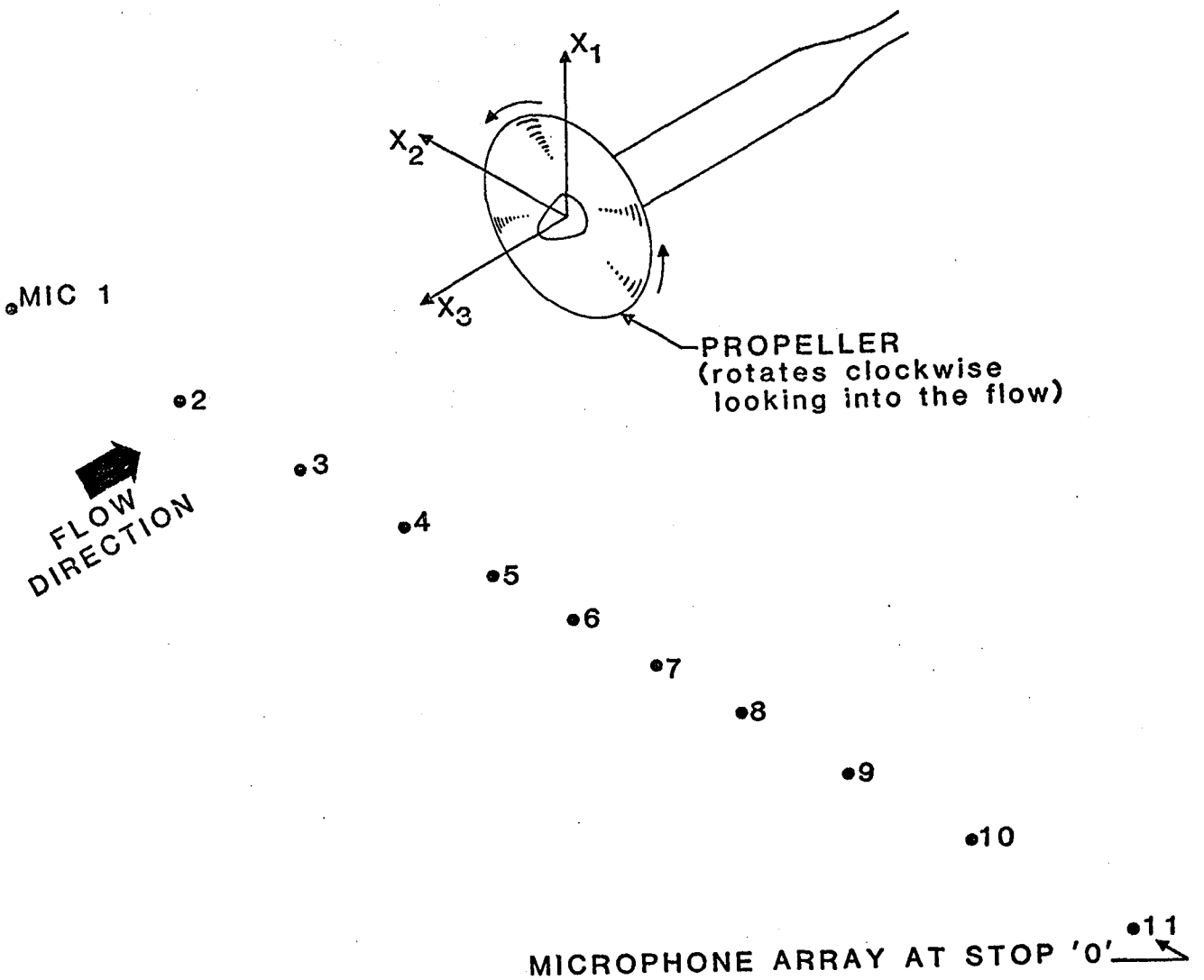

Figure 6.- Isometric sketch showing coordinate system in which microphone locations are defined.

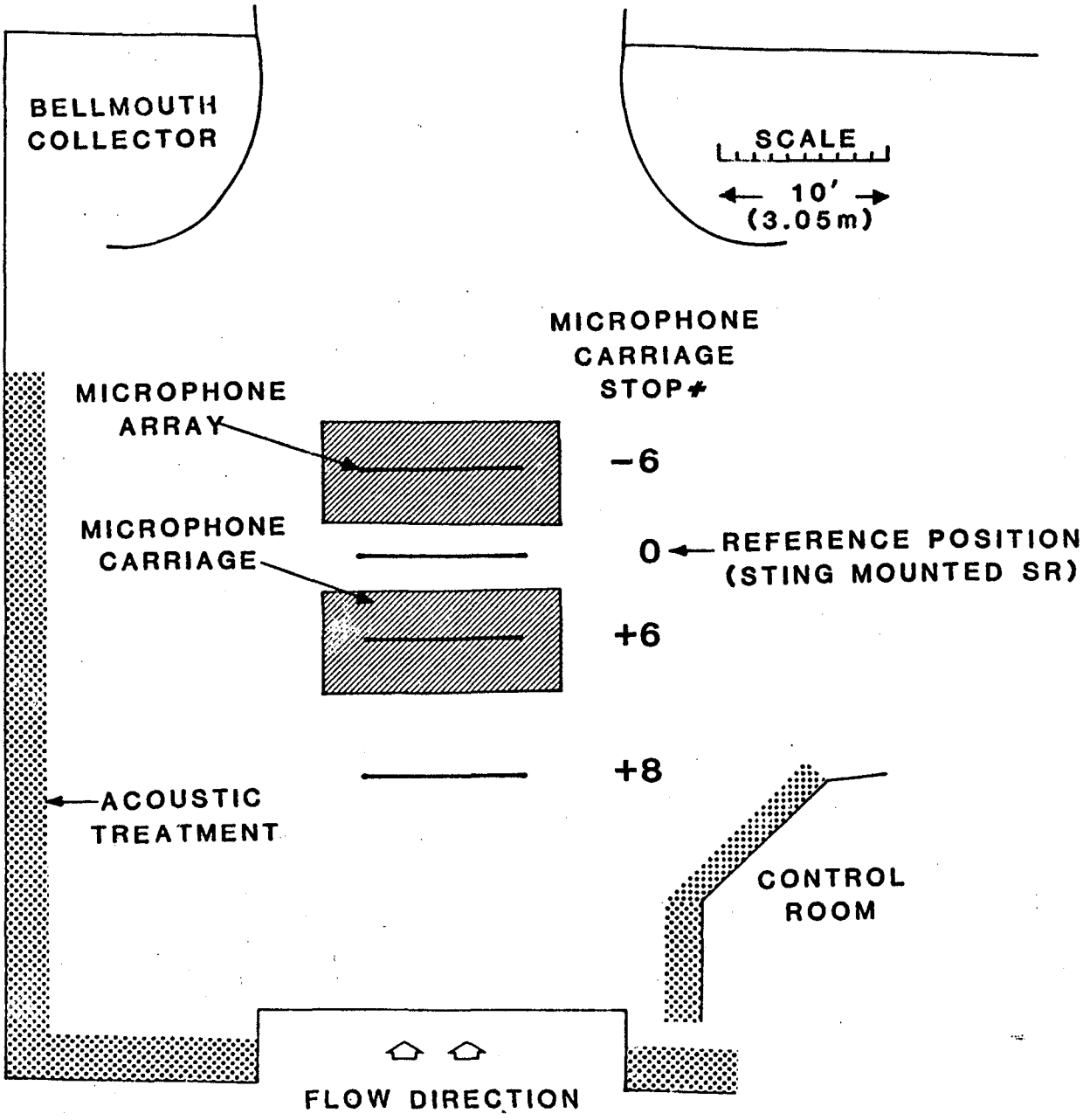

Figure 7.- Planview of the 4- x 7-Meter Tunnel open test section showing microphone carriage locations.

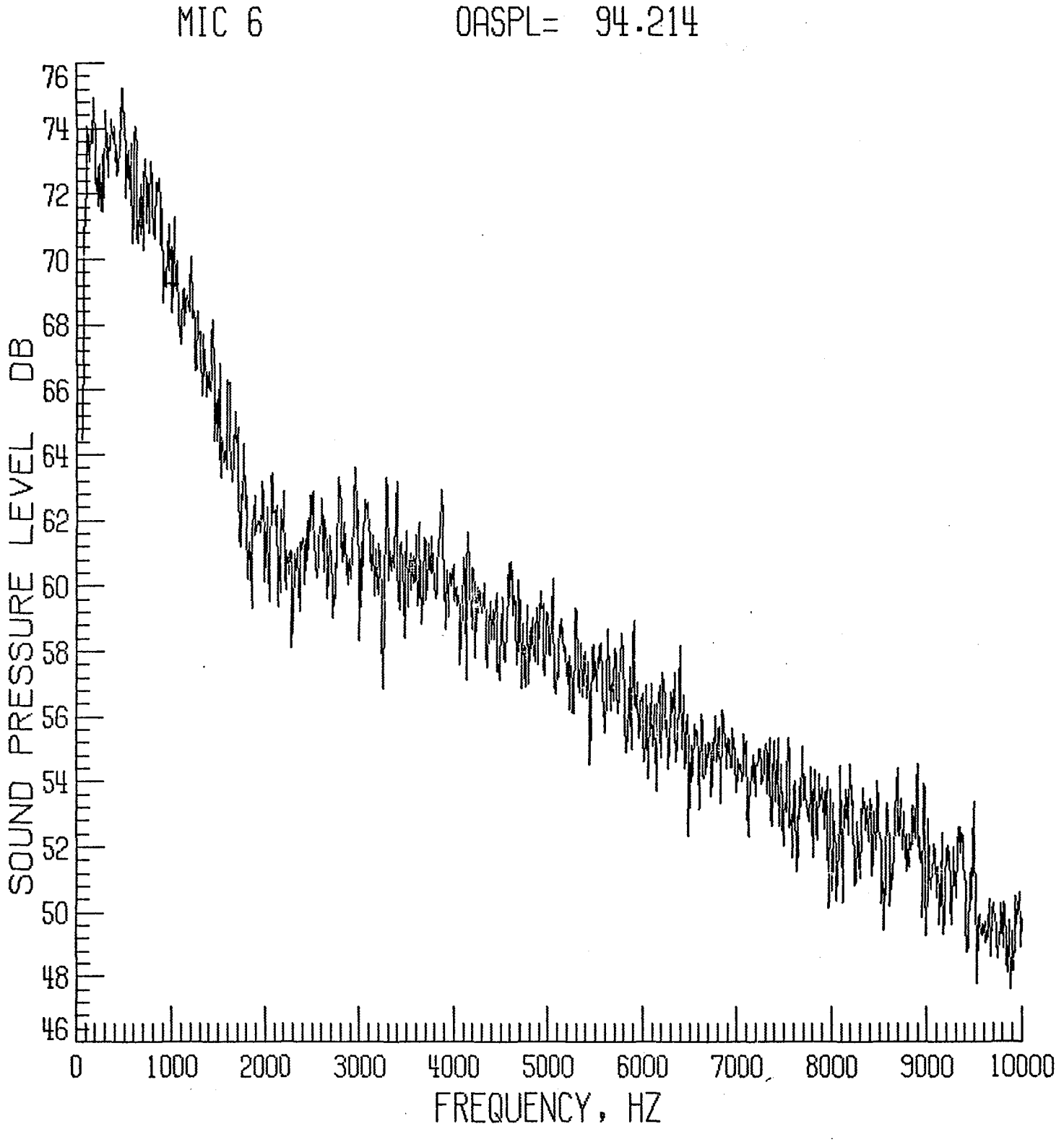

Figure 8.- Typical background noise spectra of the 4- x 7-M Tunnel open test section; U=100 fps (30.5 m/s).

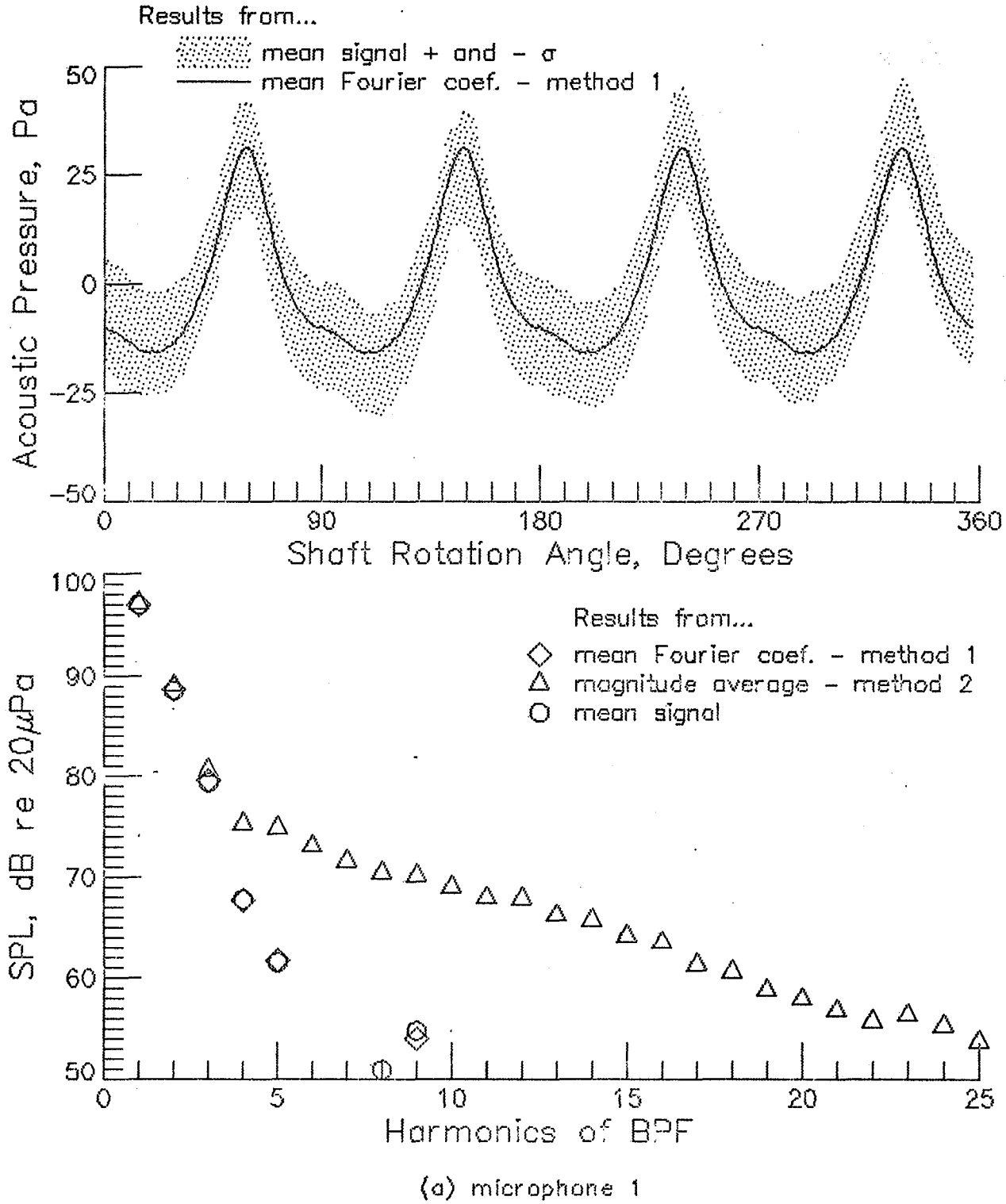

(a) microphone 1

Figure 9. - Run 54+4 . BPF= 671.7 Hz. RPM=10076.0. U_{Tip}=743.0 fps.

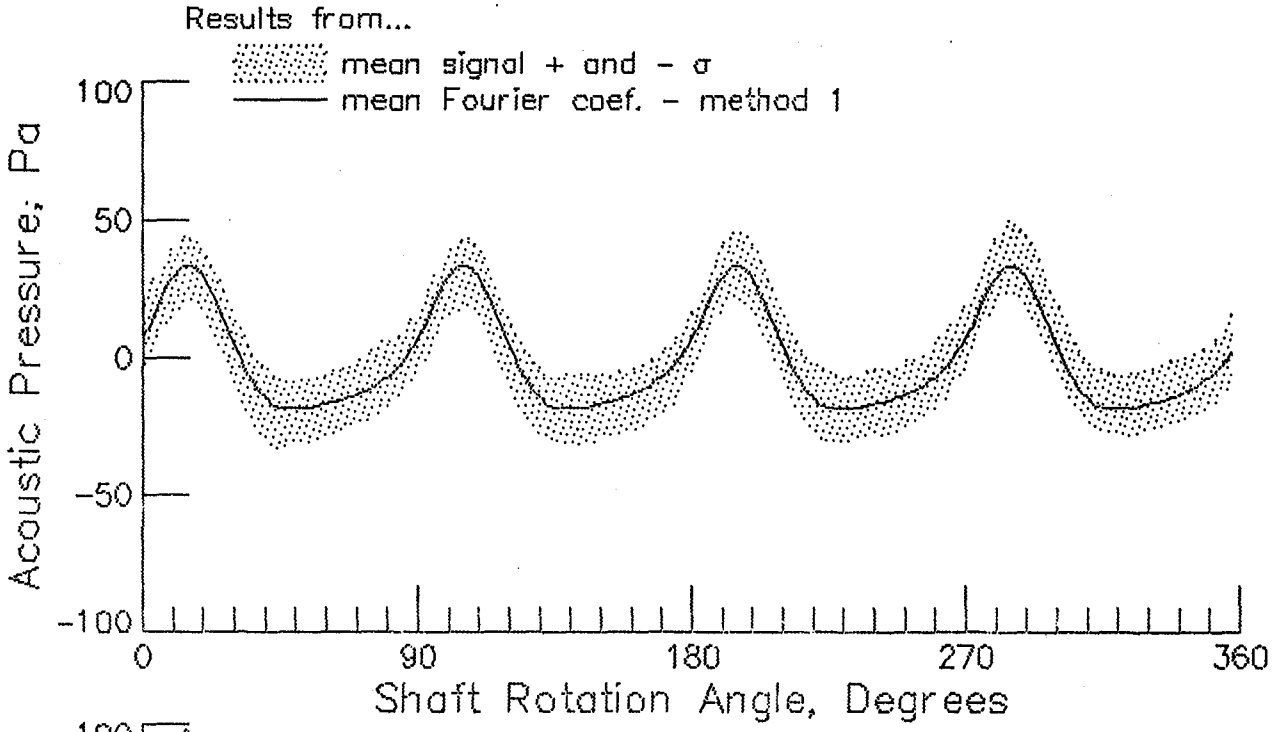

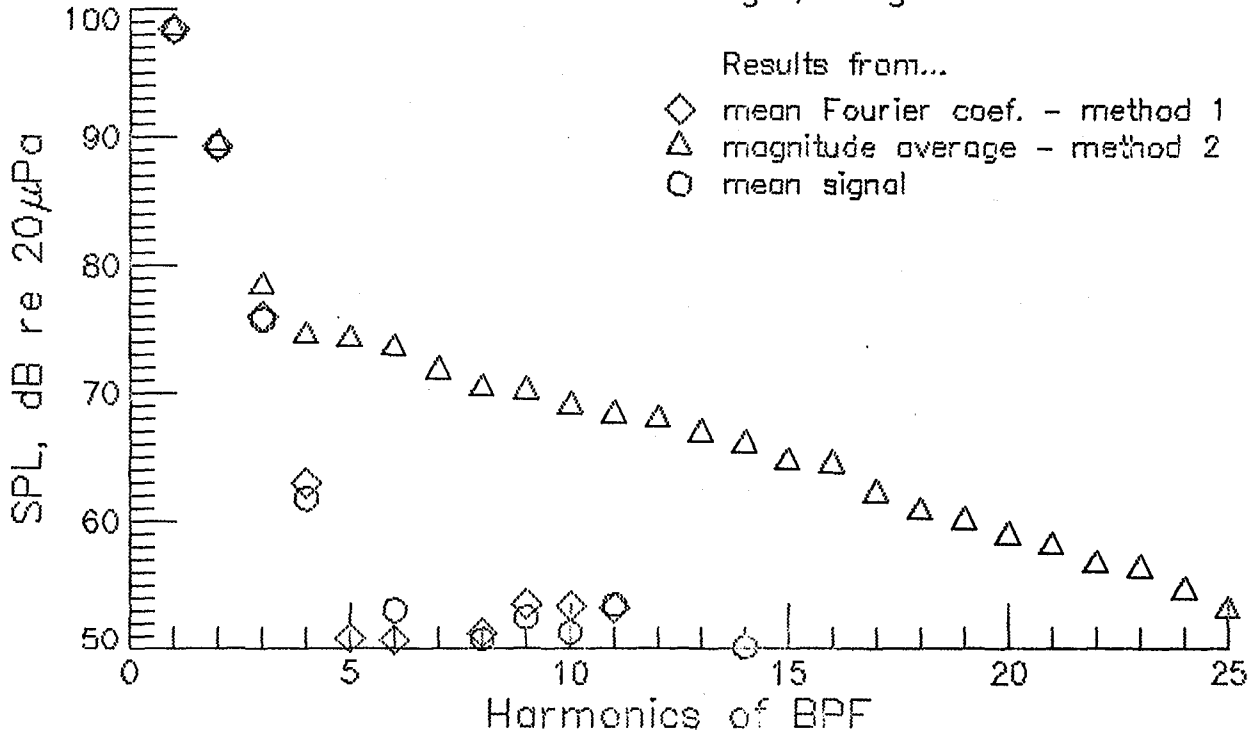

(b) microphone 2

Figure 9. - Continued.

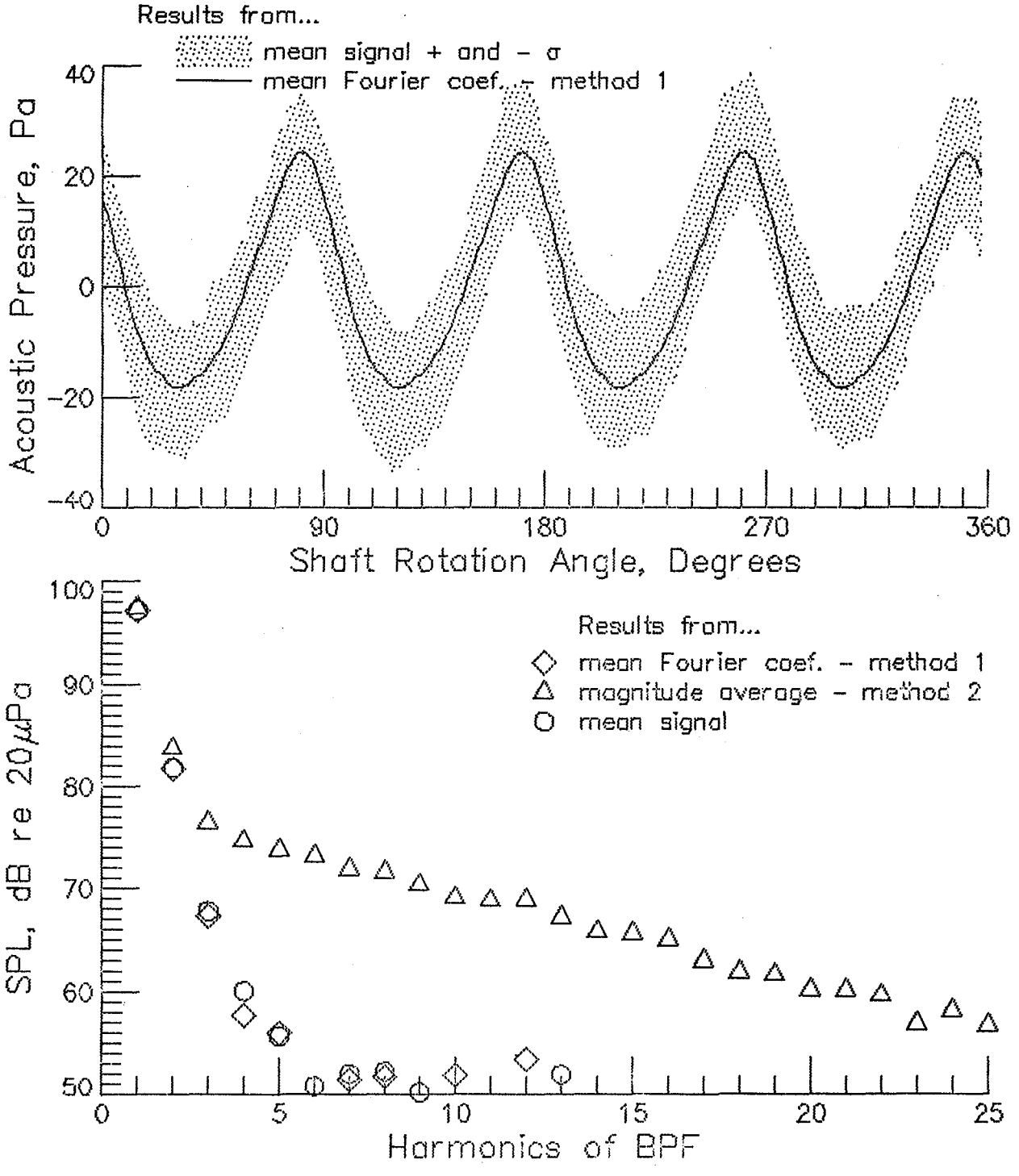

(c) microphone 3

Figure 9. - Continued.

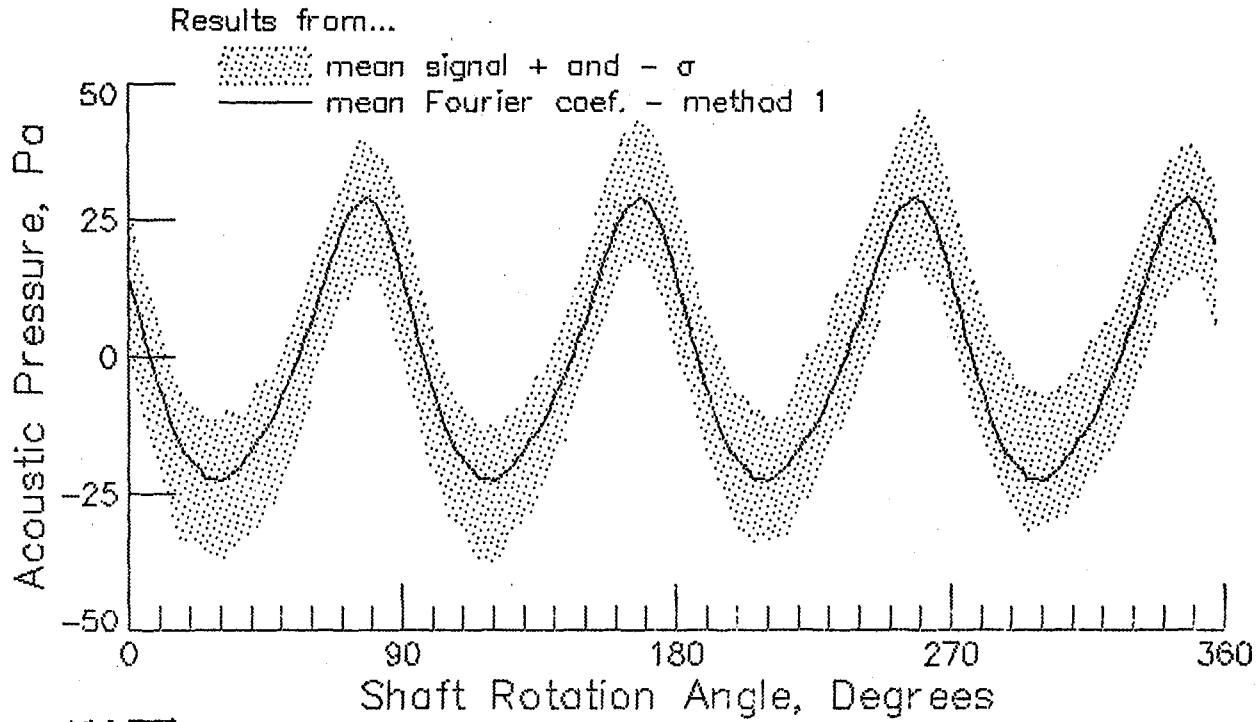

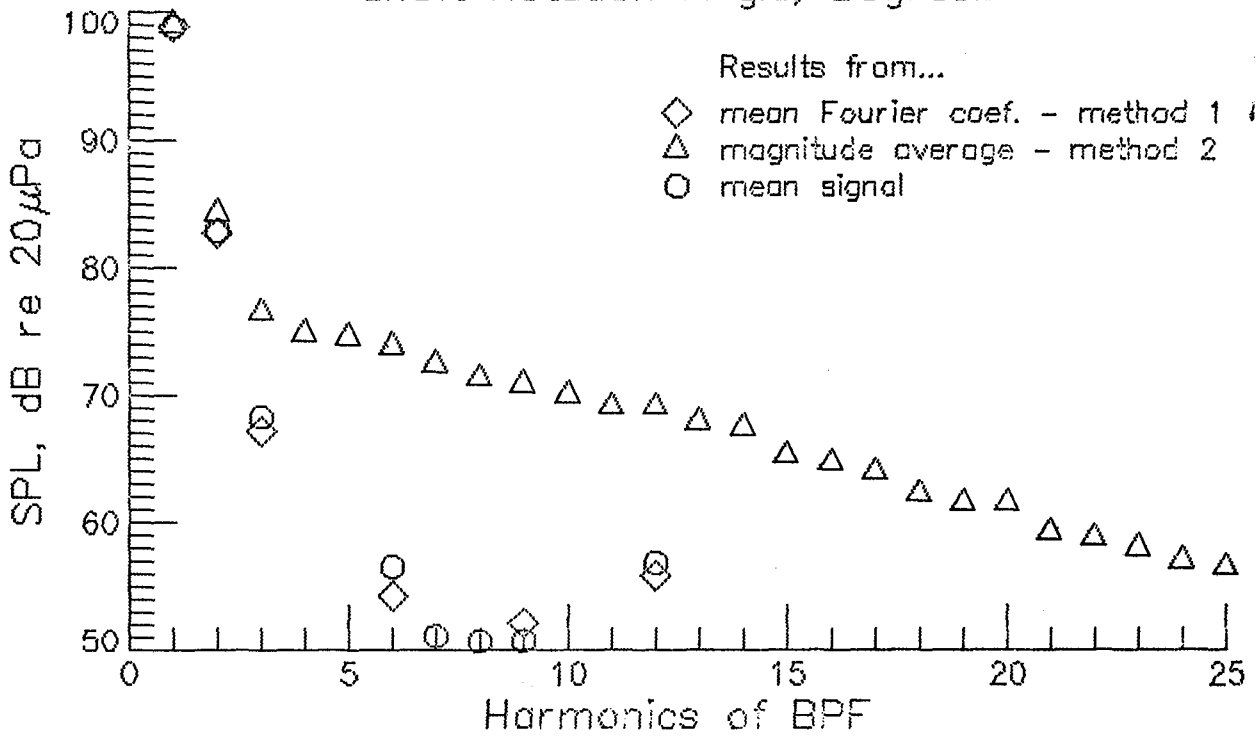

(d) microphone 4

Figure 9. - Continued.

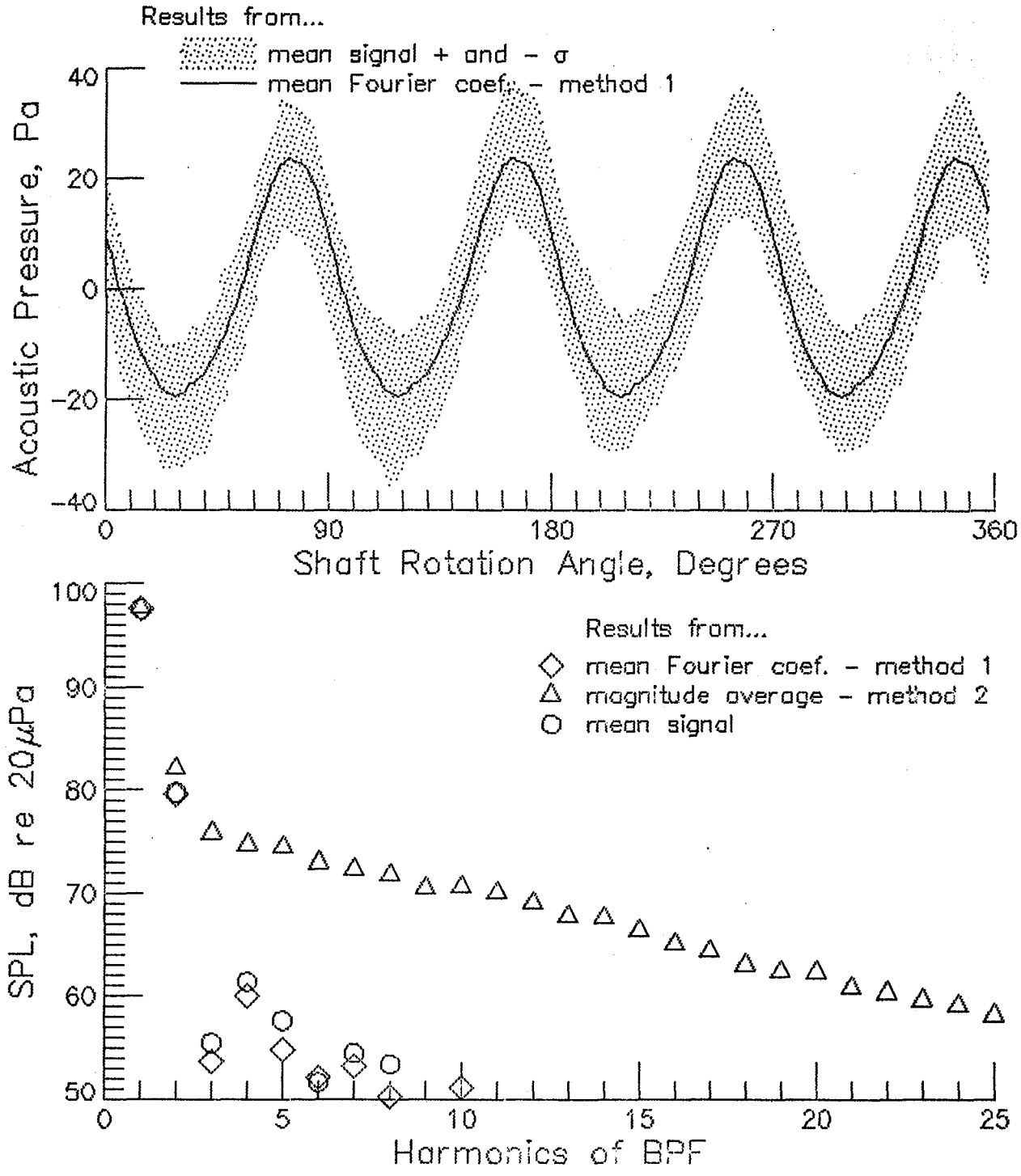

(e) microphone 5

Figure 9. - Continued.

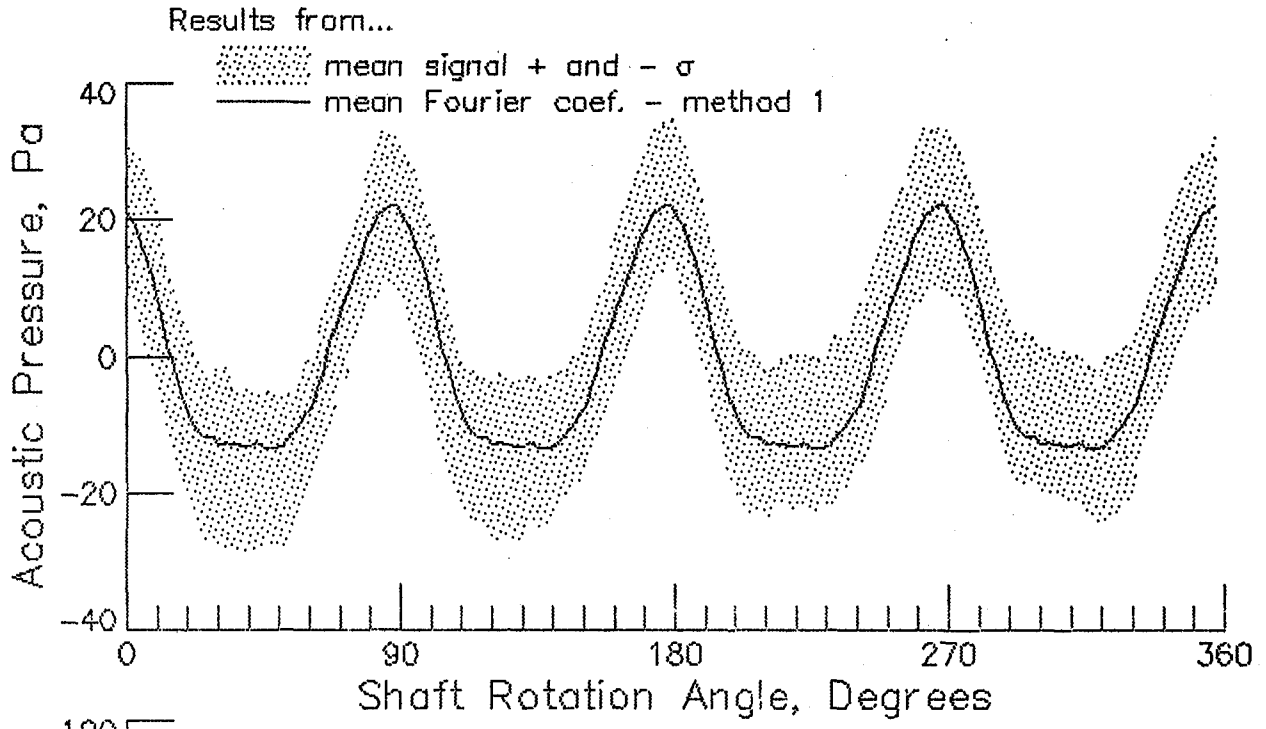

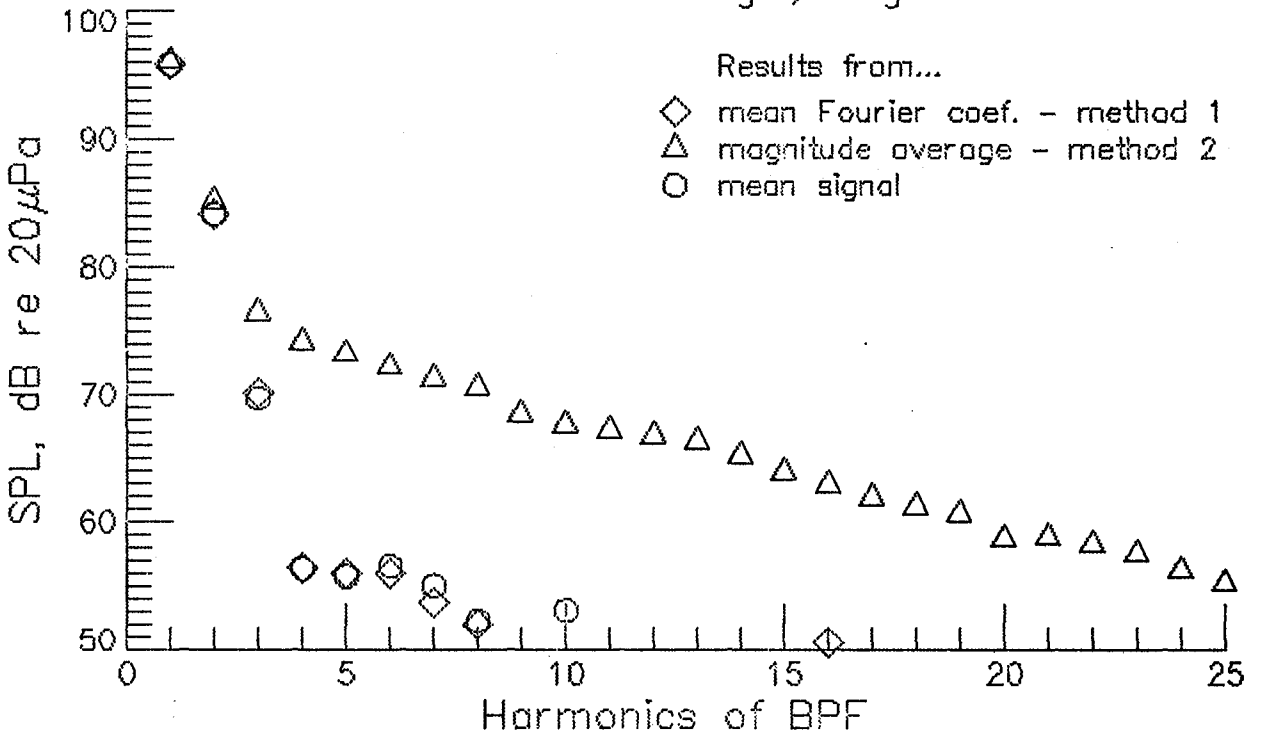

(f) microphone 6

Figure 9. - Continued.

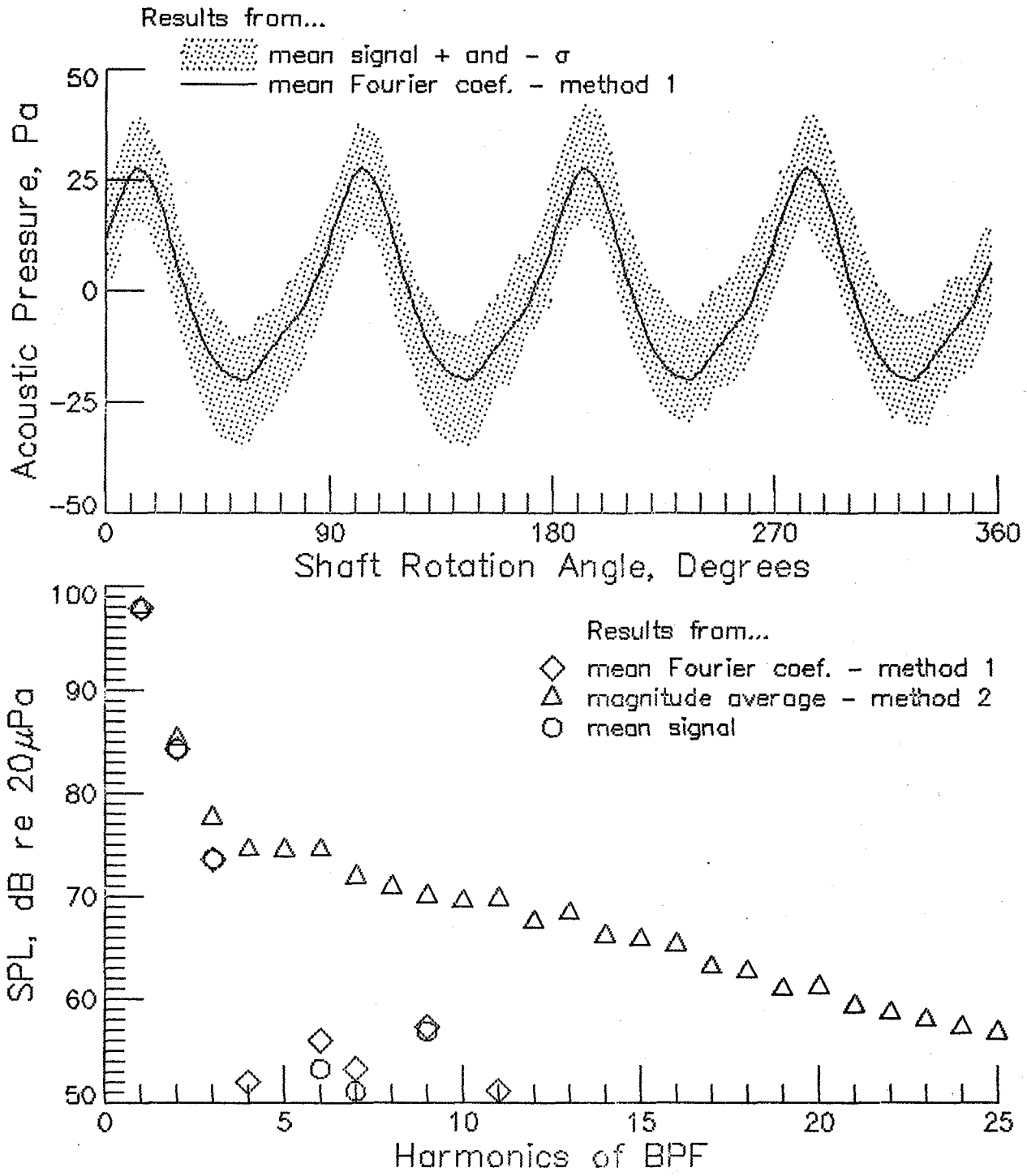

(g) microphone 7

Figure 9. - Continued.

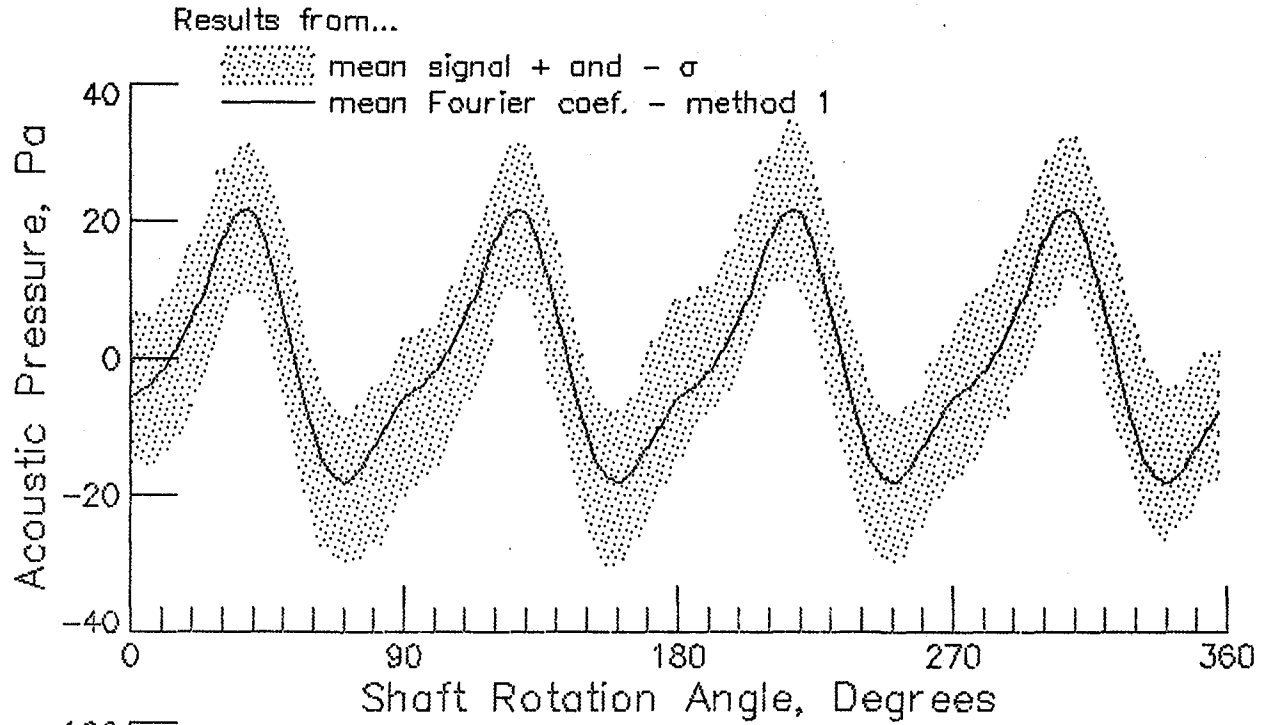

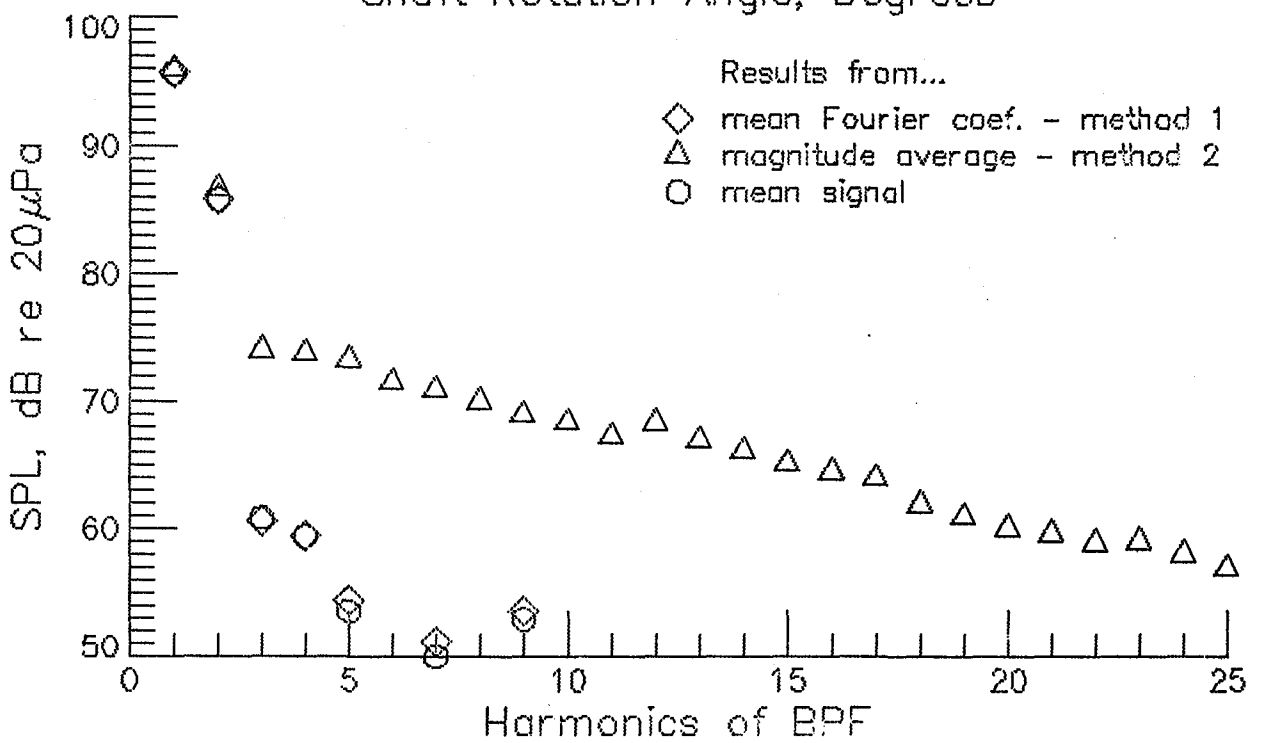

(h) microphone 8

Figure 9. - Continued.

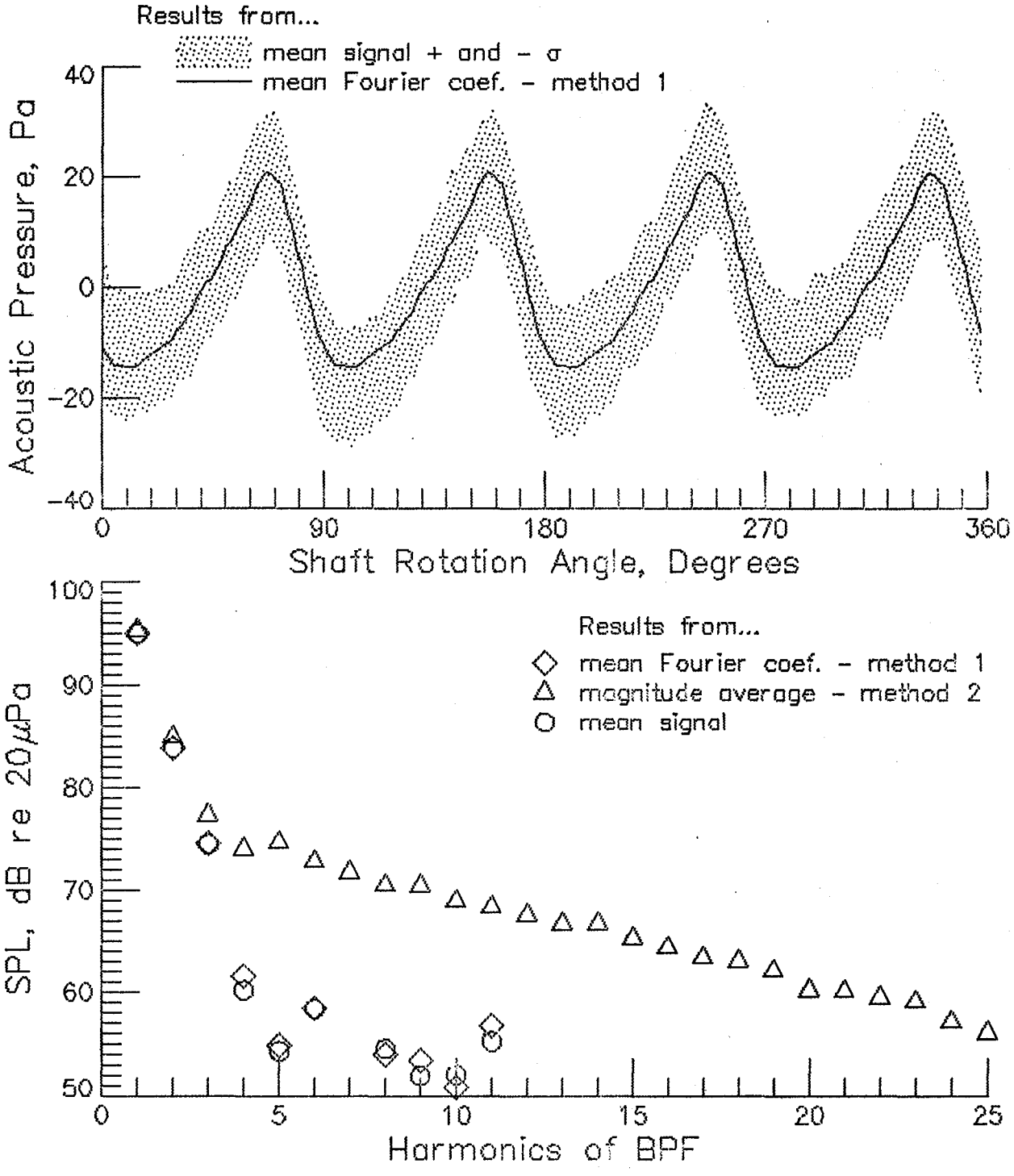

(i) microphone 9

Figure 9. - Continued.

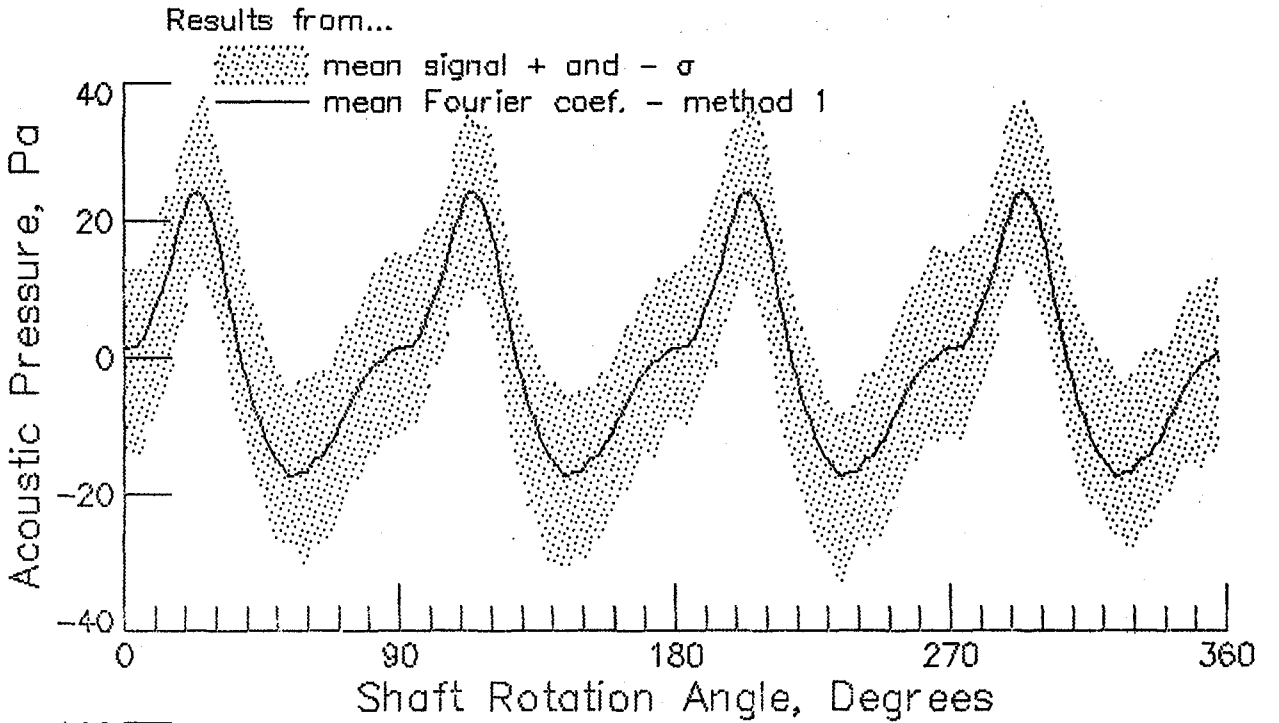

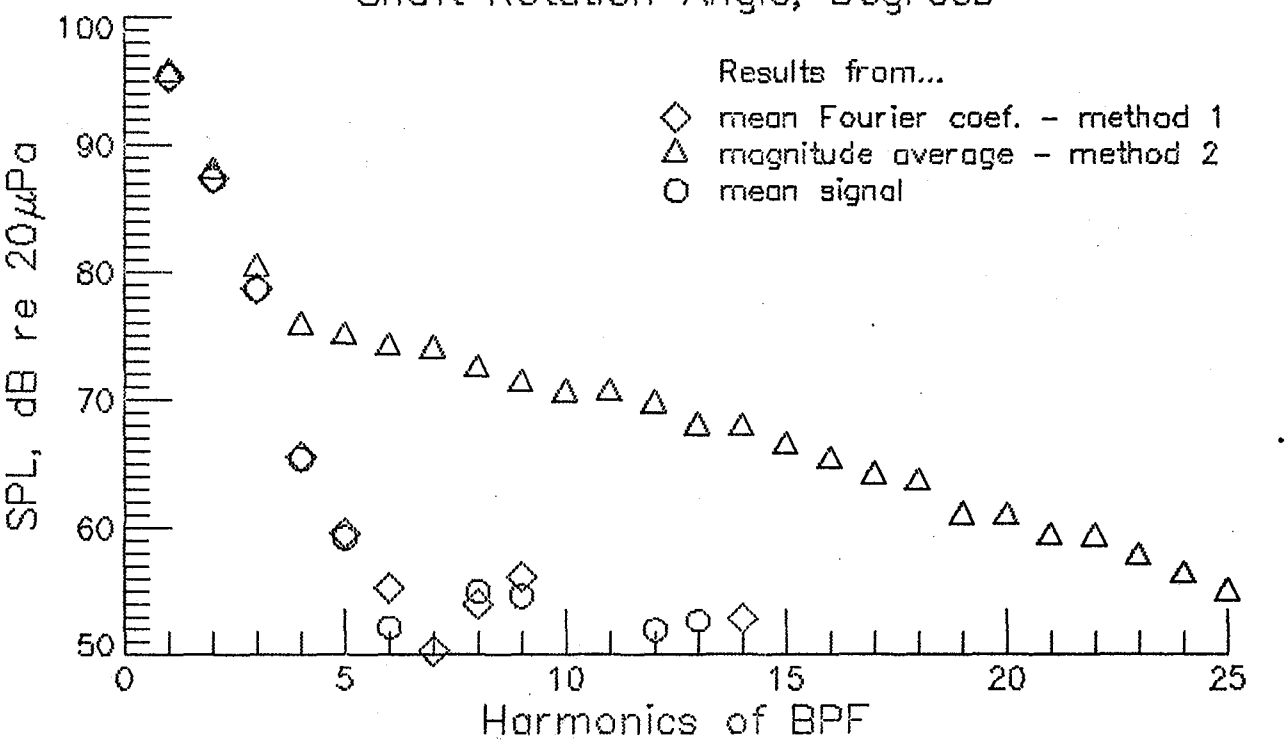

(j) microphone 10

Figure 9. - Continued.

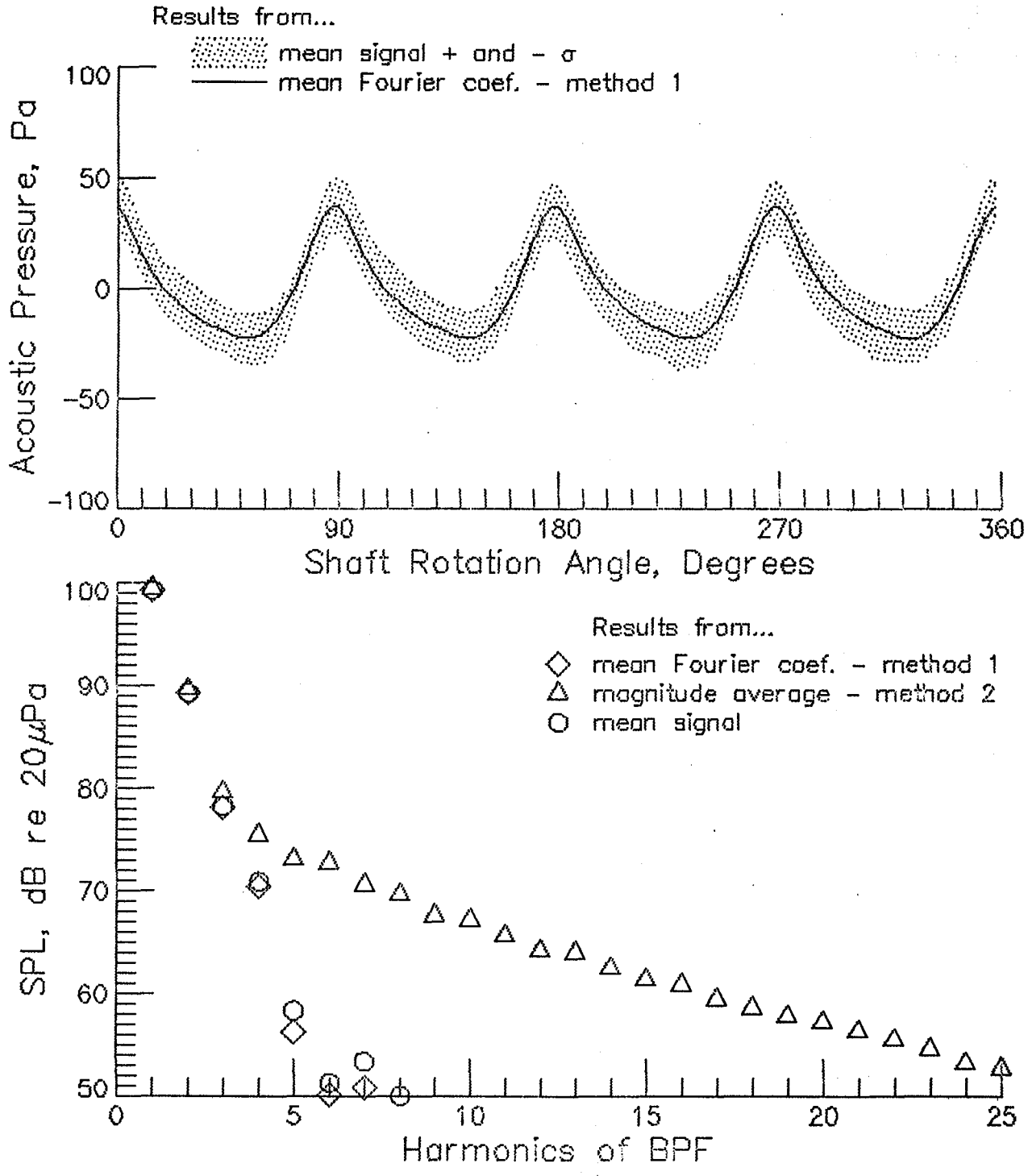

(k) microphone 11

Figure 9. - Continued.

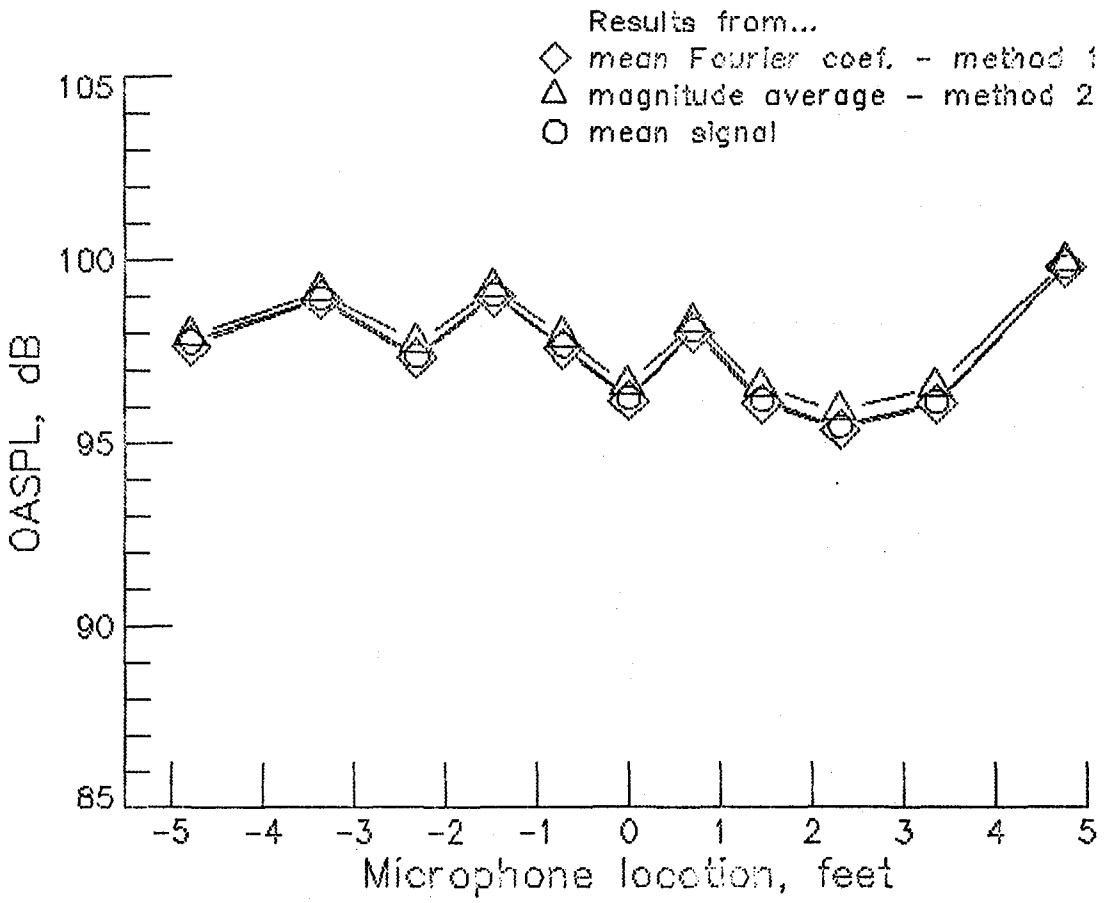

(l) Summary of Stop 4

Figure 9. - Run 54+4 . BPF= 671.7 Hz. RPM=10076.0. U_{Tip}=743.0 fps.

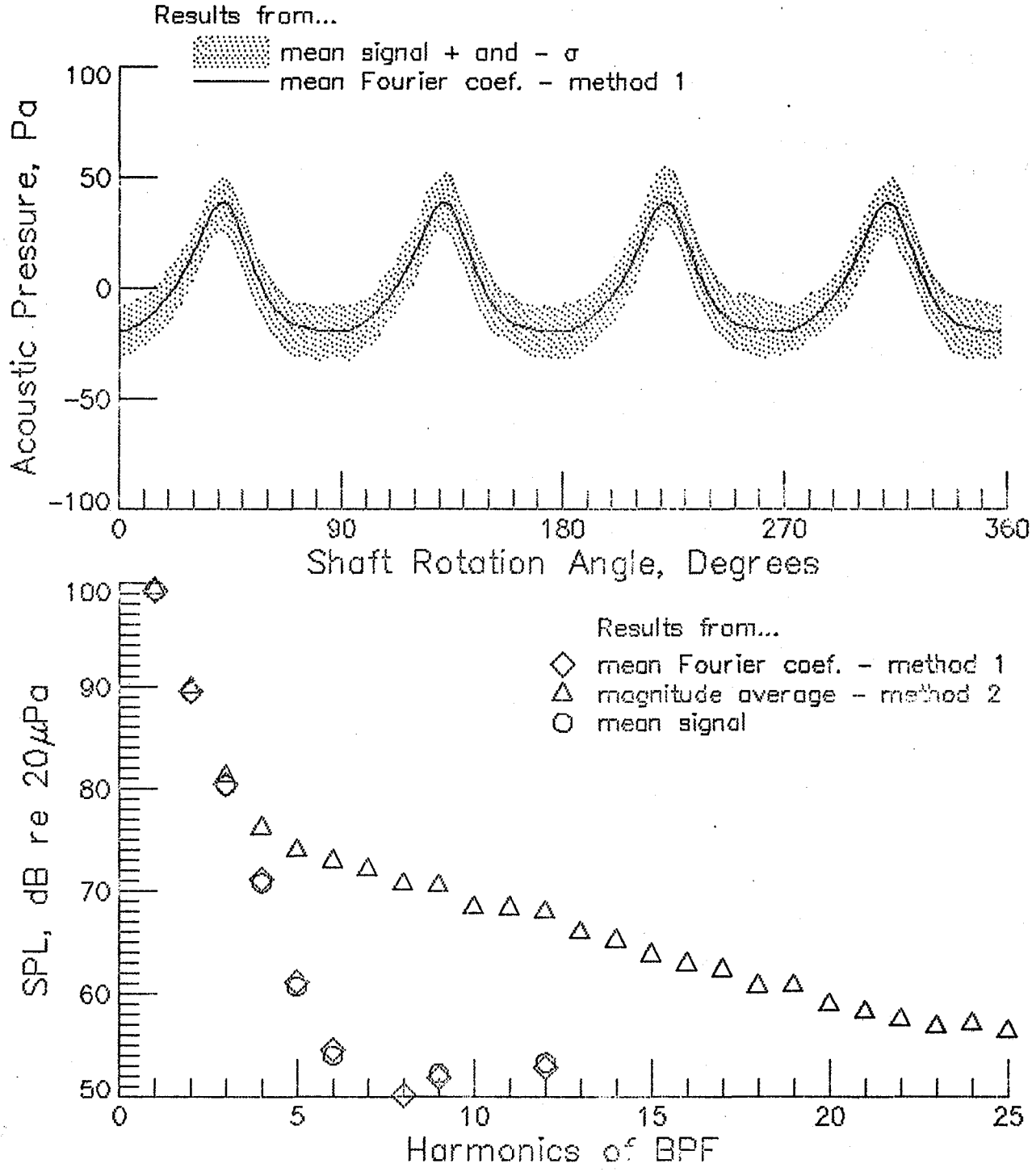

(a) microphone 1

Figure 10. - Run 67+4 . BPF= 670.8 Hz. RPM=10062.5. U_{Tip}=742.0 fps.

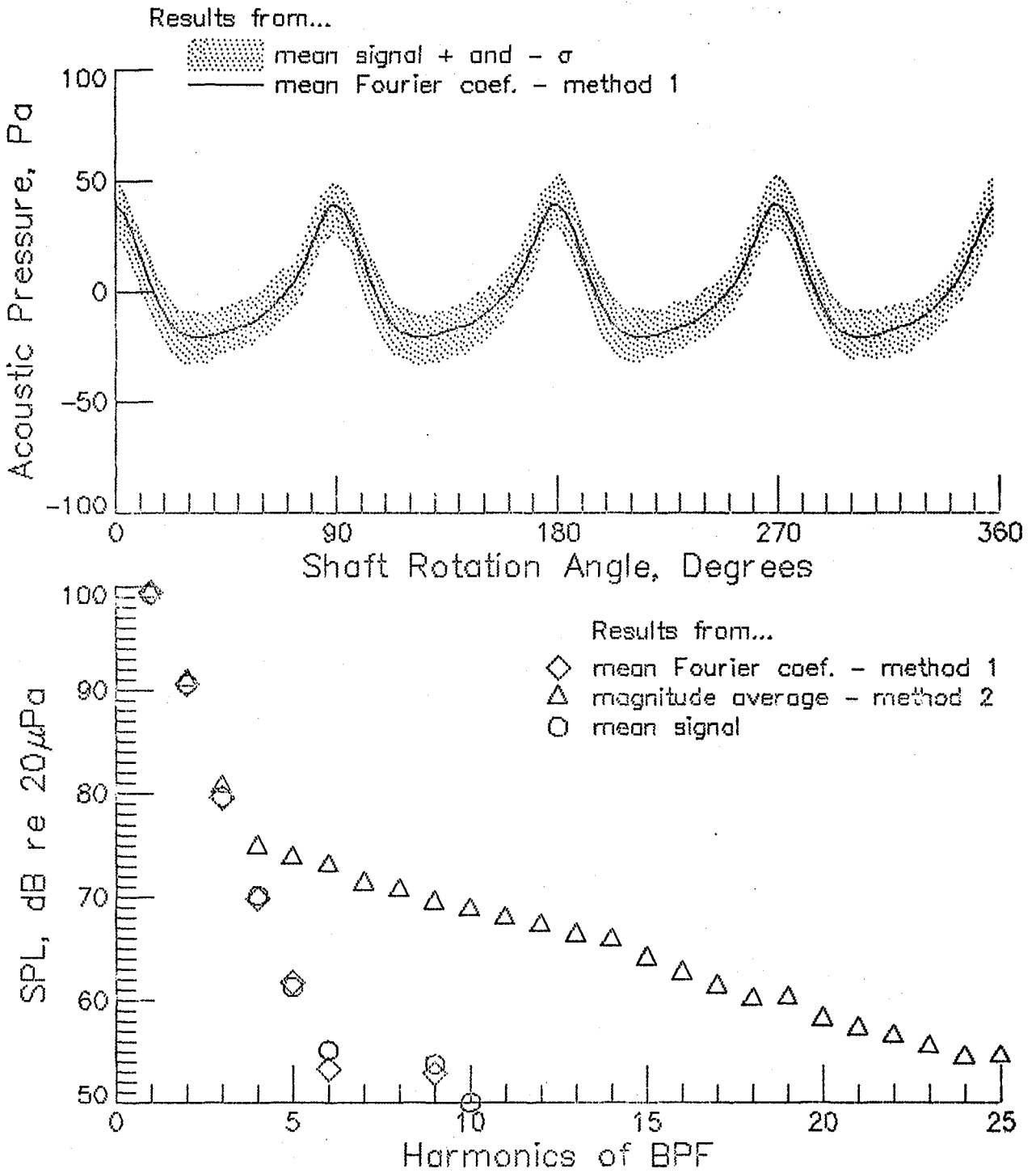

(b) microphone 2

Figure 10. - Continued.

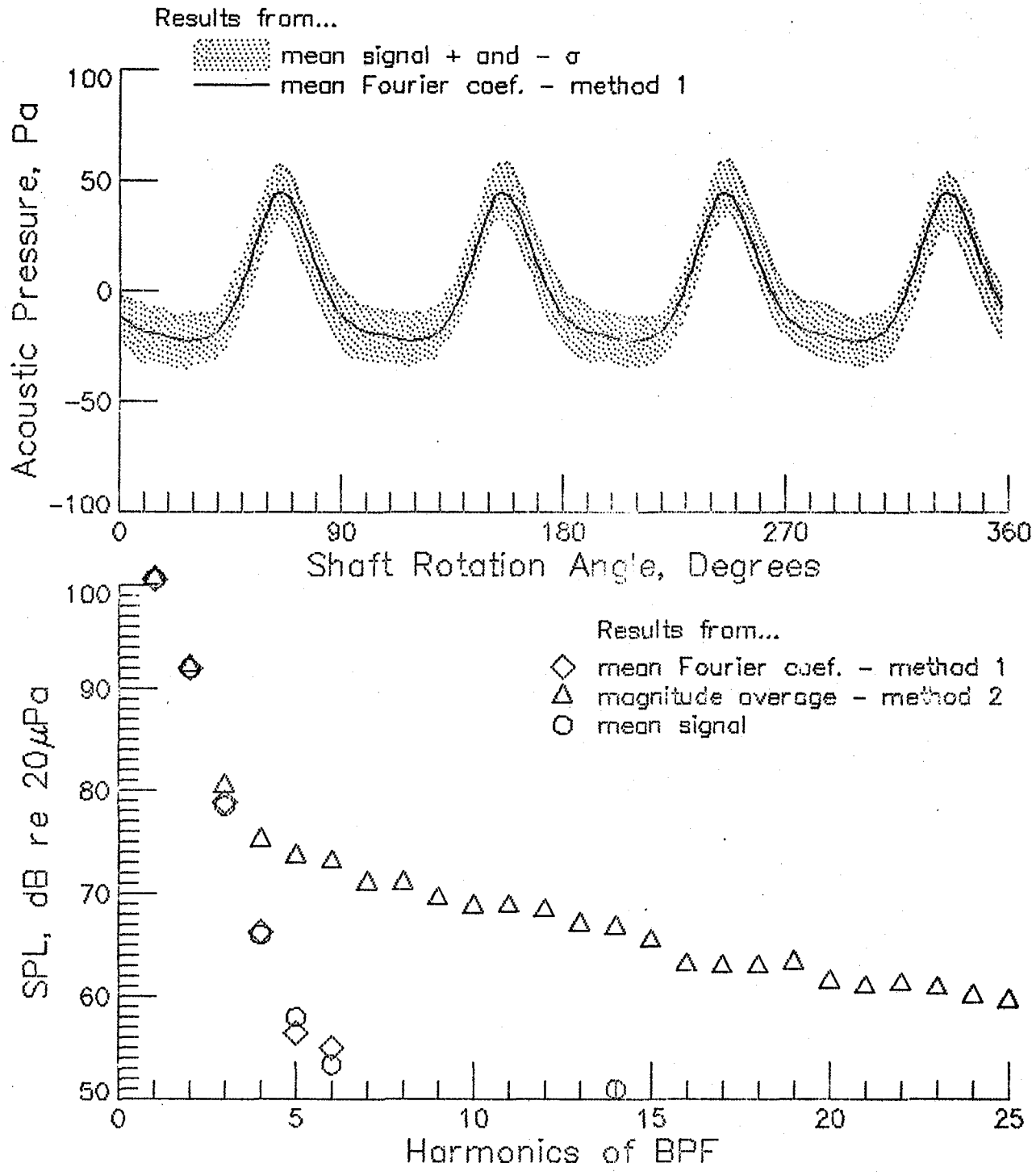

(c) microphone 3

Figure 10. - Continued.

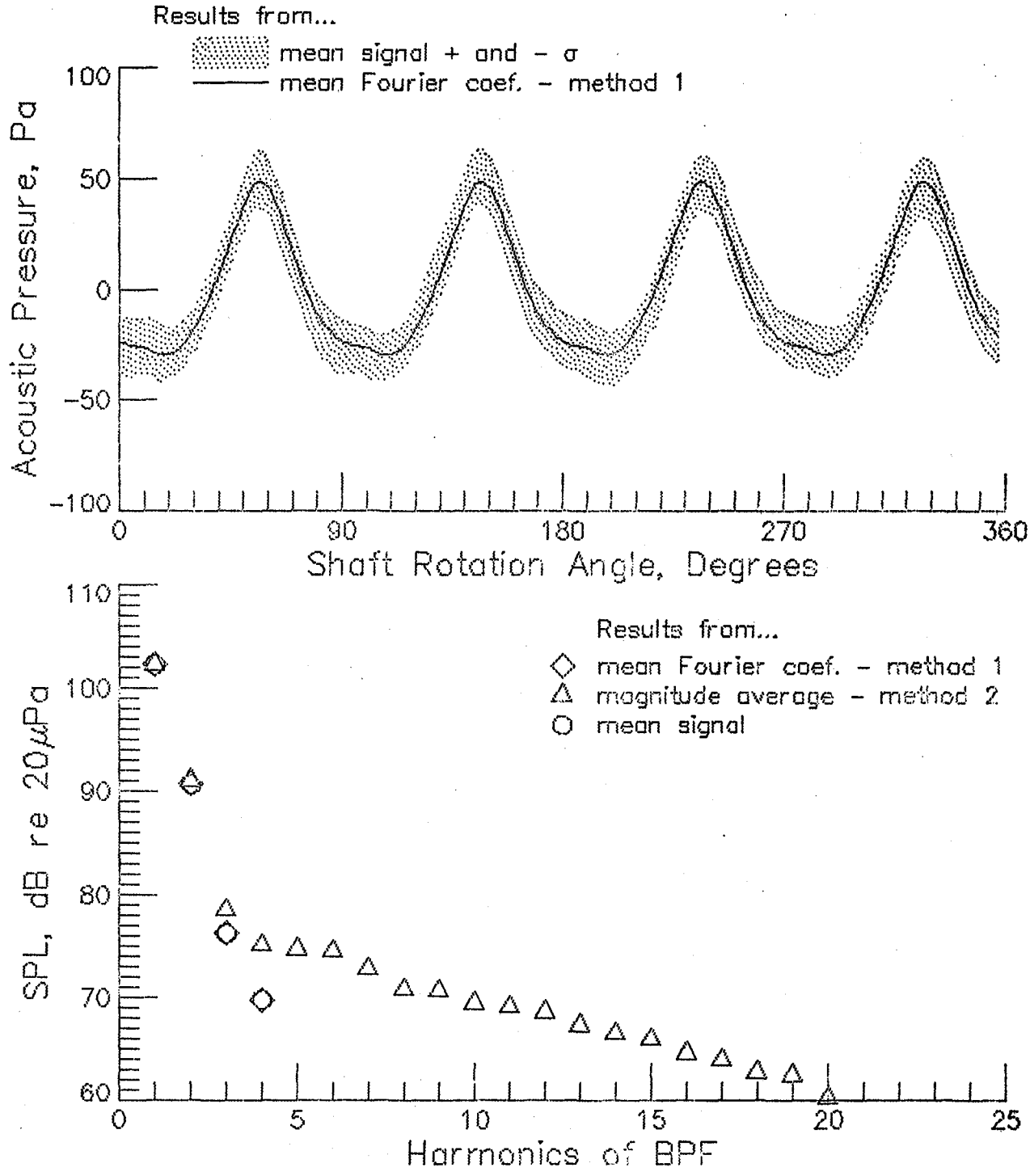

(d) microphone 4

Figure 10. - Continued.

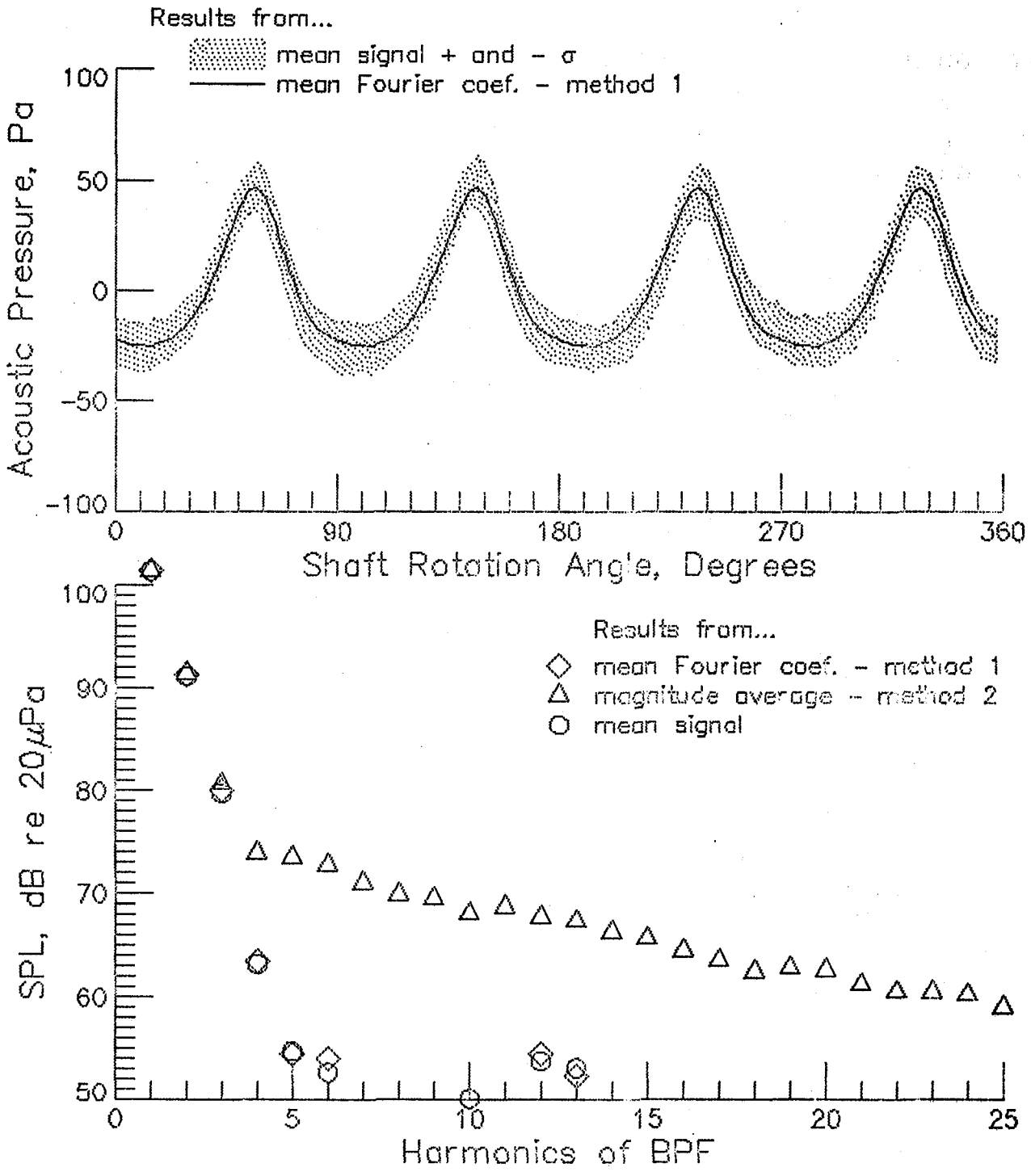

(e) microphone 5

Figure 10. - Continued.

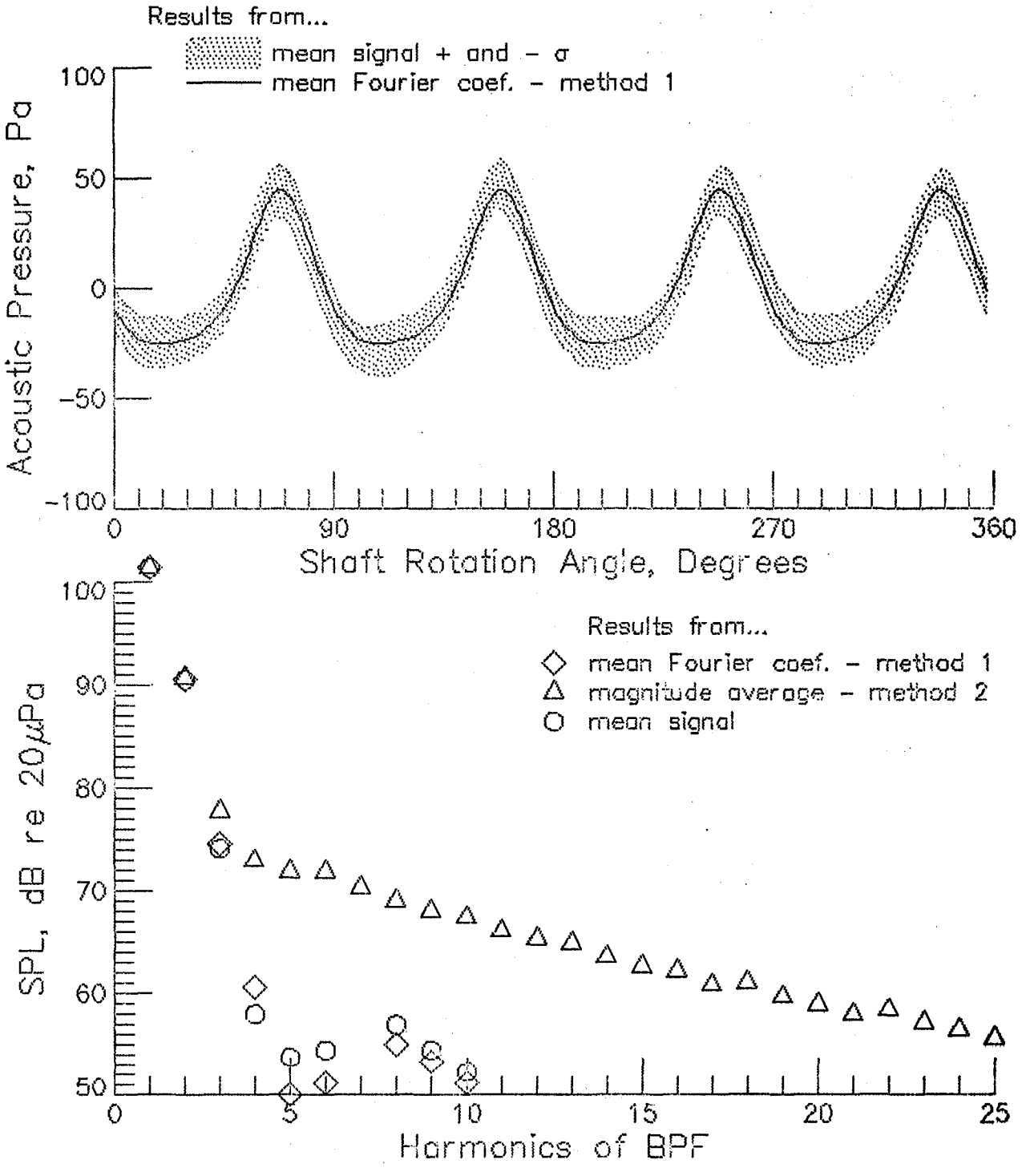

(f) microphone 6

Figure 10. - Continued.

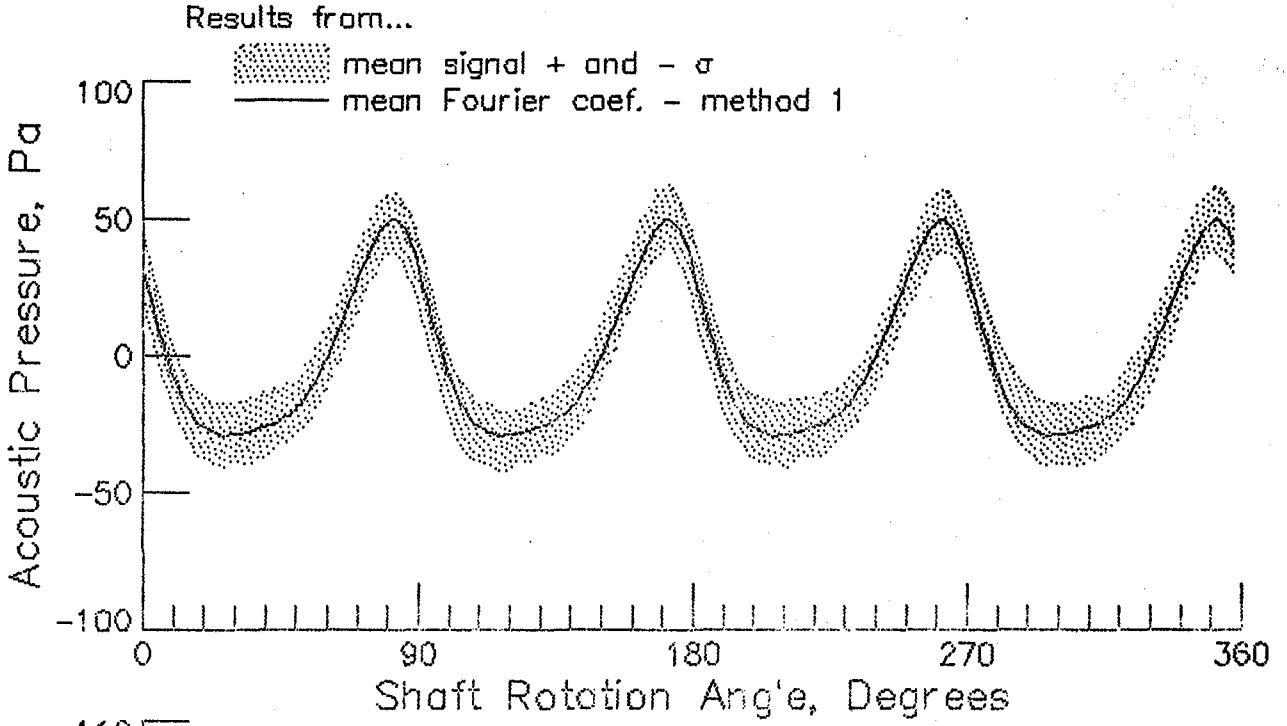

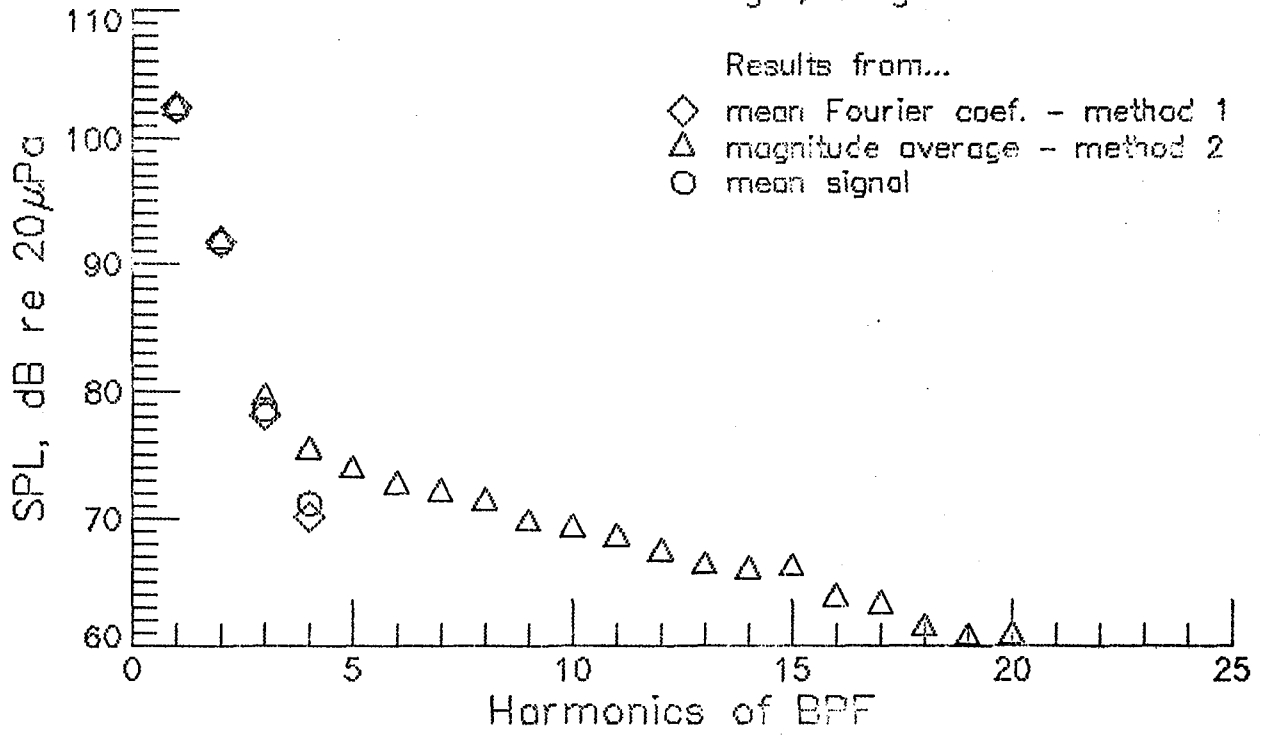

(g) microphone 7

Figure 10. - Continued.

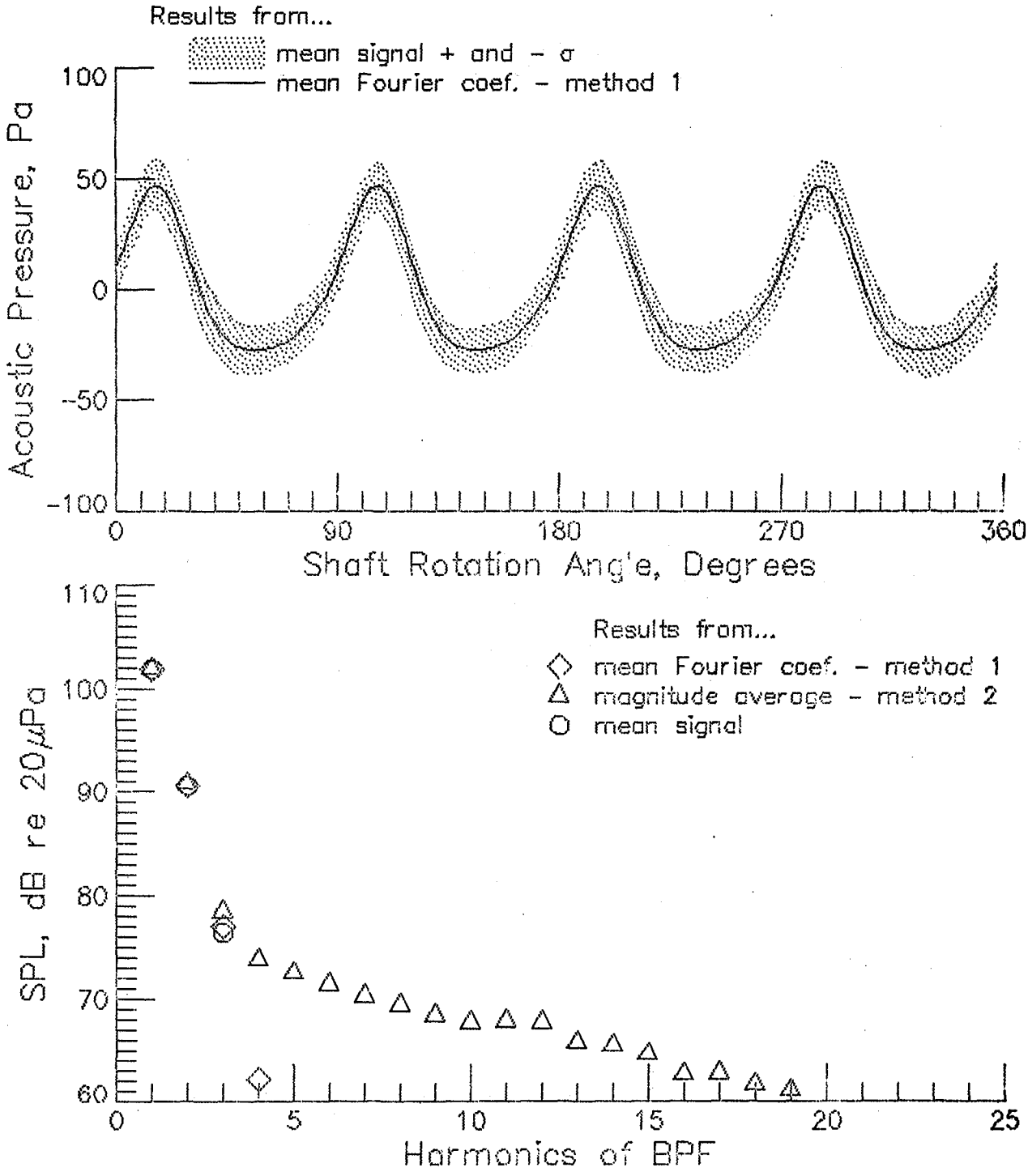

(h) microphone 8

Figure 10. - Continued.

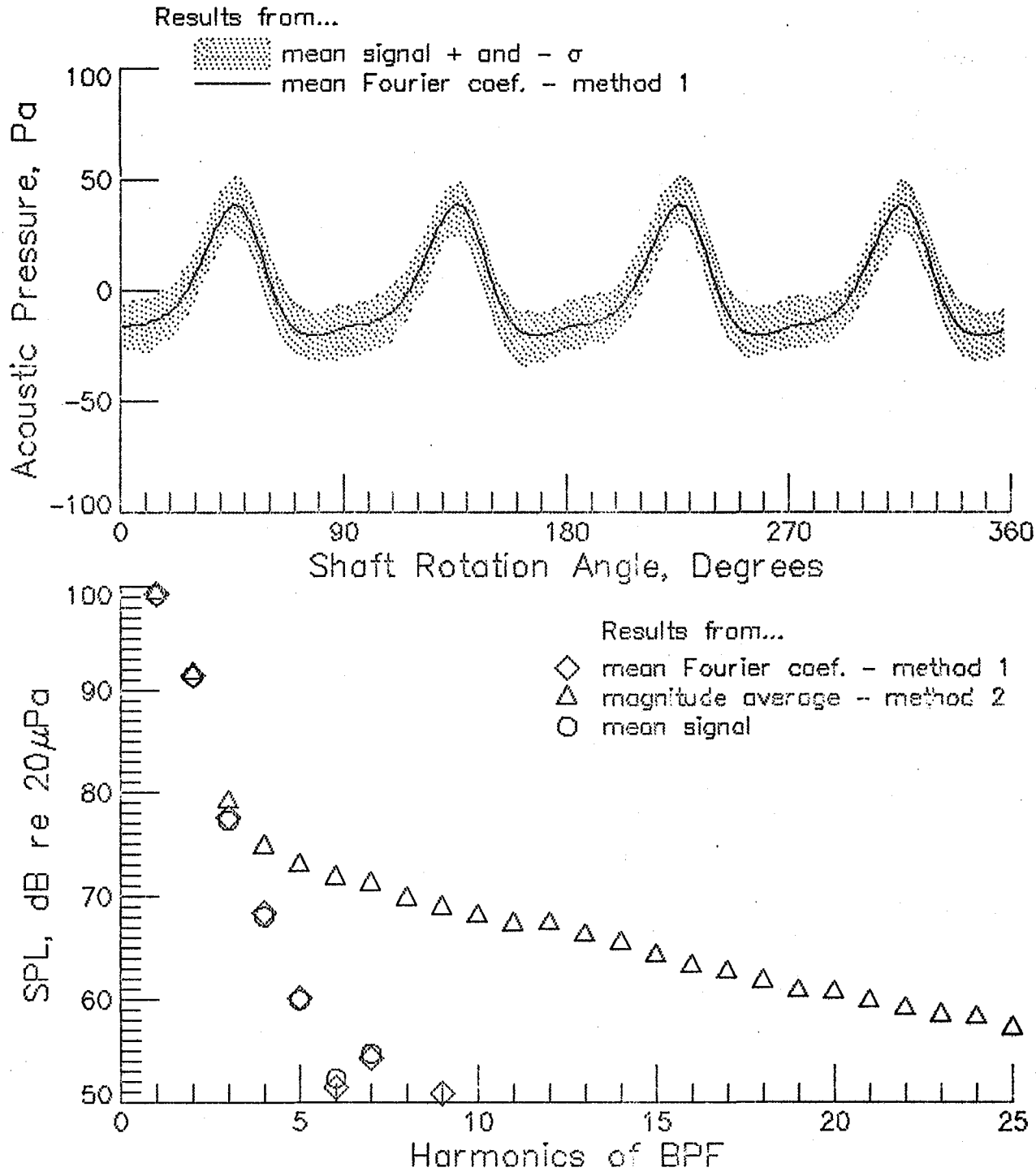

(i) microphone 9

Figure 10. - Continued.

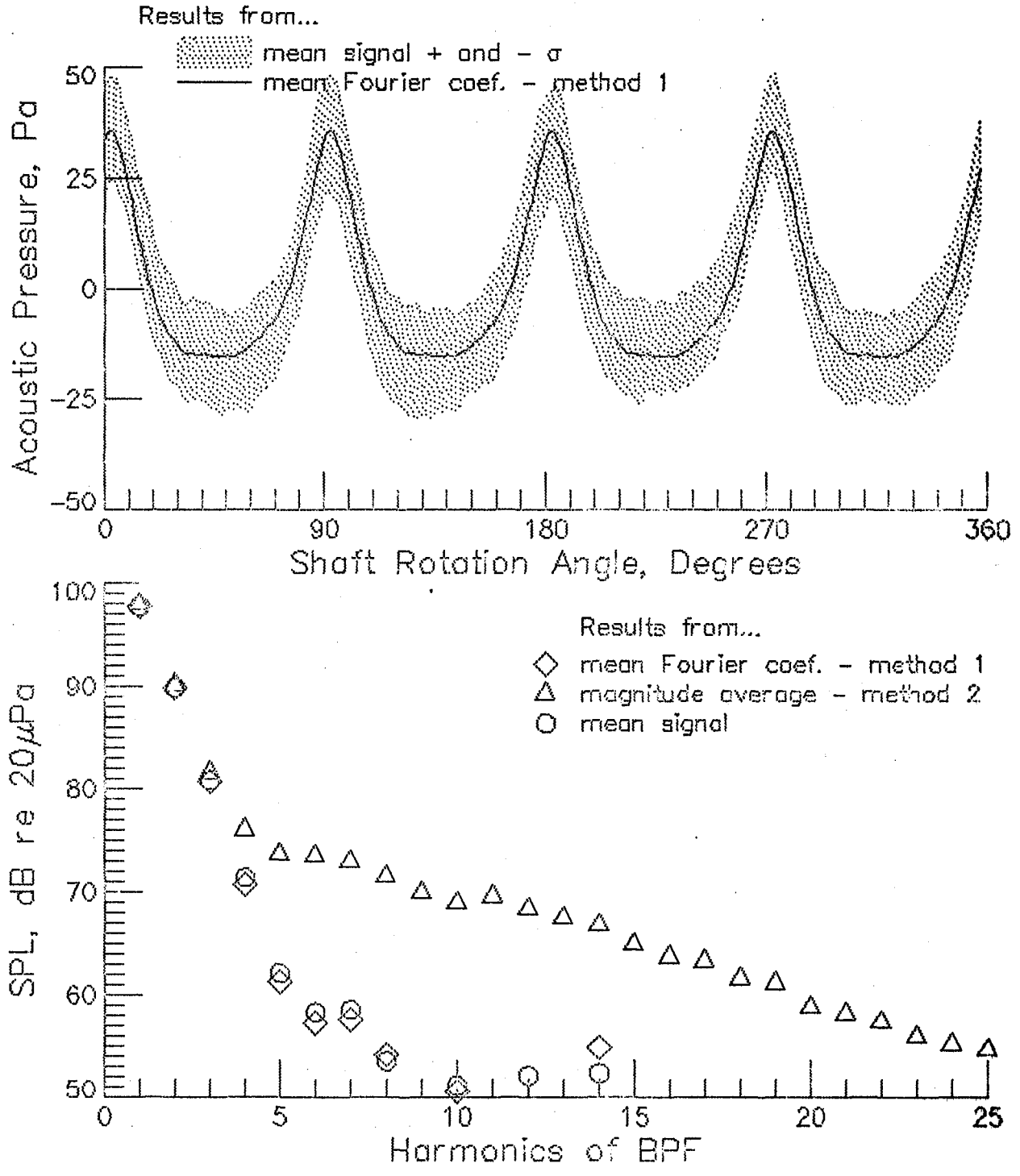

(j) microphone 10

Figure 10. - Continued.

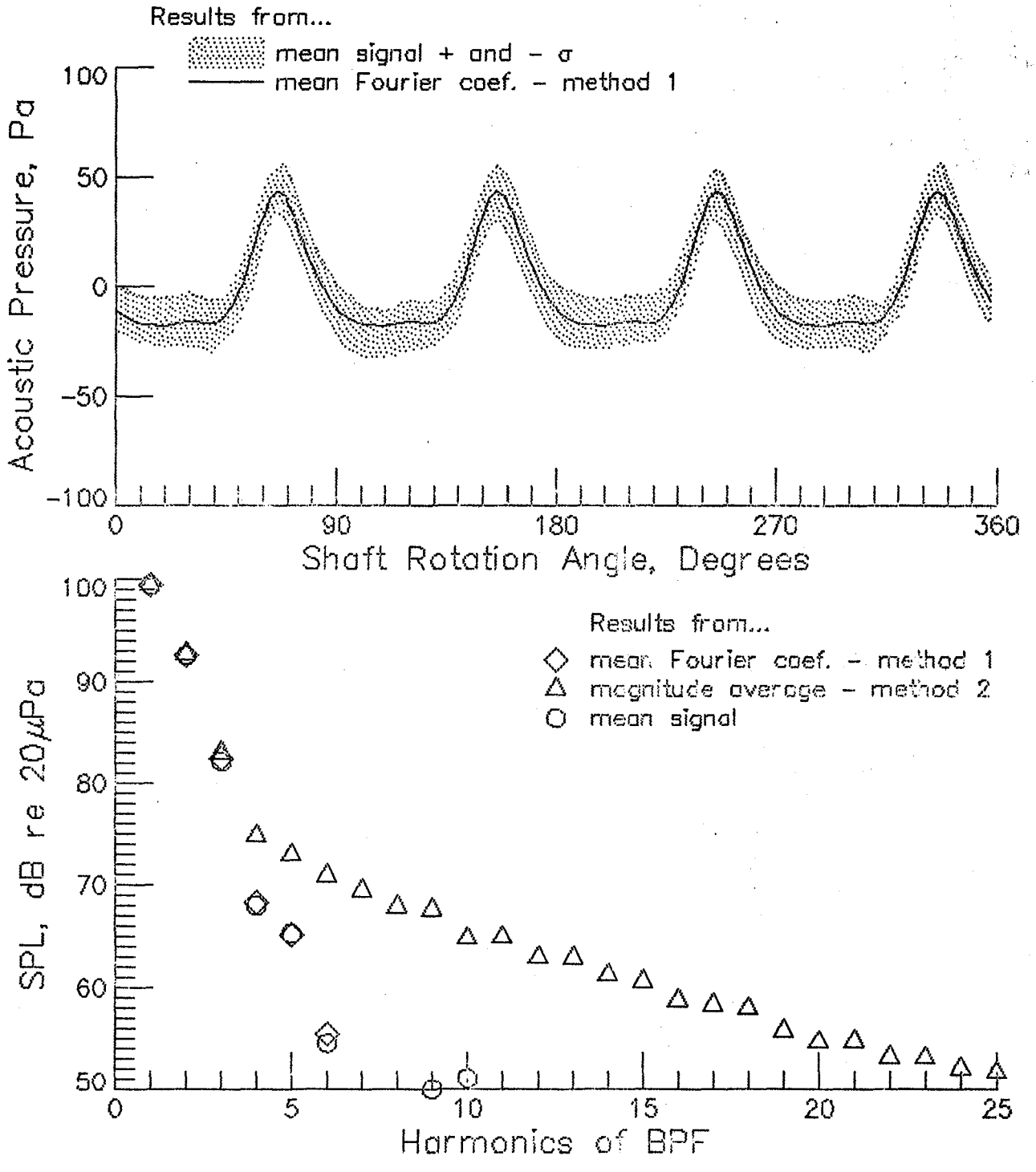

(k) microphone 11

Figure 10. - Continued.

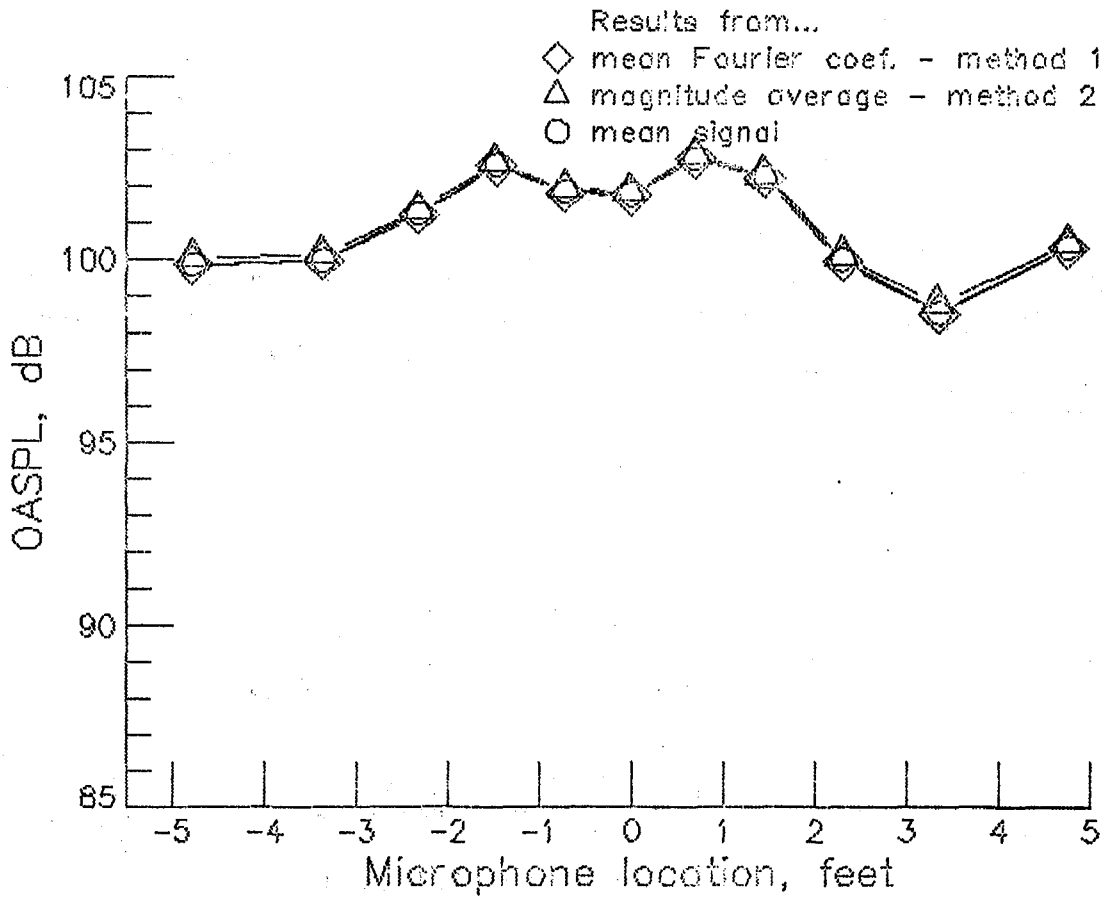

(l) Summary of Stop 4

Figure 10. - Run 67+4 . BPF= 670.8 Hz. RPM=10062.5. U_{Tip}=742.0 fps.

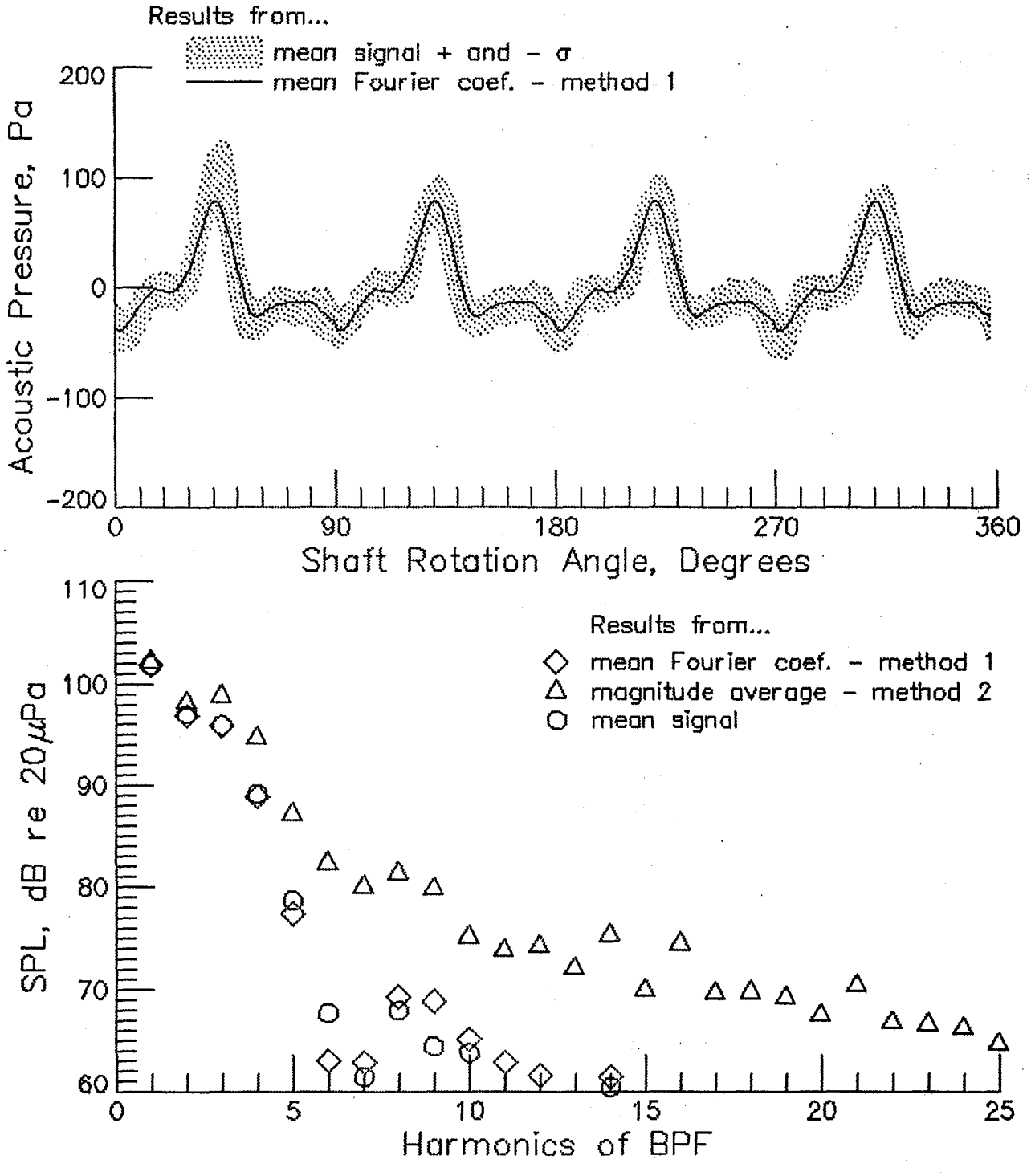

(a) microphone 1

Figure 11. - Run 84+4 . BPF= 665.9 Hz. RPM= 9988.9. U_{Tip}=701.7 fps.

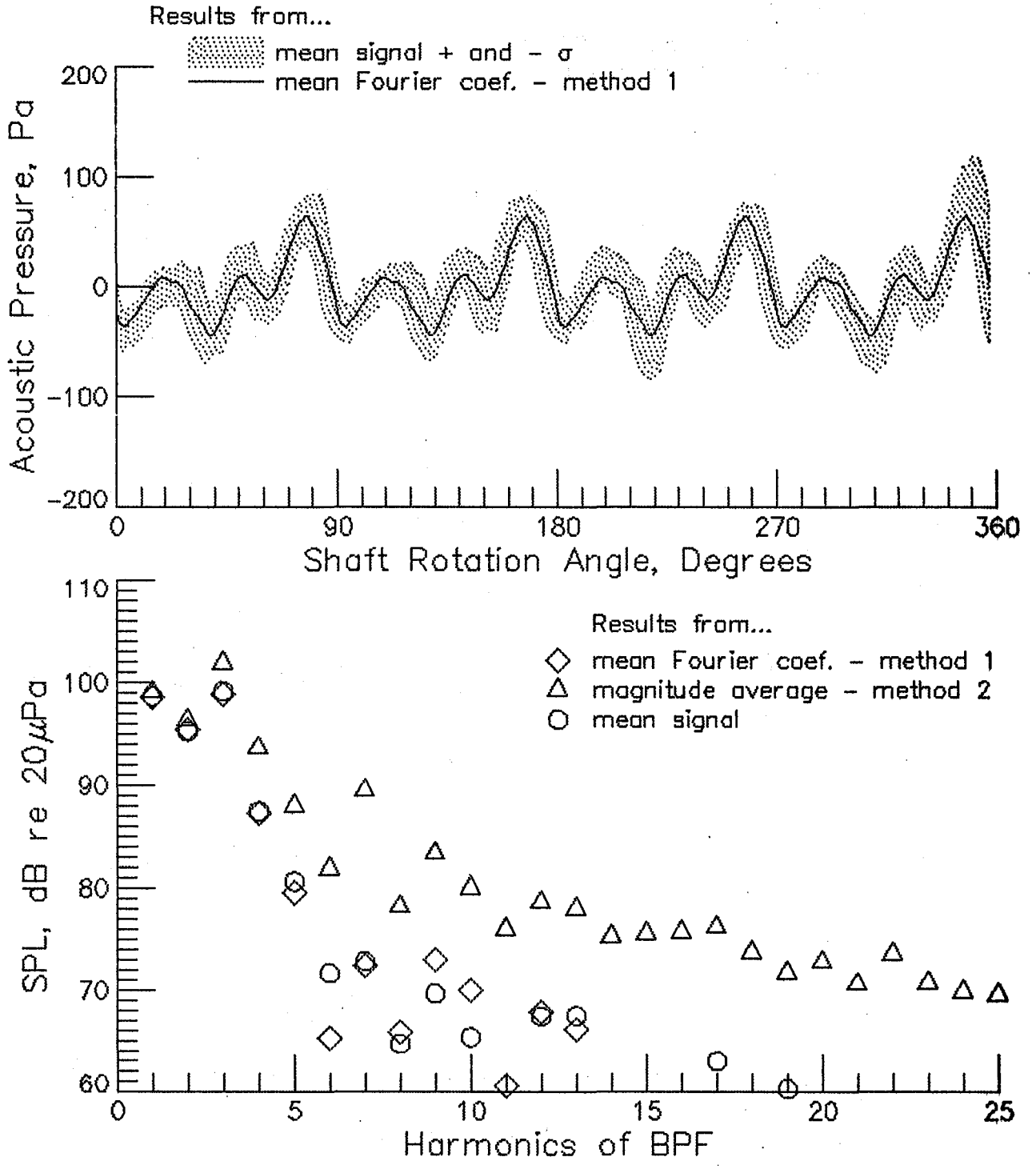

(b) microphone 2

Figure 11. - Continued.

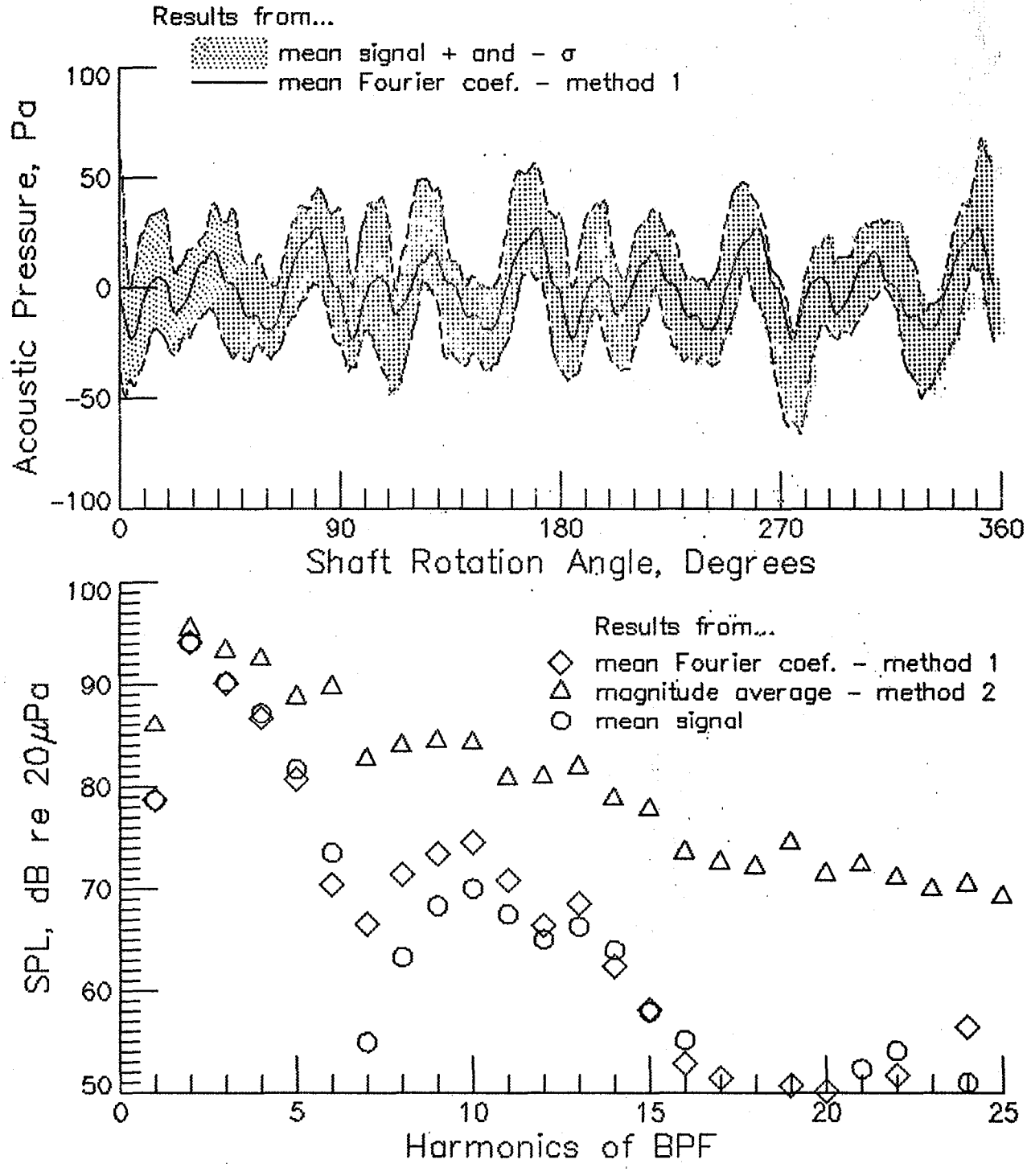

(c) microphone 3

Figure 11. - Continued.

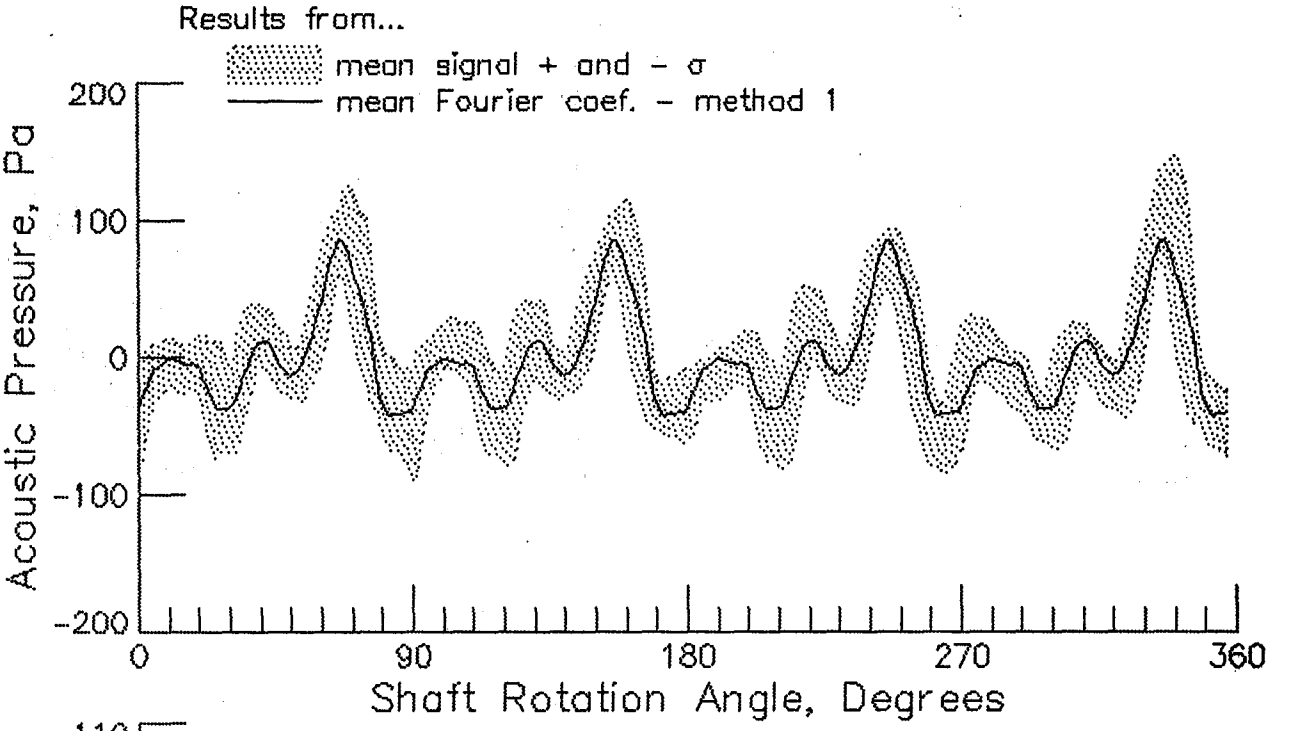

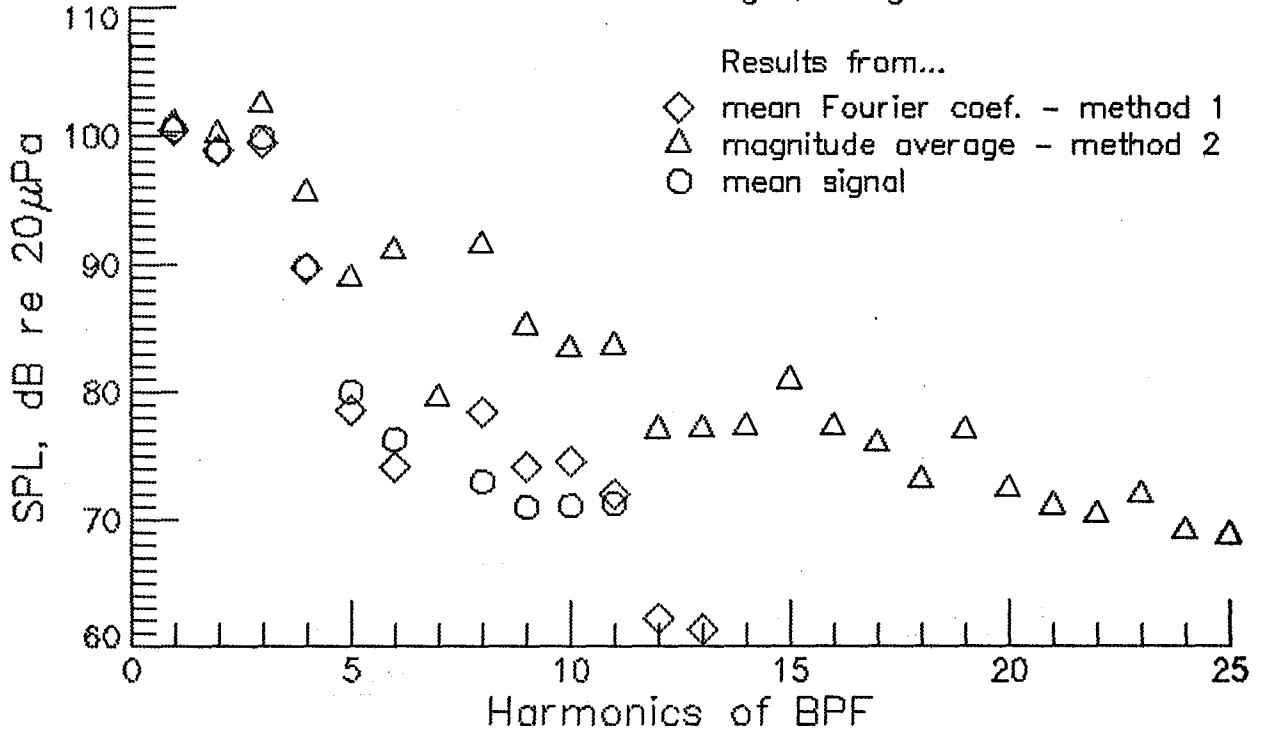

(d) microphone 4

Figure 11. - Continued.

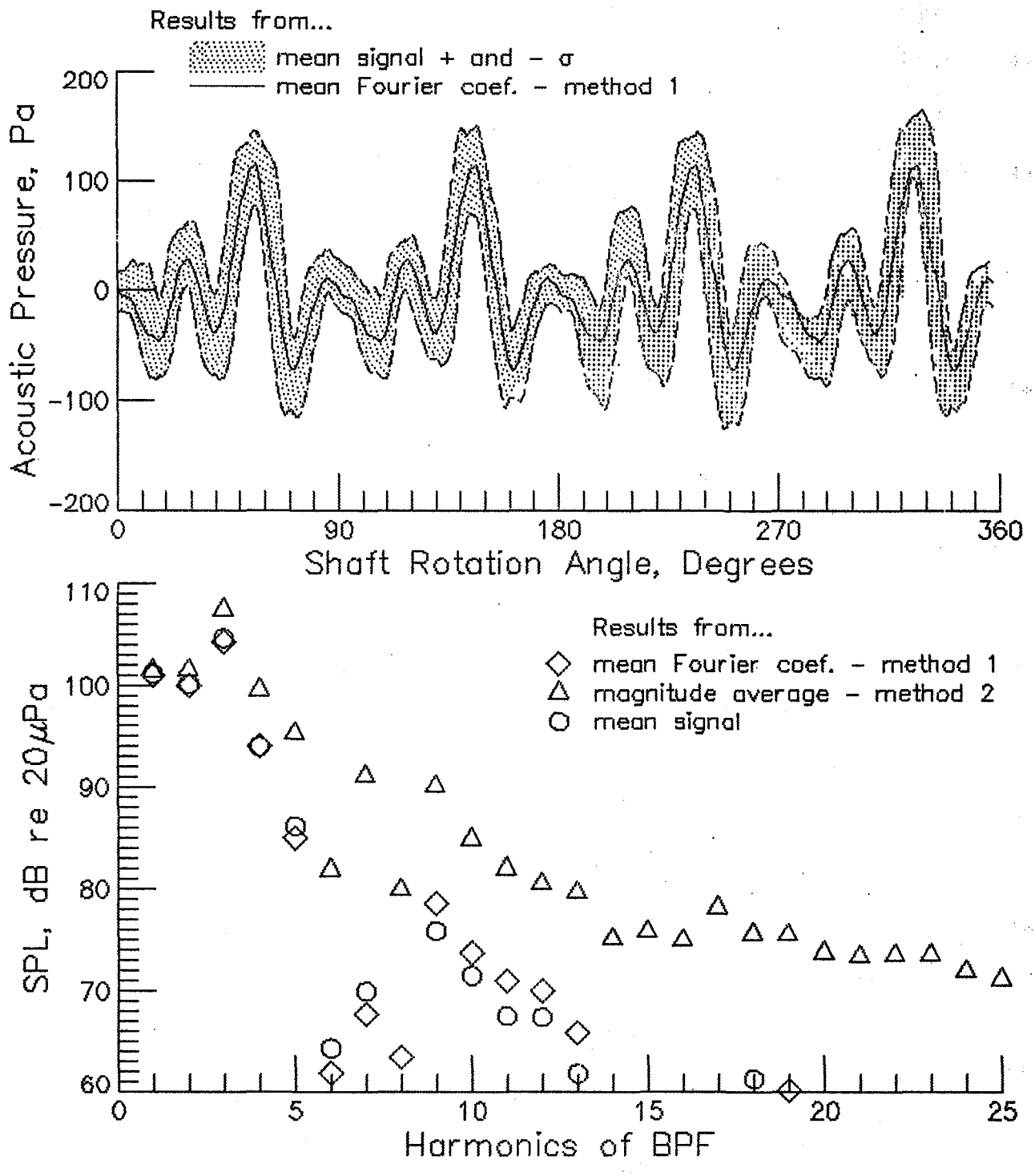

(e) microphone 5

Figure 11. - Continued.

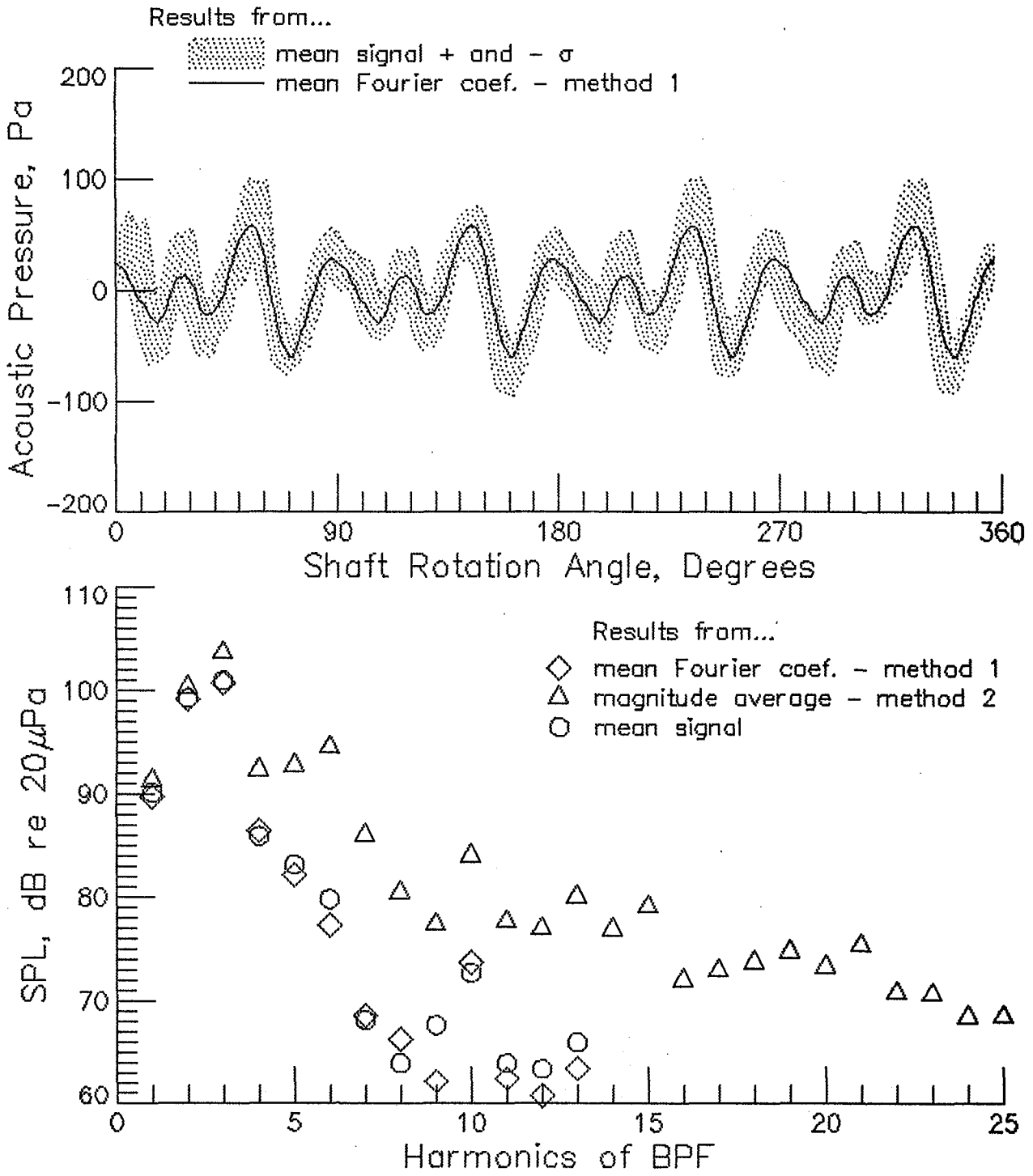

(f) microphone 6

Figure 11. - Continued.

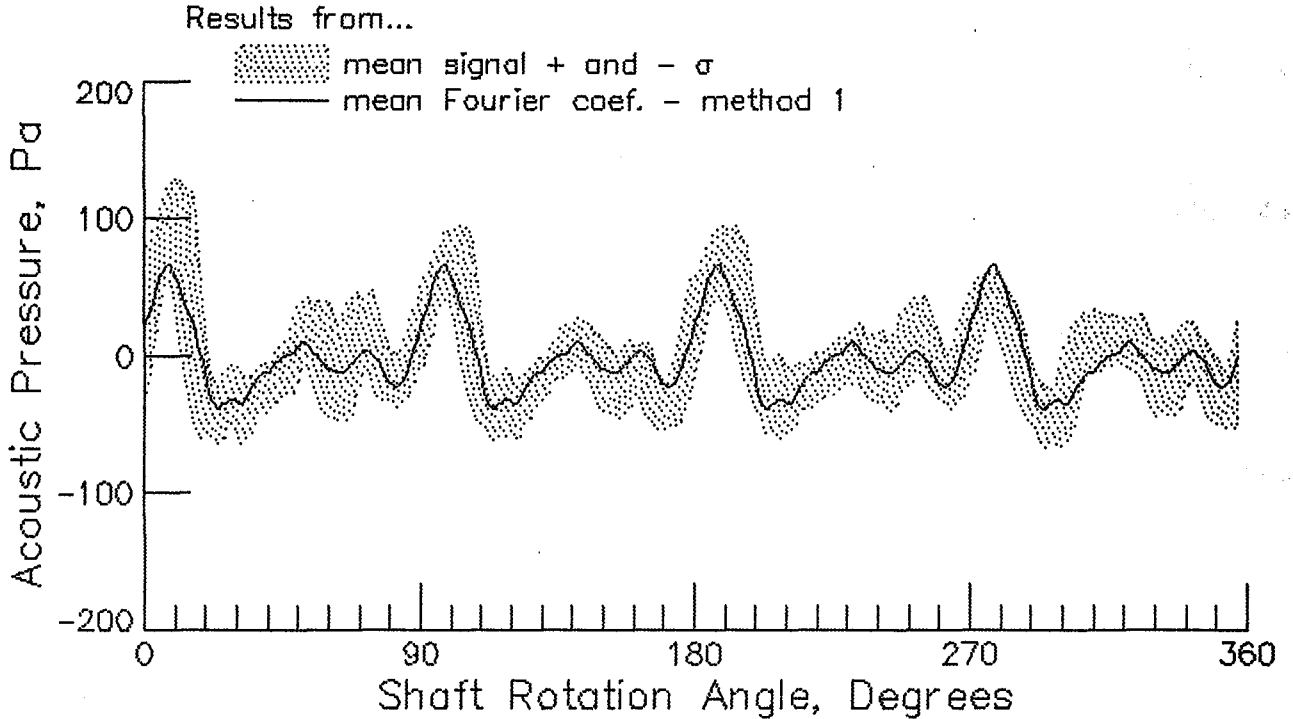

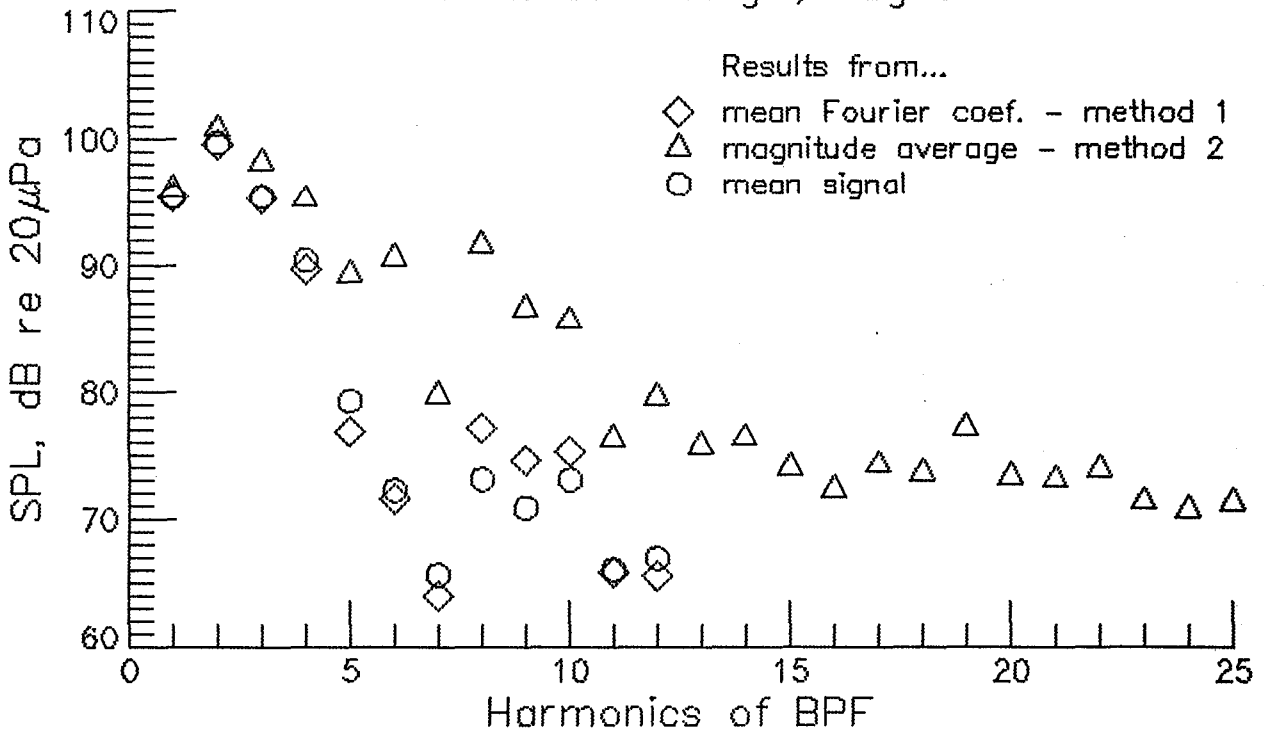

(g) microphone 7

Figure 11. - Continued.

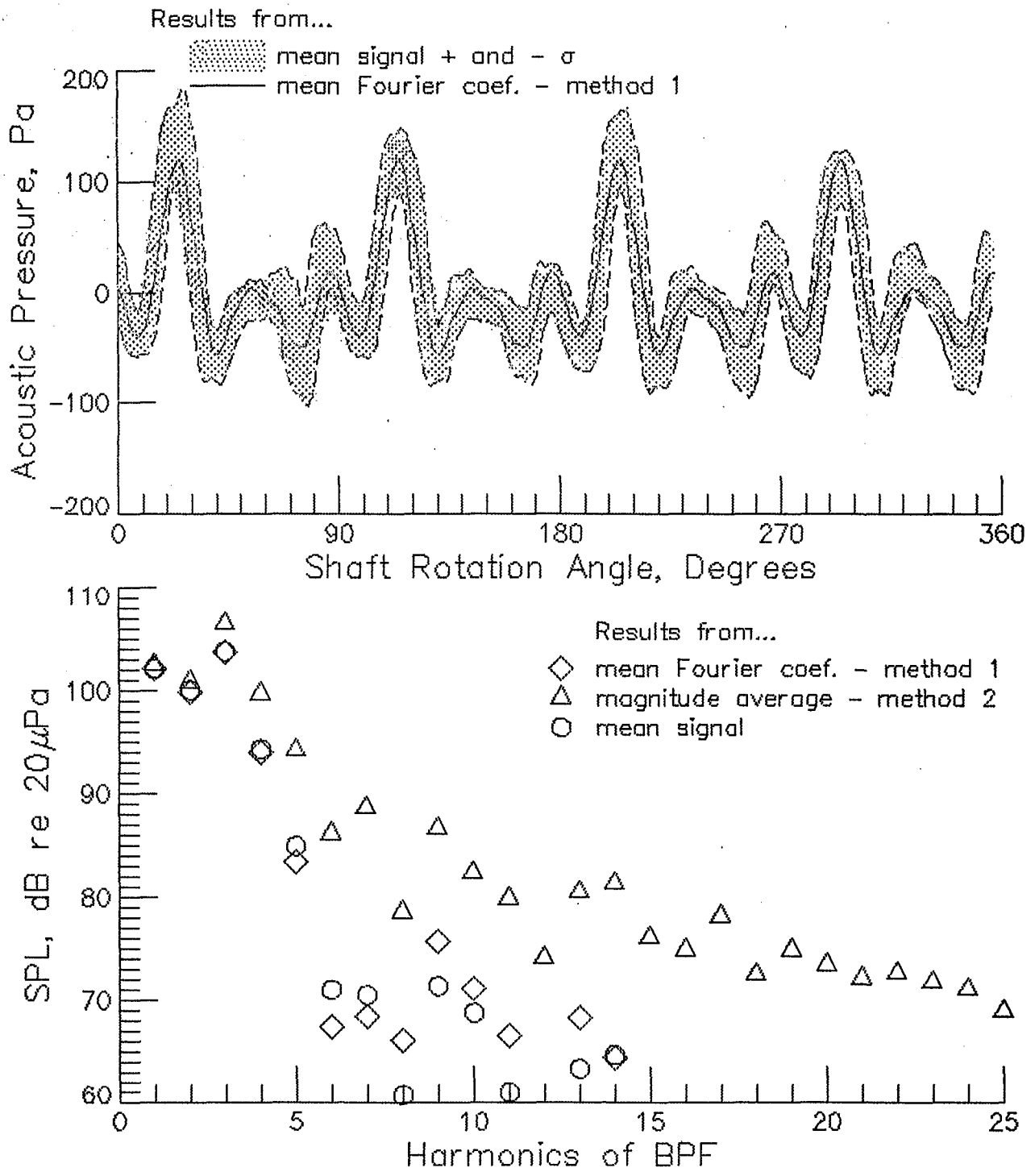

(h) microphone 8

Figure 11. - Continued.

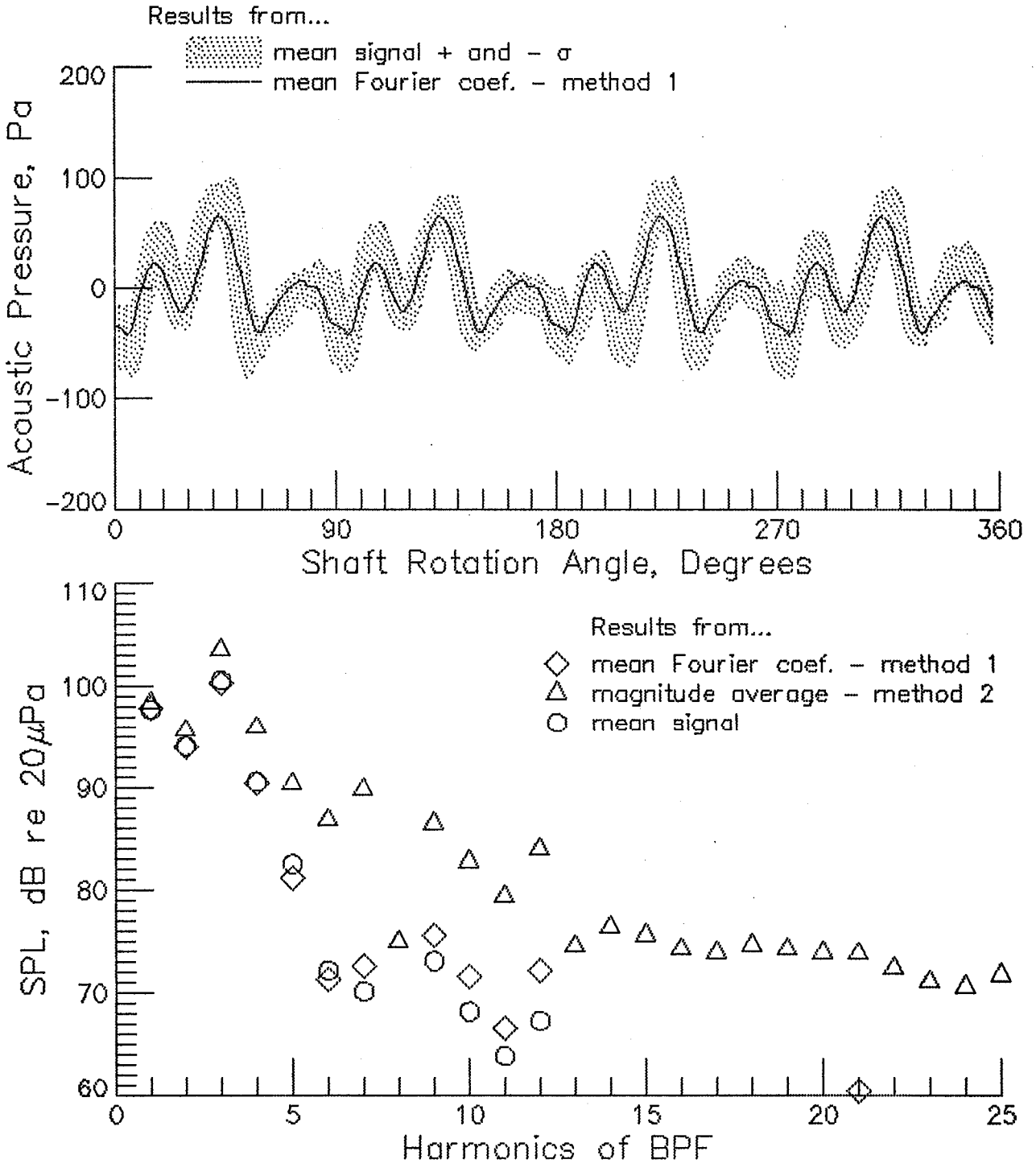

(i) microphone 9

Figure 11 - Continued.

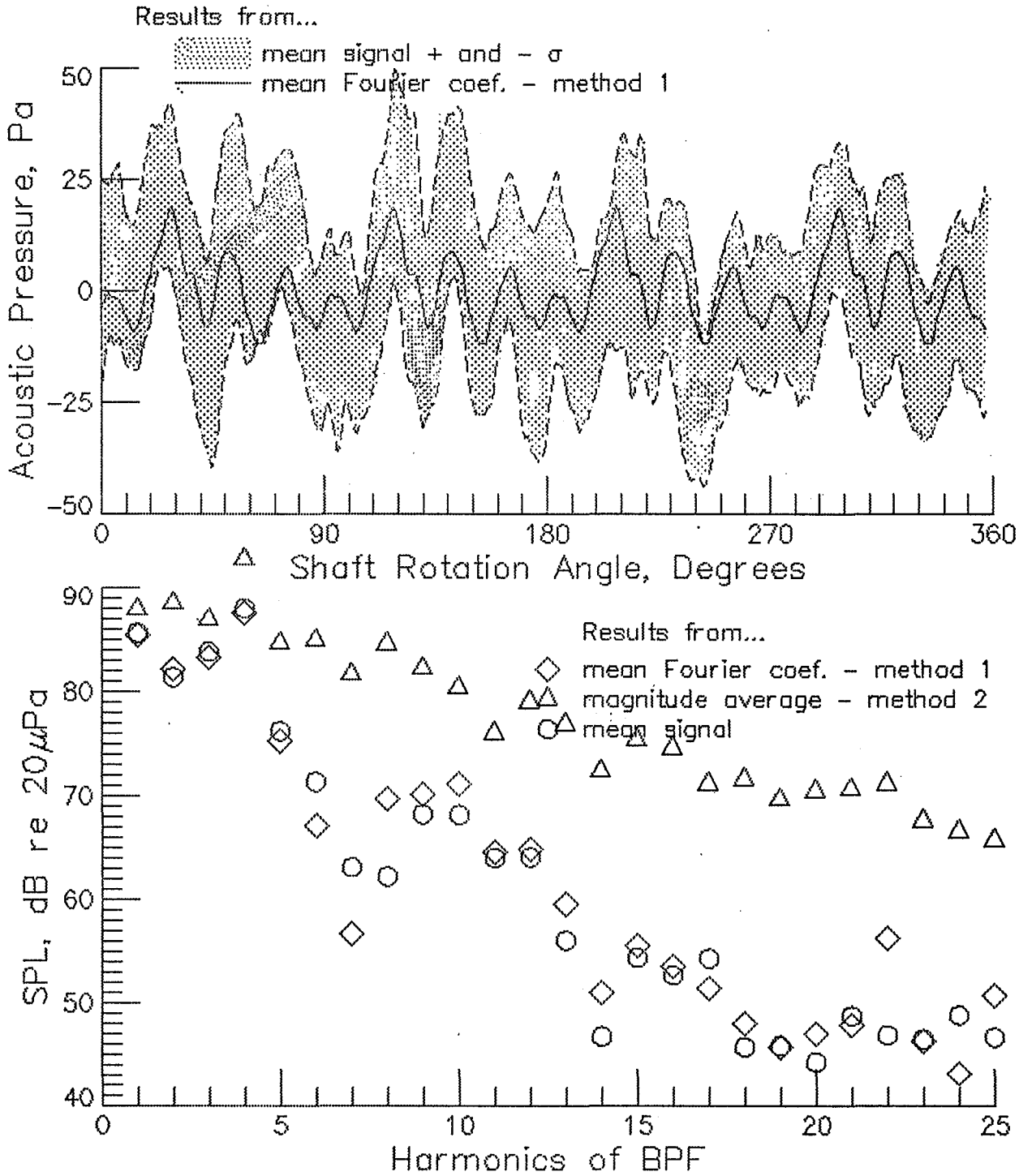

(j) microphone 10

Figure 11. - Continued.

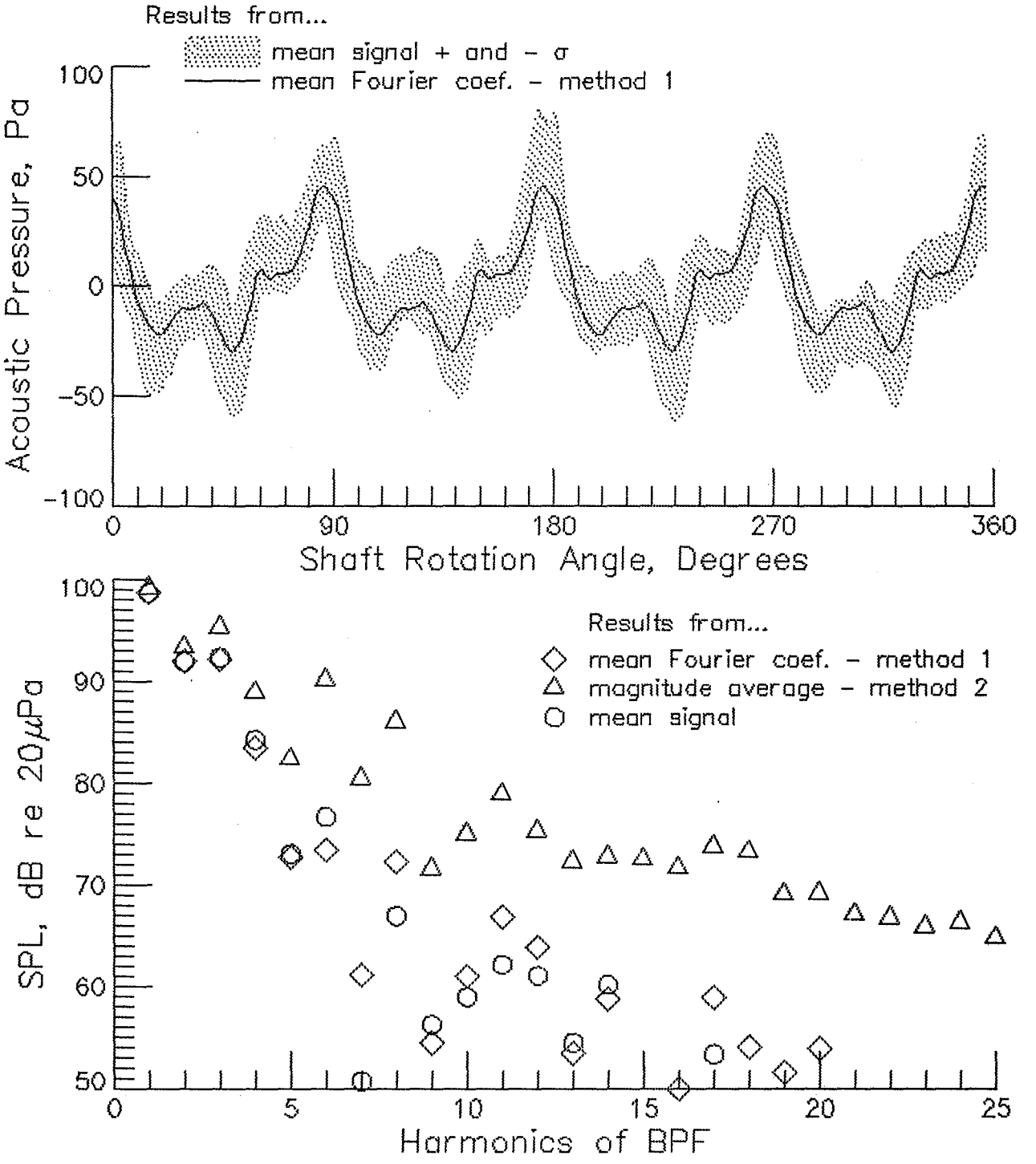

(k) microphone 11

Figure 11. - Continued.

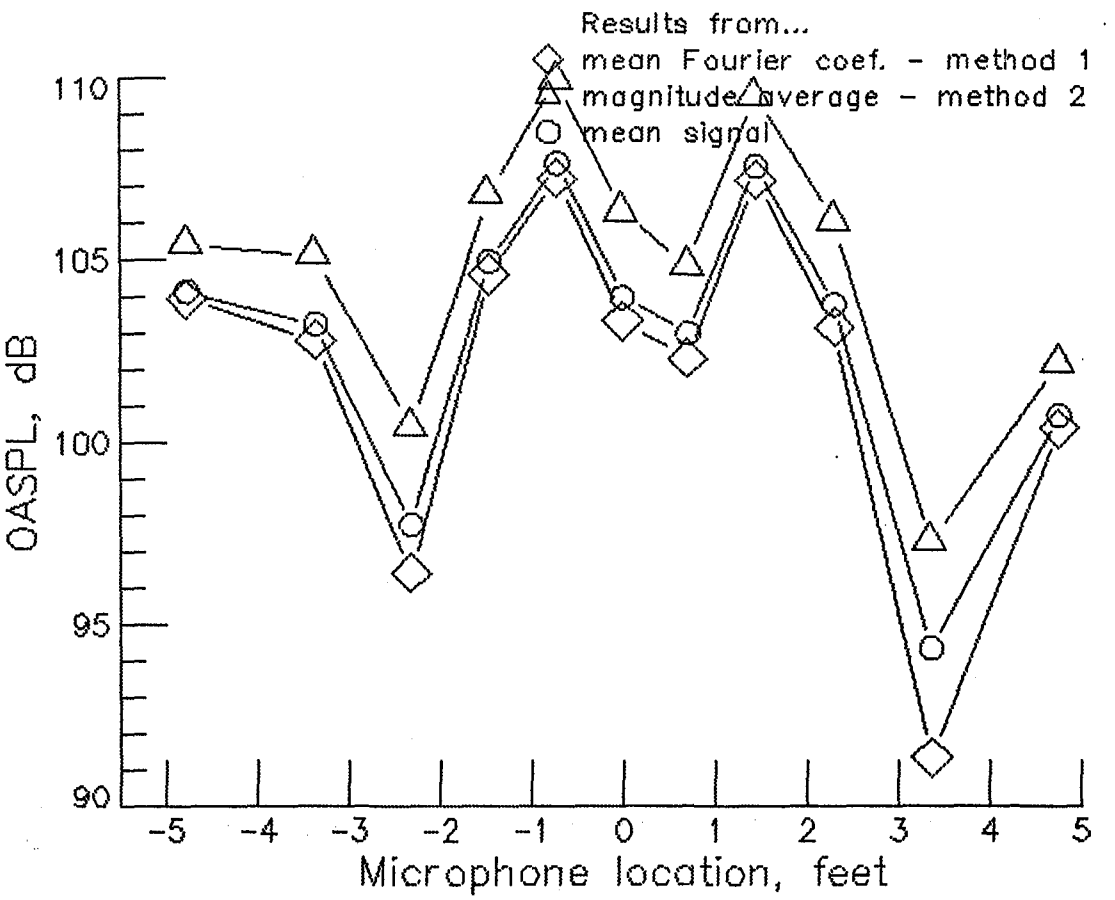

(l) Summary of Stop 4

Figure 11. - Run 84+4 . BPF= 665.9 Hz. RPM= 9988.9. U_{Tip}=701.7 fps.

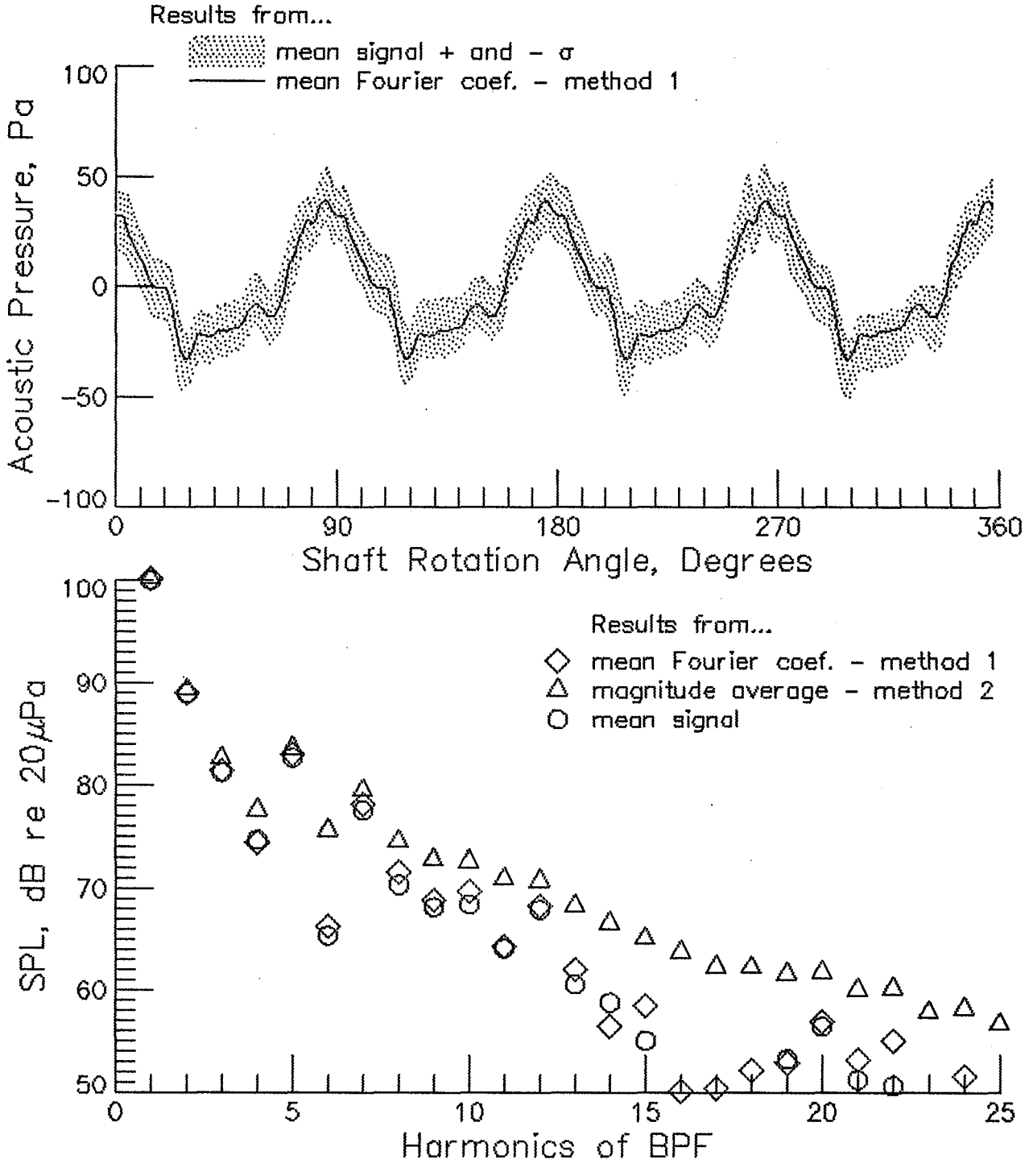

(a) microphone 1

Figure 12. - Run 132-2. BPF= 670.9 Hz. RPM=10063.2. U_{Tip}=742.1 fps.

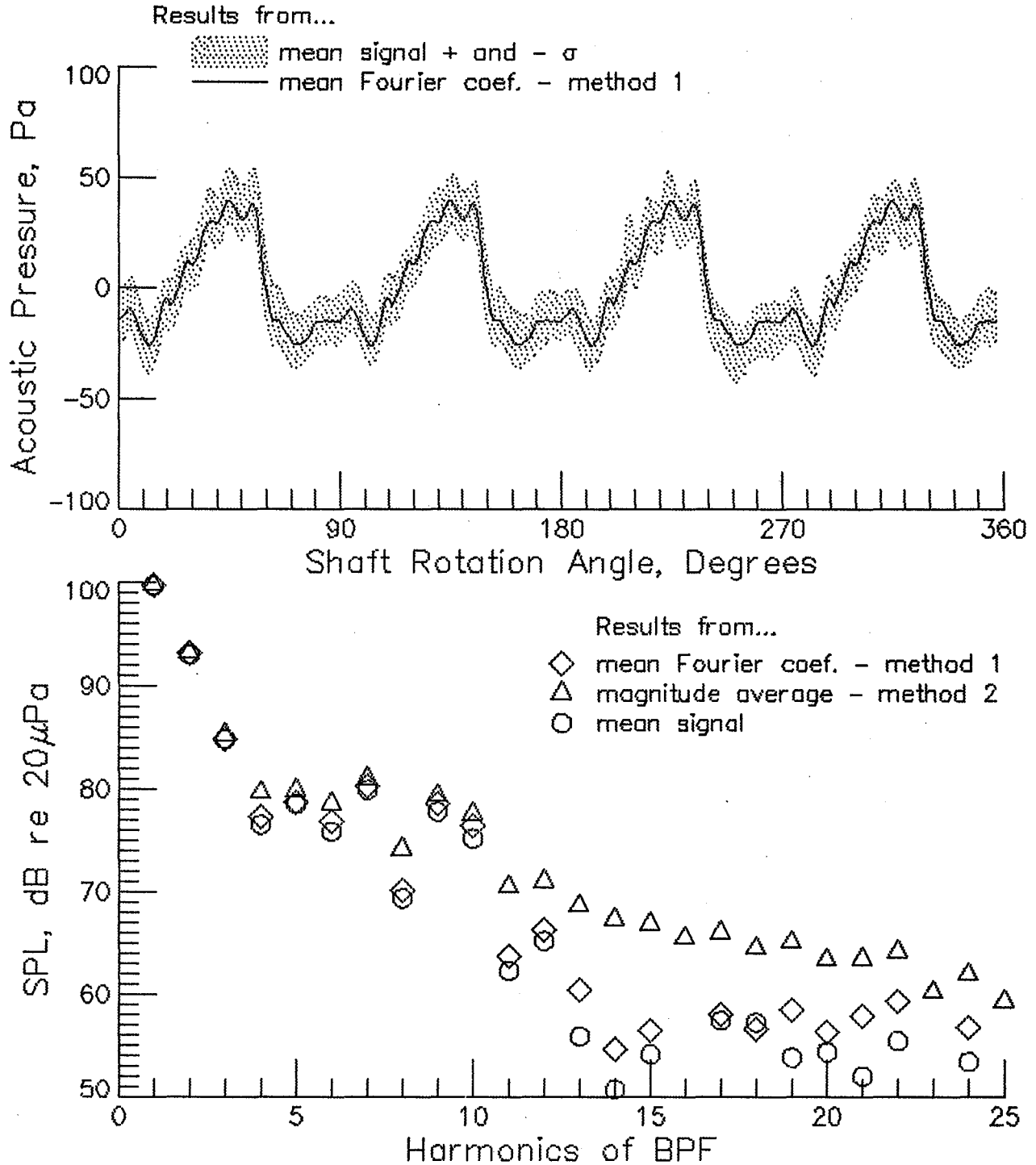

(b) microphone 2

Figure 12. - Continued.

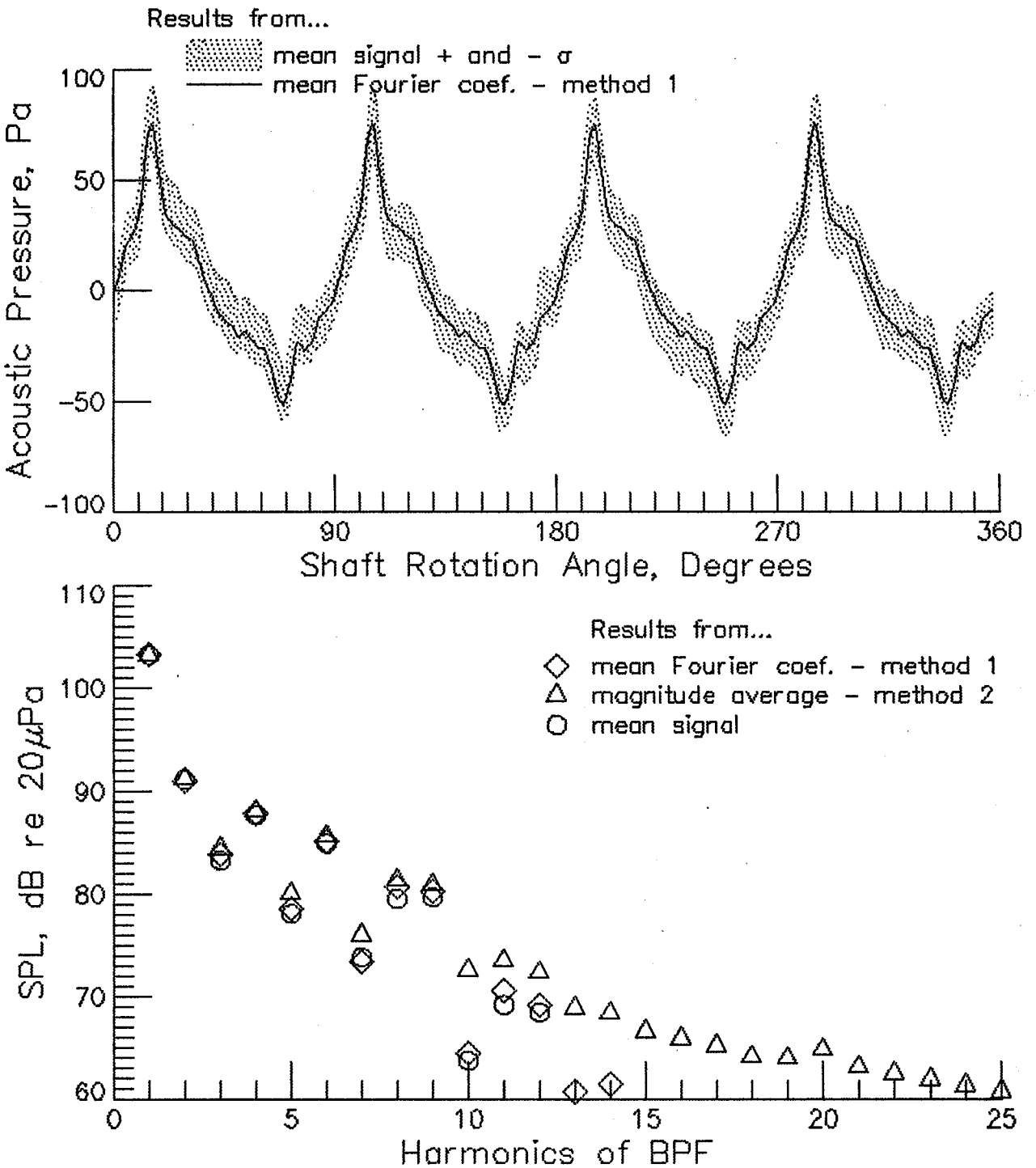

(c) microphone 3

Figure 12. - Continued.

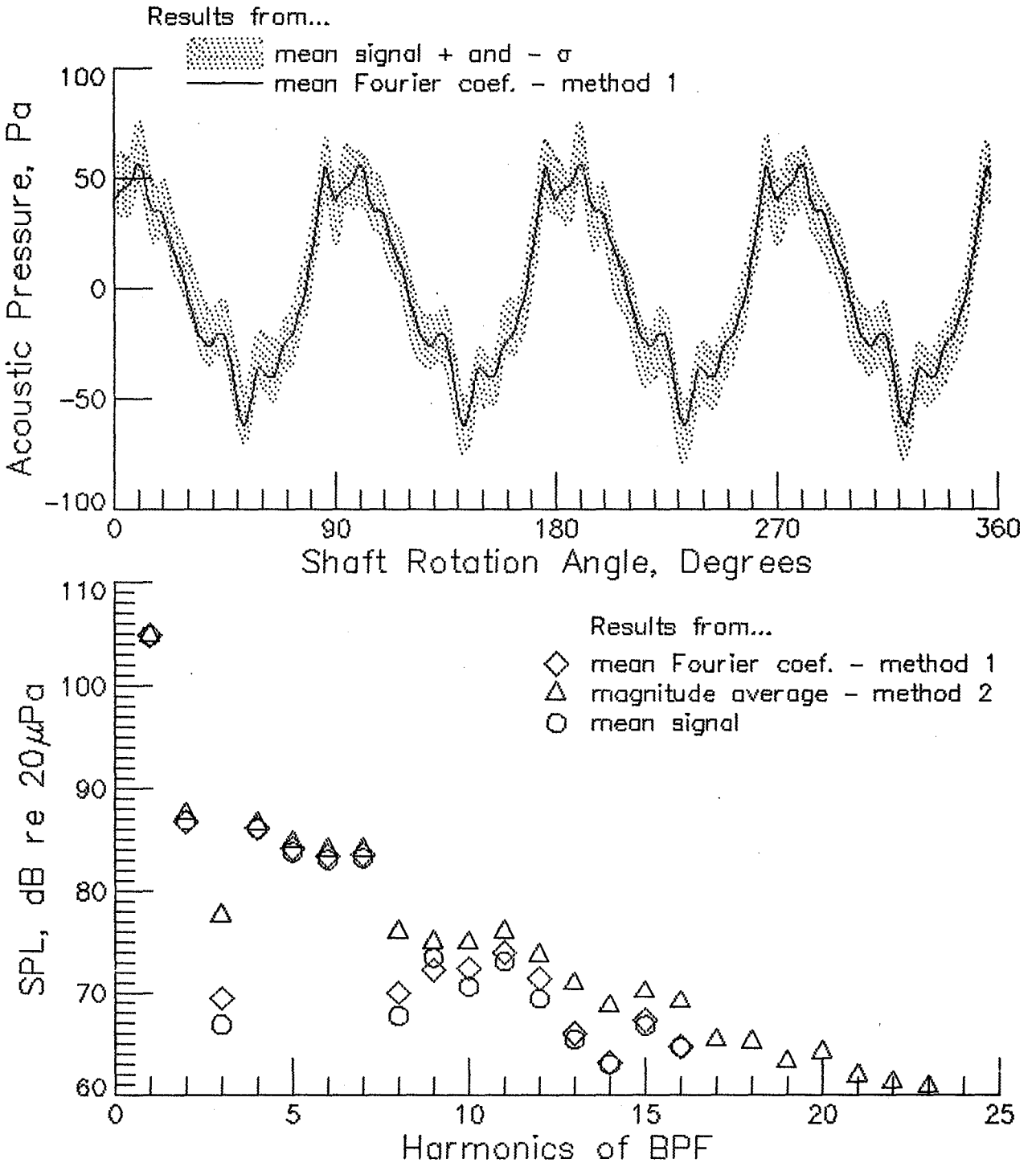

(d) microphone 4

Figure 12. - Continued.

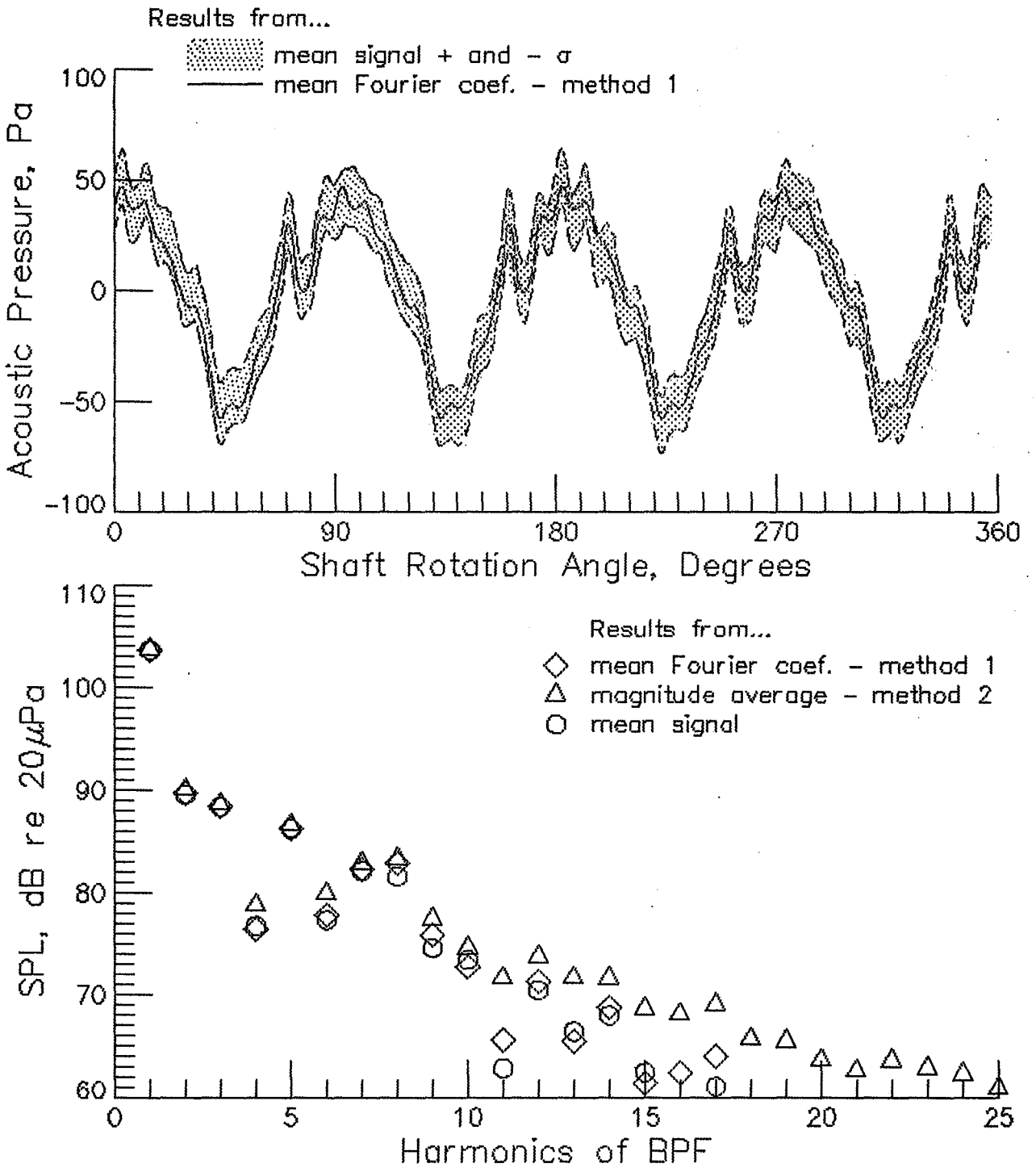

(e) microphone 5

Figure 12 - Continued.

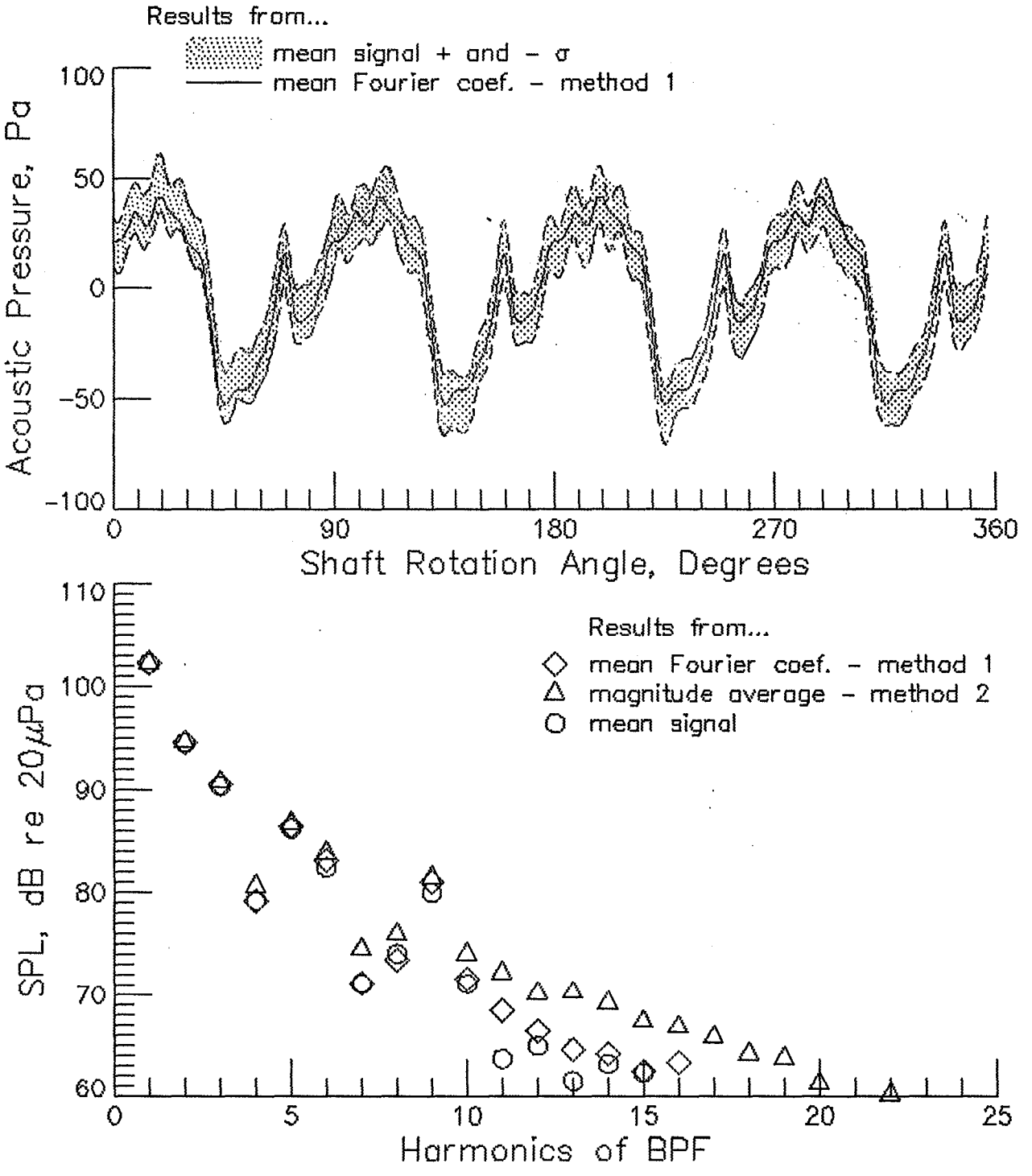

(f) microphone 6

Figure 12 - Continued.

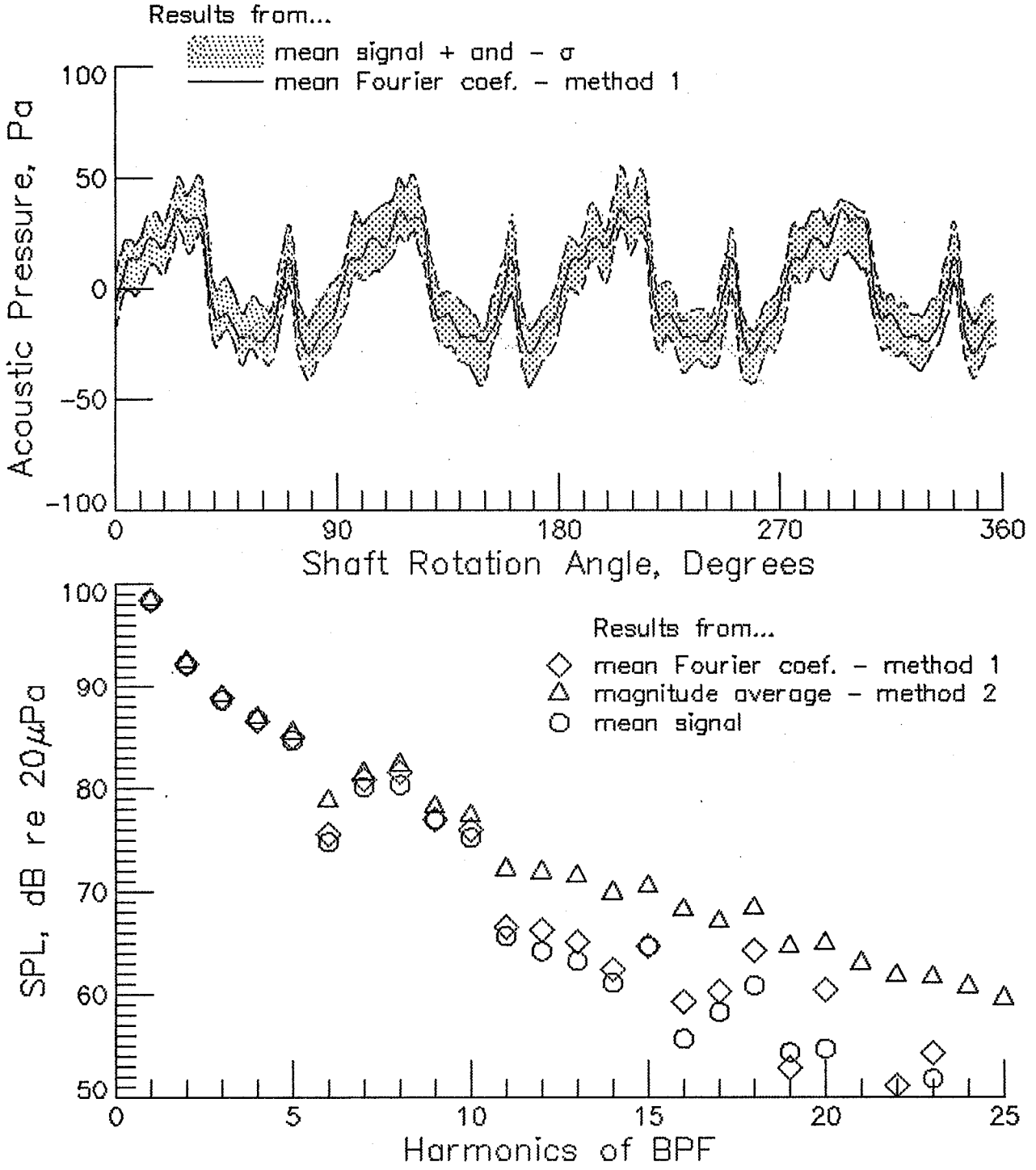

(g) microphone 7

Figure 12. - Continued.

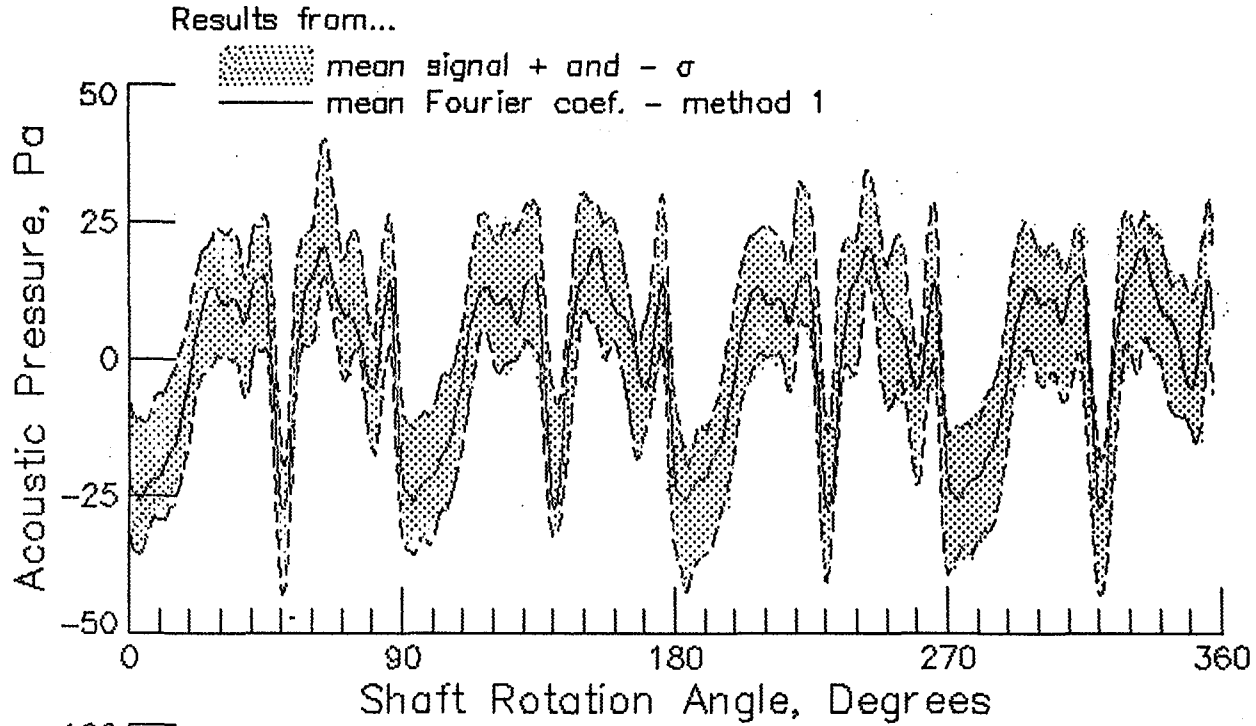

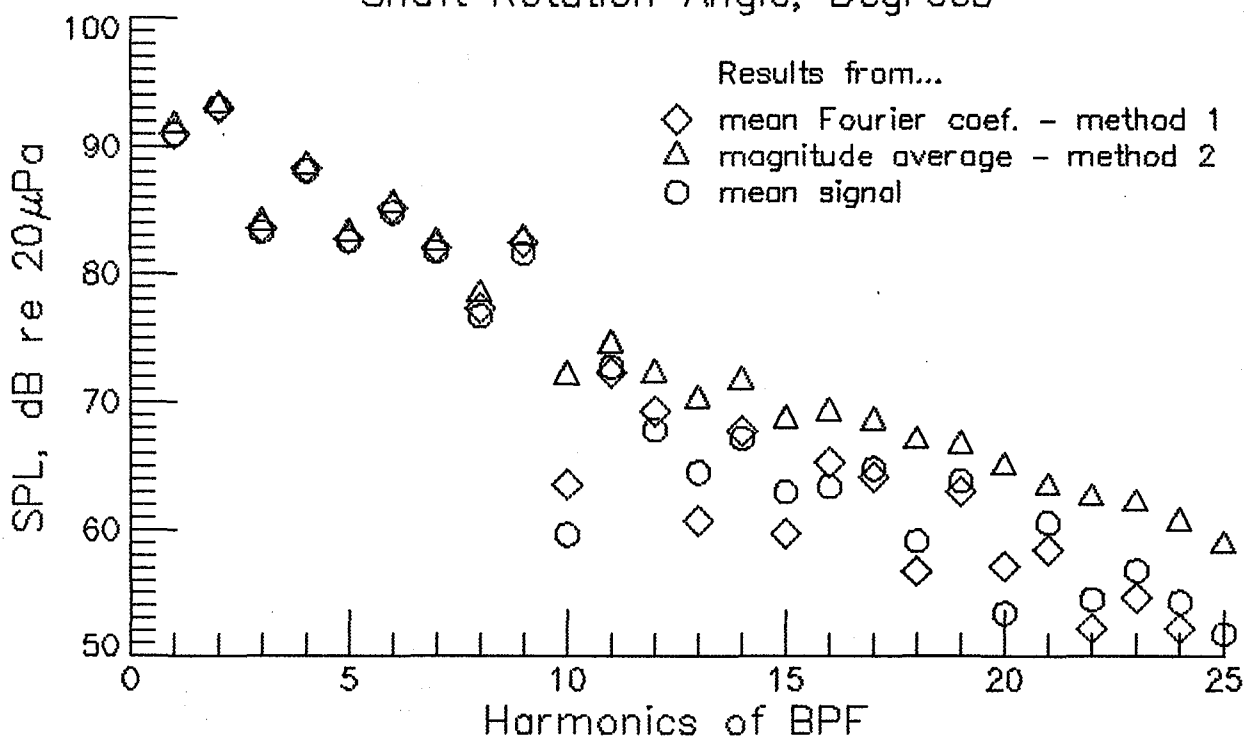

(h) microphone 8

Figure 12. - Continued.

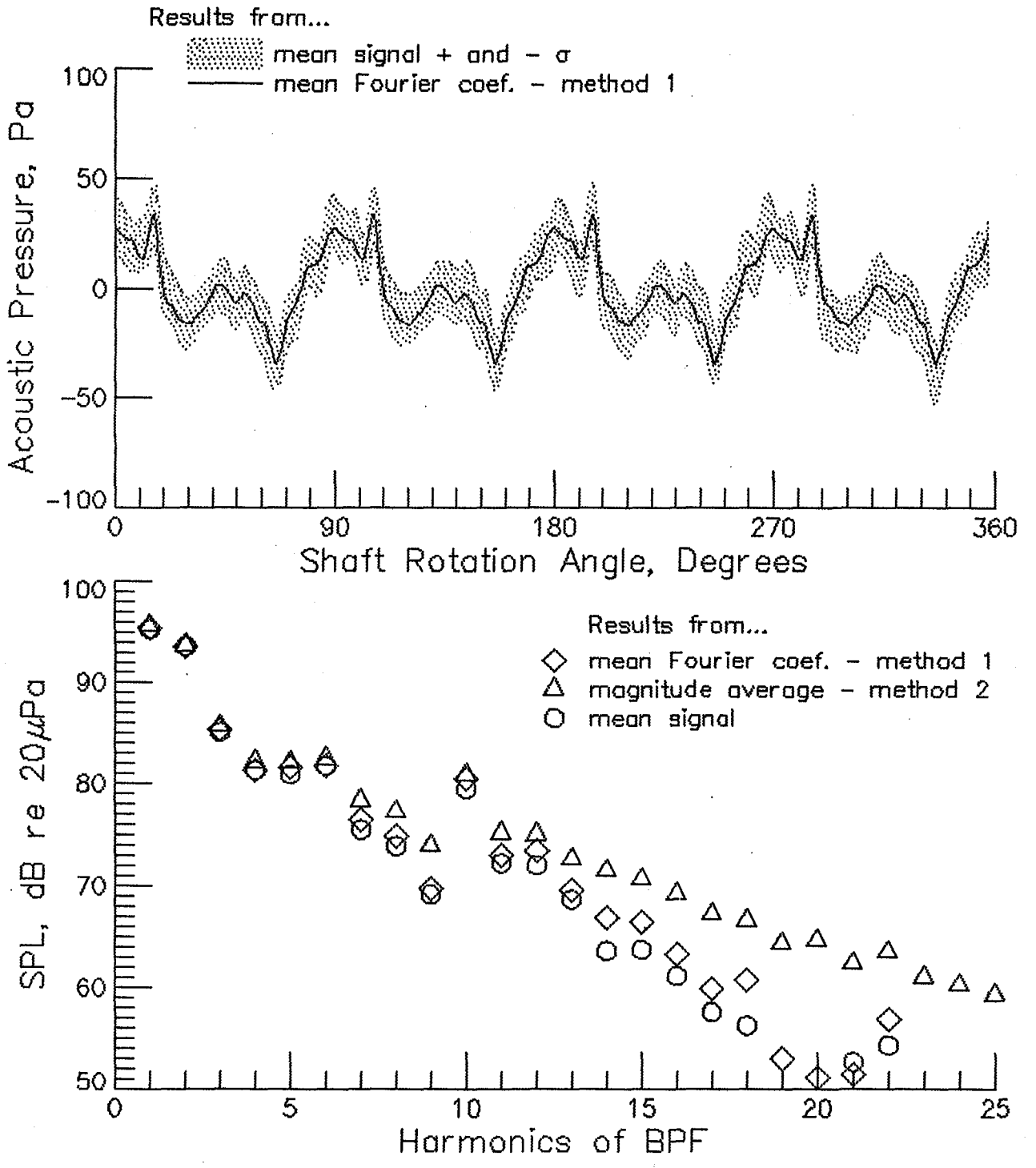

(l) microphone 9

Figure 12. - Continued.

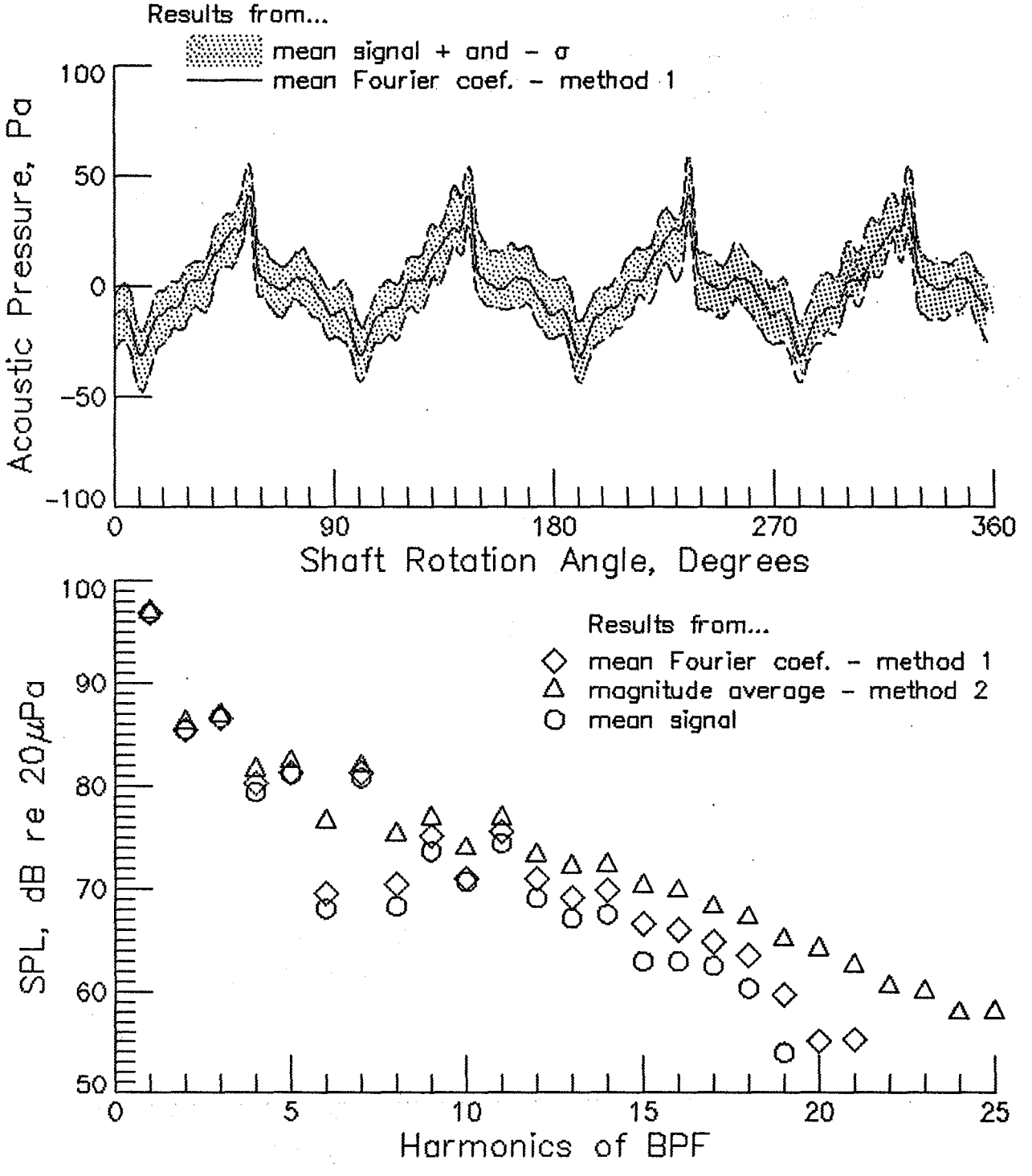

(j) microphone 10

Figure 12. - Continued.

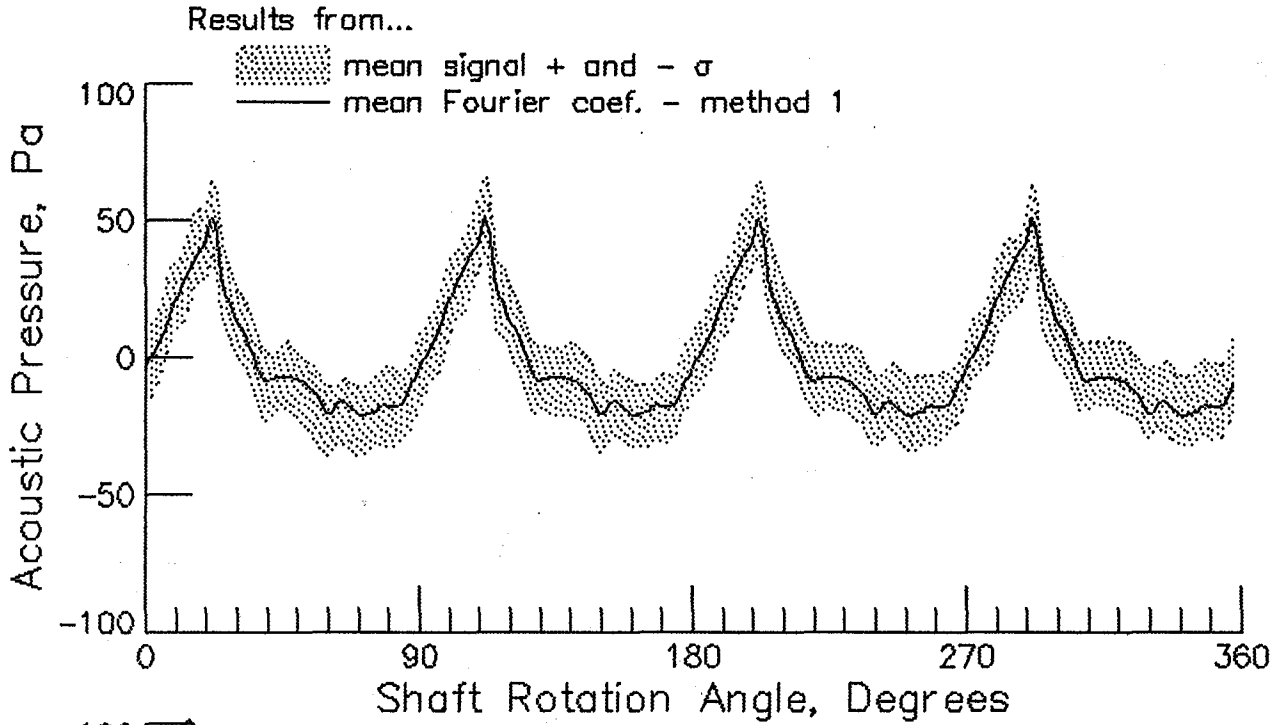

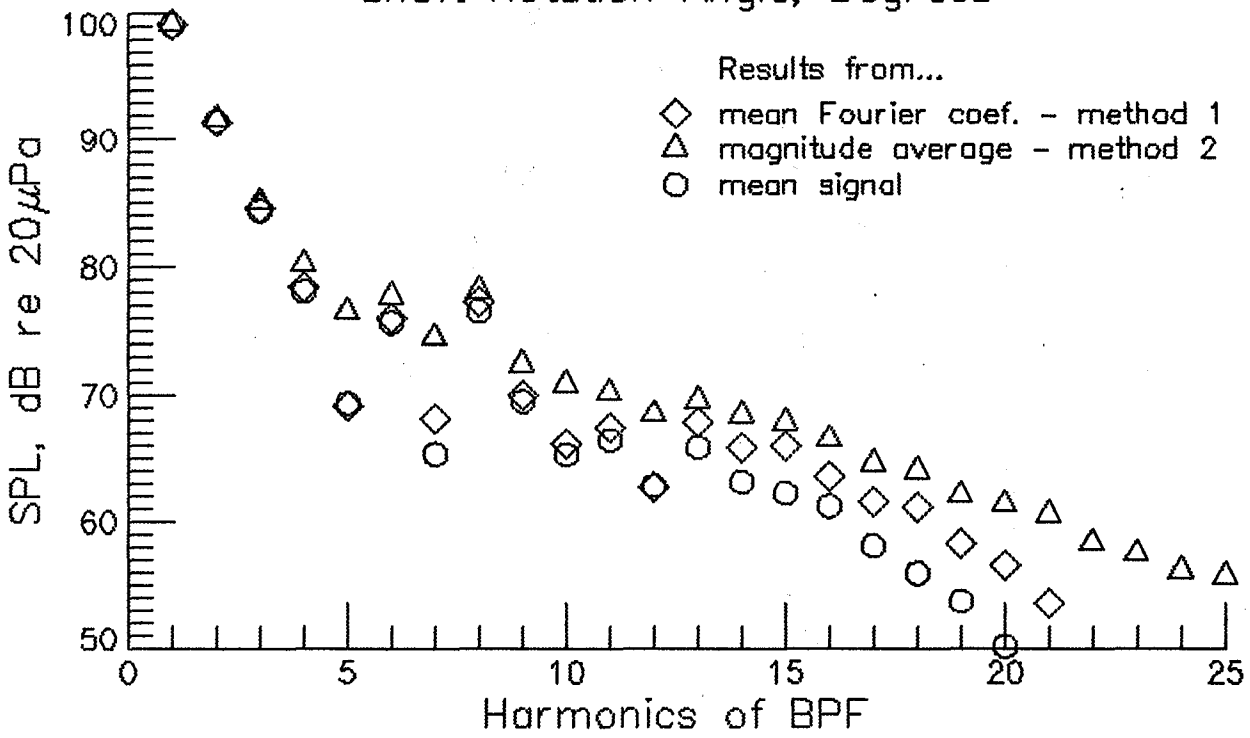

(k) microphone 11

Figure 12. - Continued.

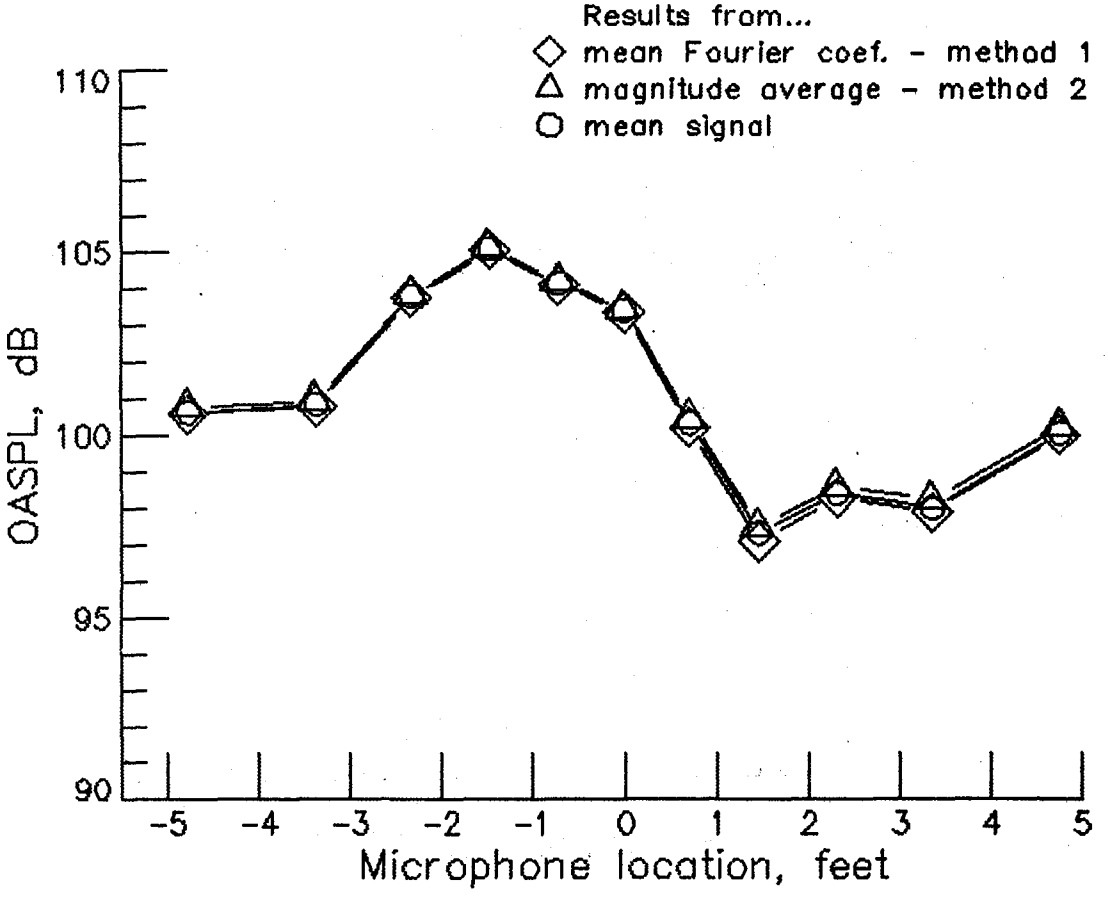

(l) Summary of Stop -2

Figure 12. - Run 132-2. BPF= 670.9 Hz. RPM=10063.2. U_{Tip}=742.1 fps.

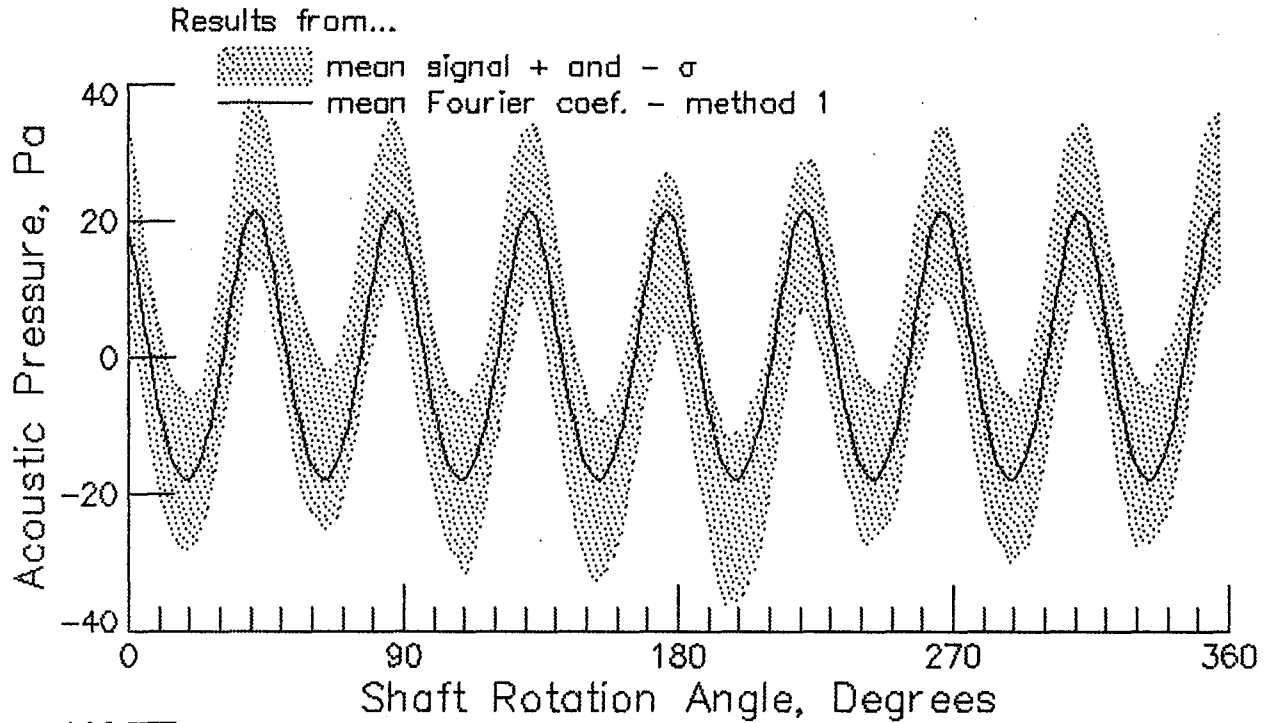

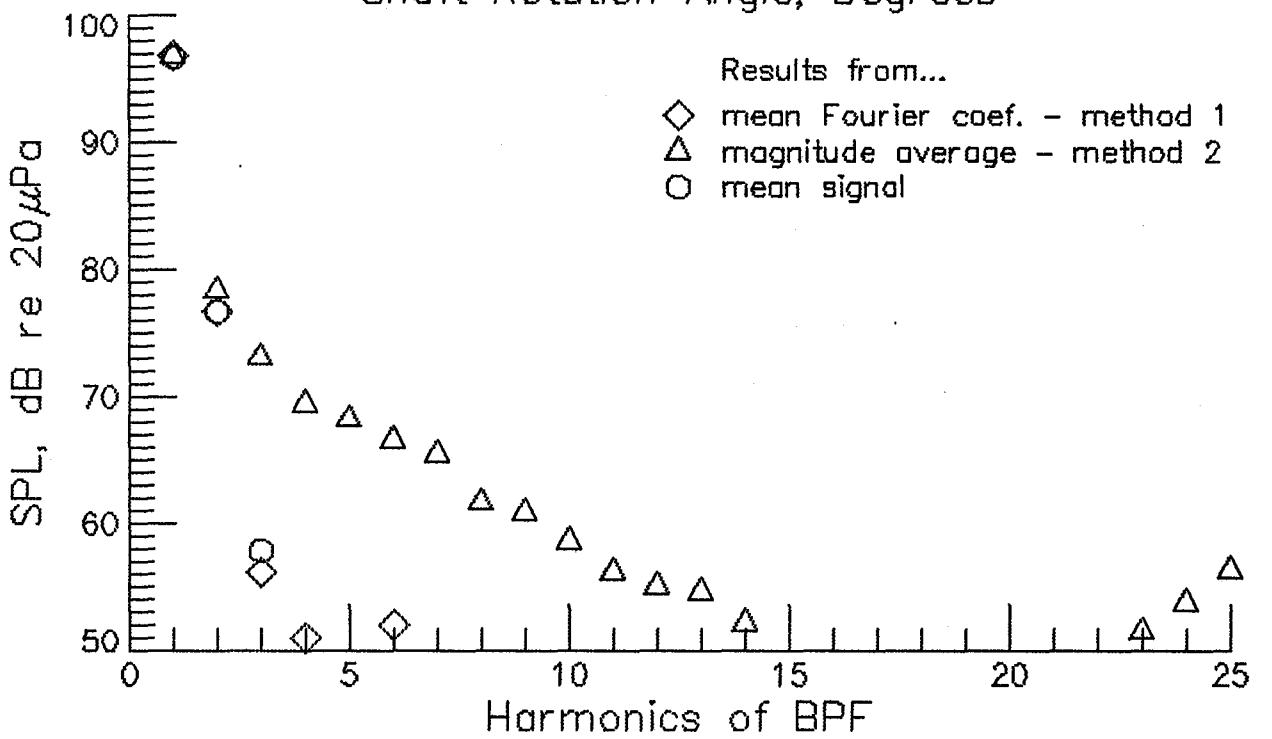

(a) microphone 1

Figure 13 - Run 141+3. BPF=1348.6 Hz. RPM=10114.6. U_{Tip}=745.9 fps.

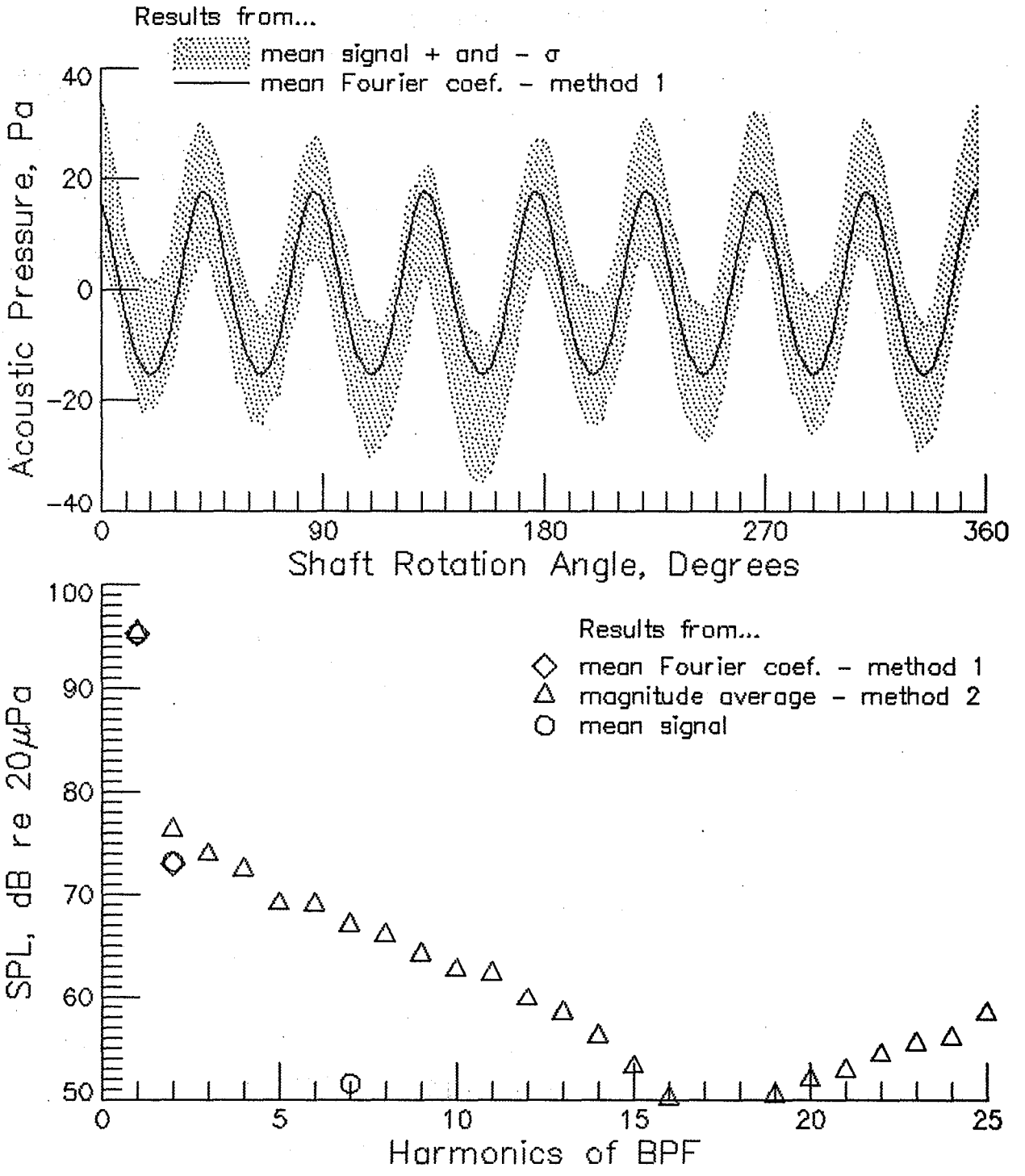

(b) microphone 2

Figure 13. - Continued.

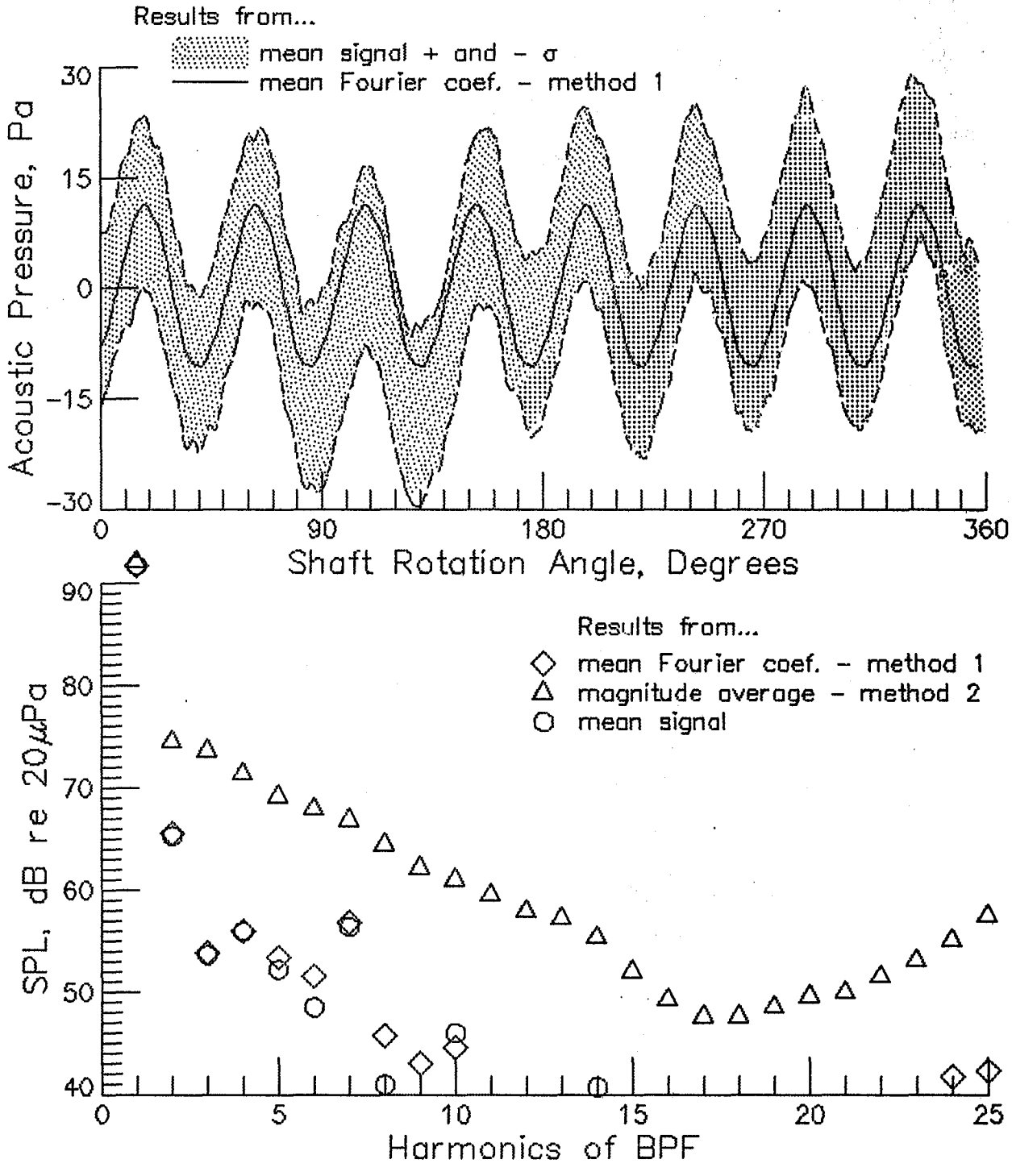

(c) microphone 3

Figure 13. - Continued.

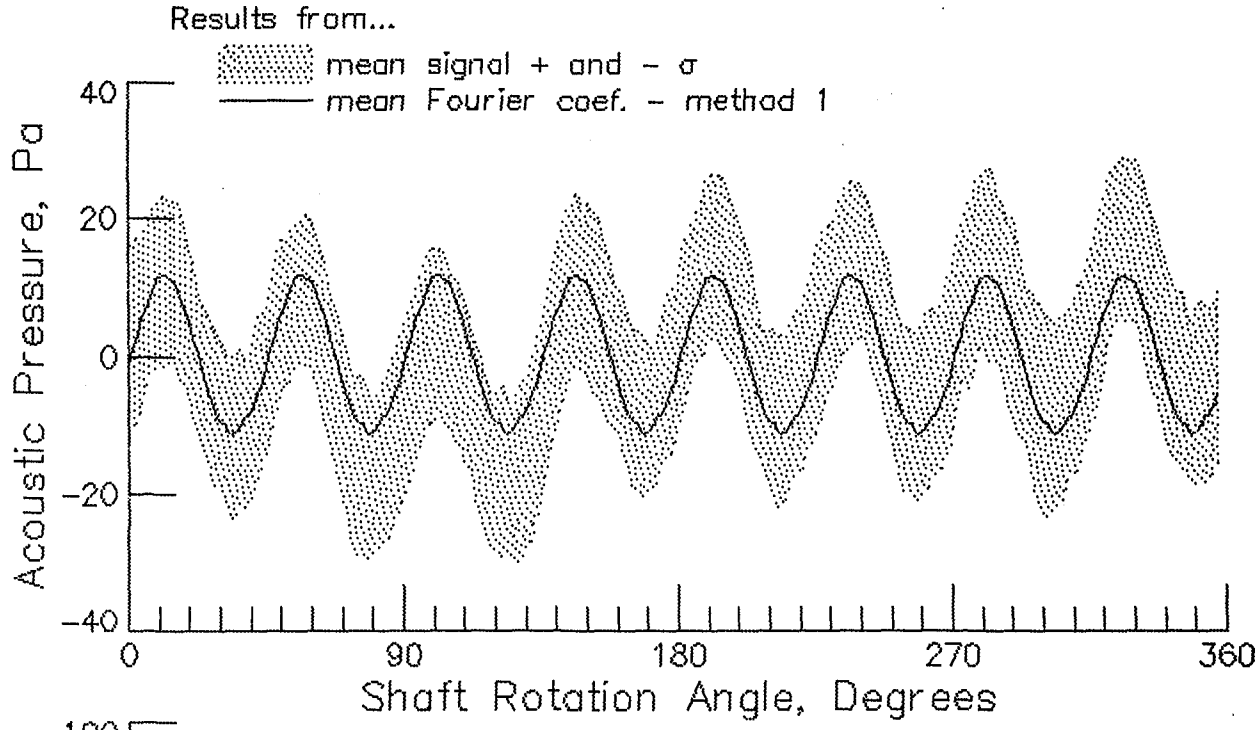

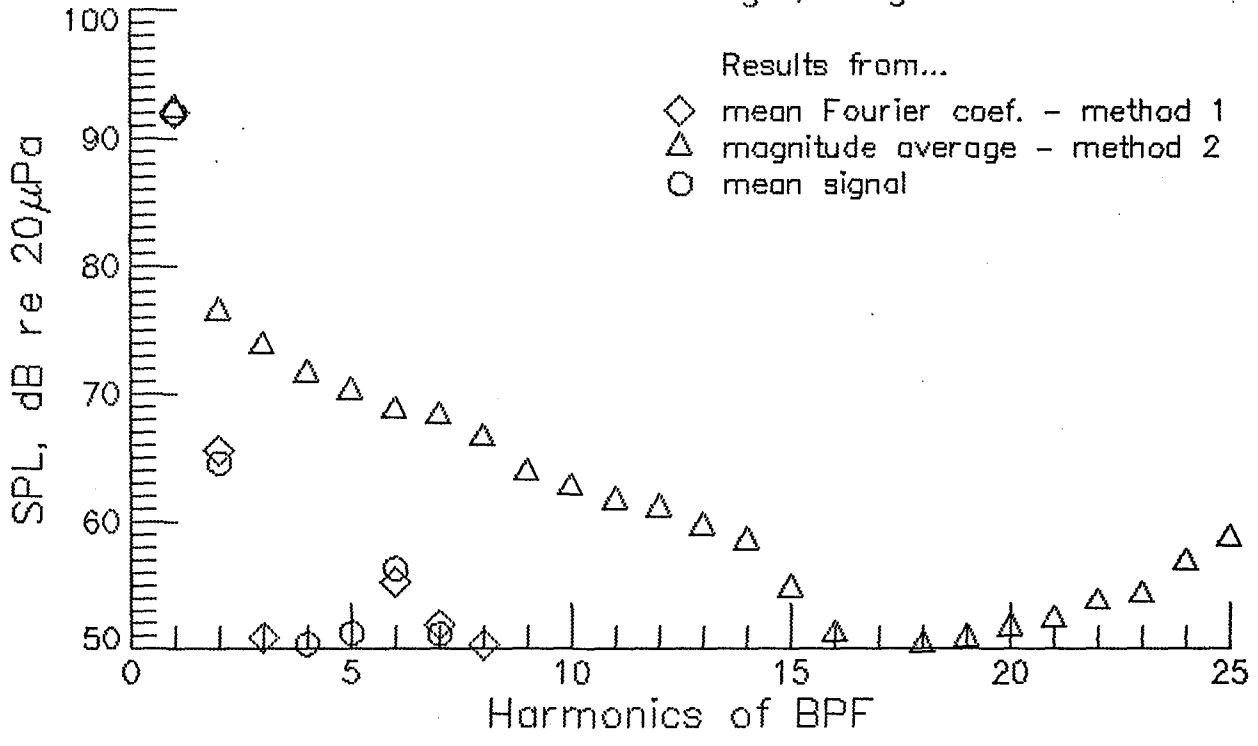

(d) microphone 4

Figure 13. - Continued.

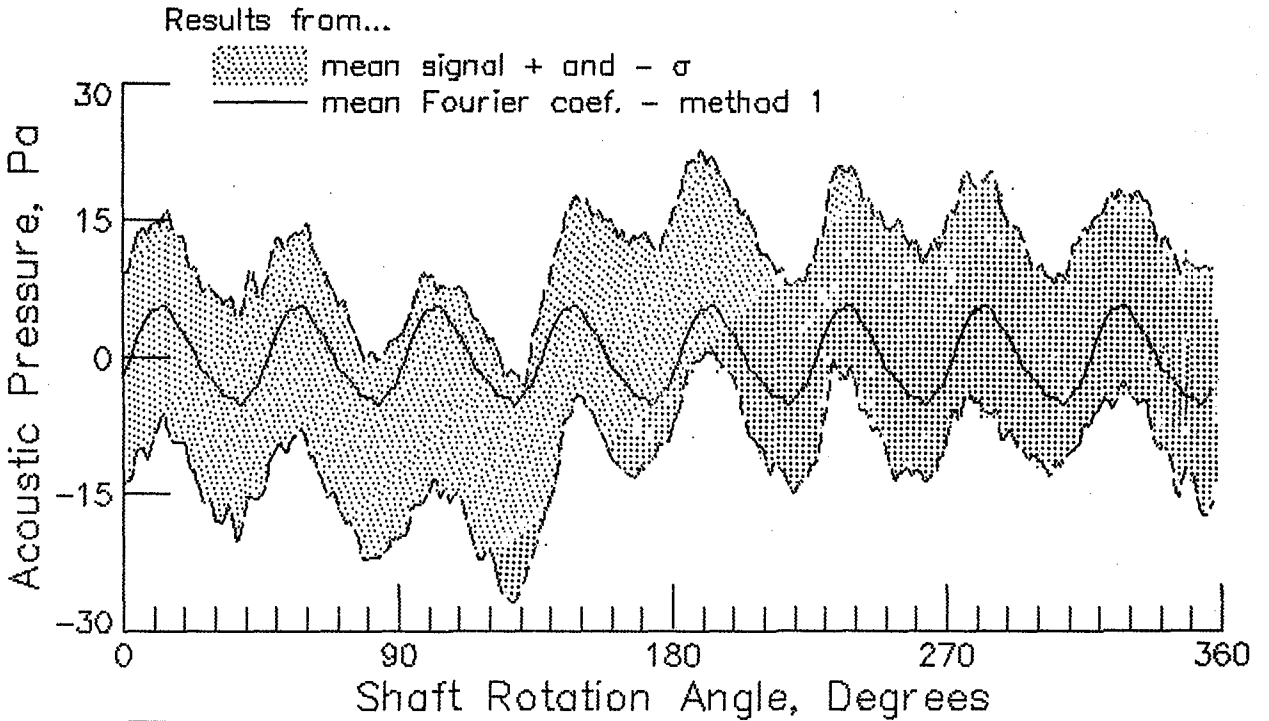

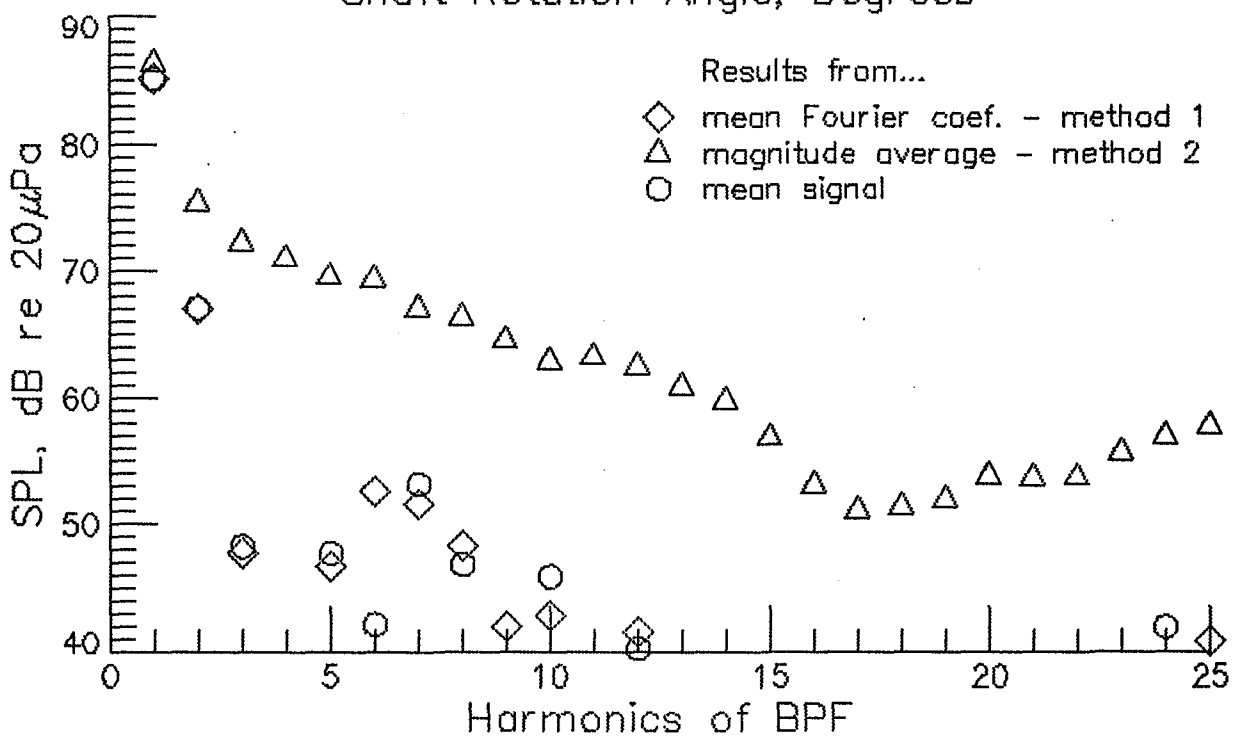

(e) microphone 5

Figure 13. - Continued.

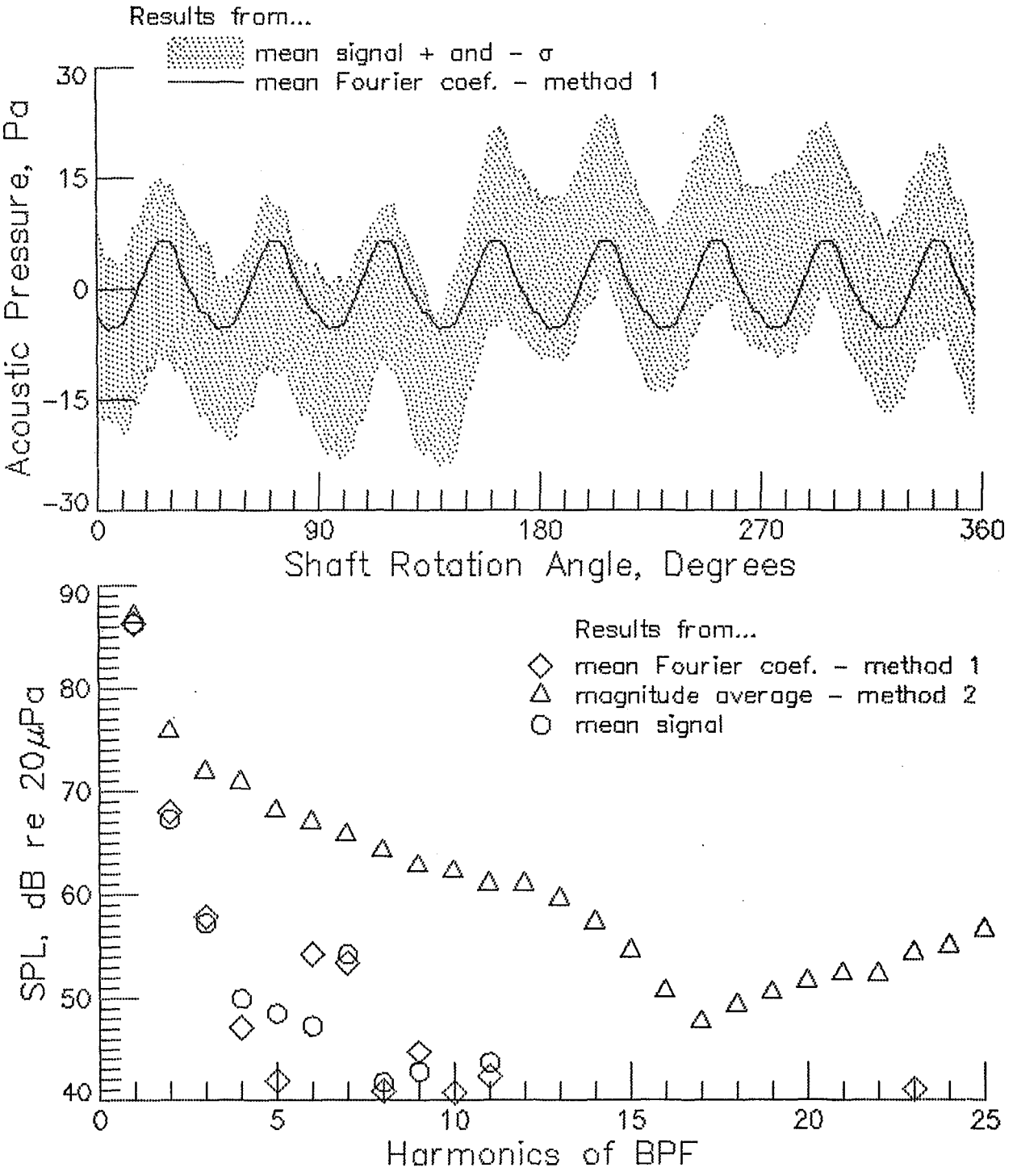

(f) microphone 6

Figure 13 - Continued.

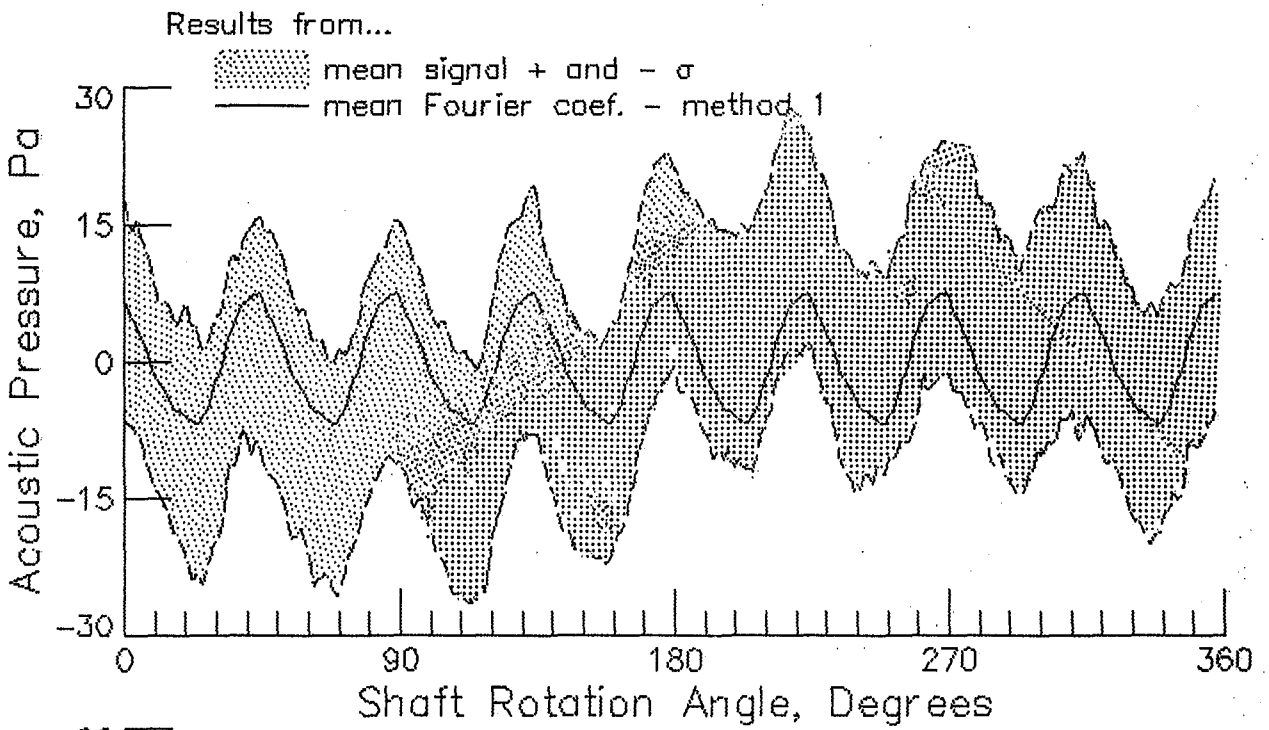

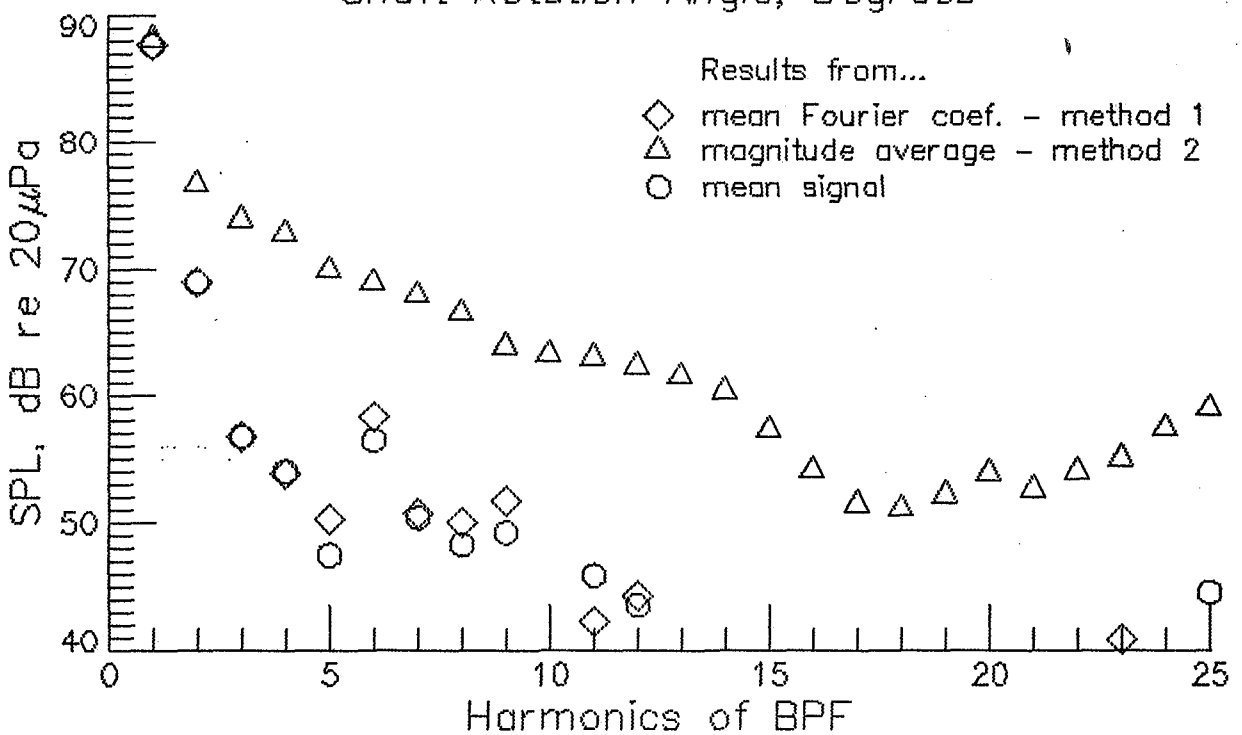

(g) microphone 7

Figure 13. - Continued.

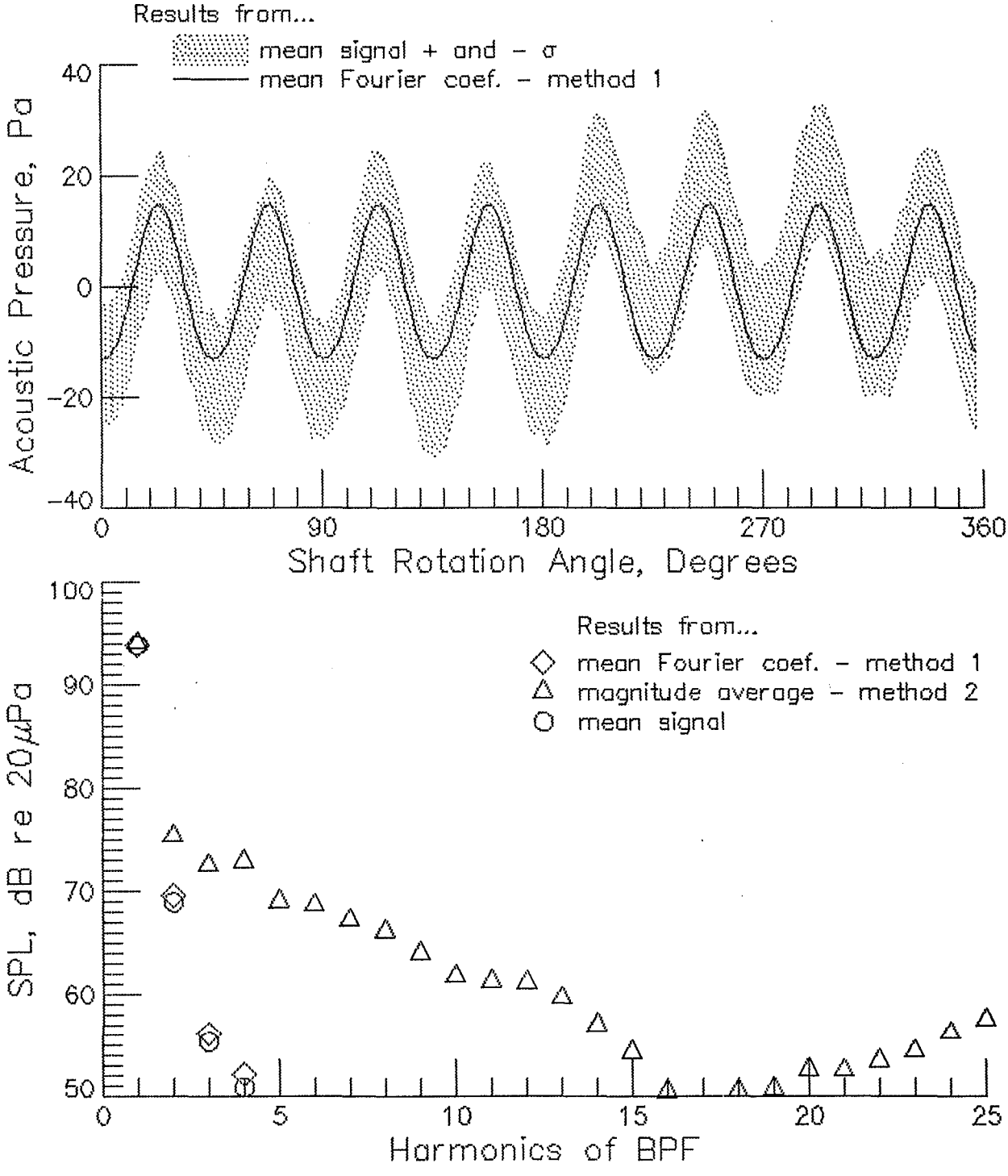

(h) microphone 8

Figure 13 - Continued.

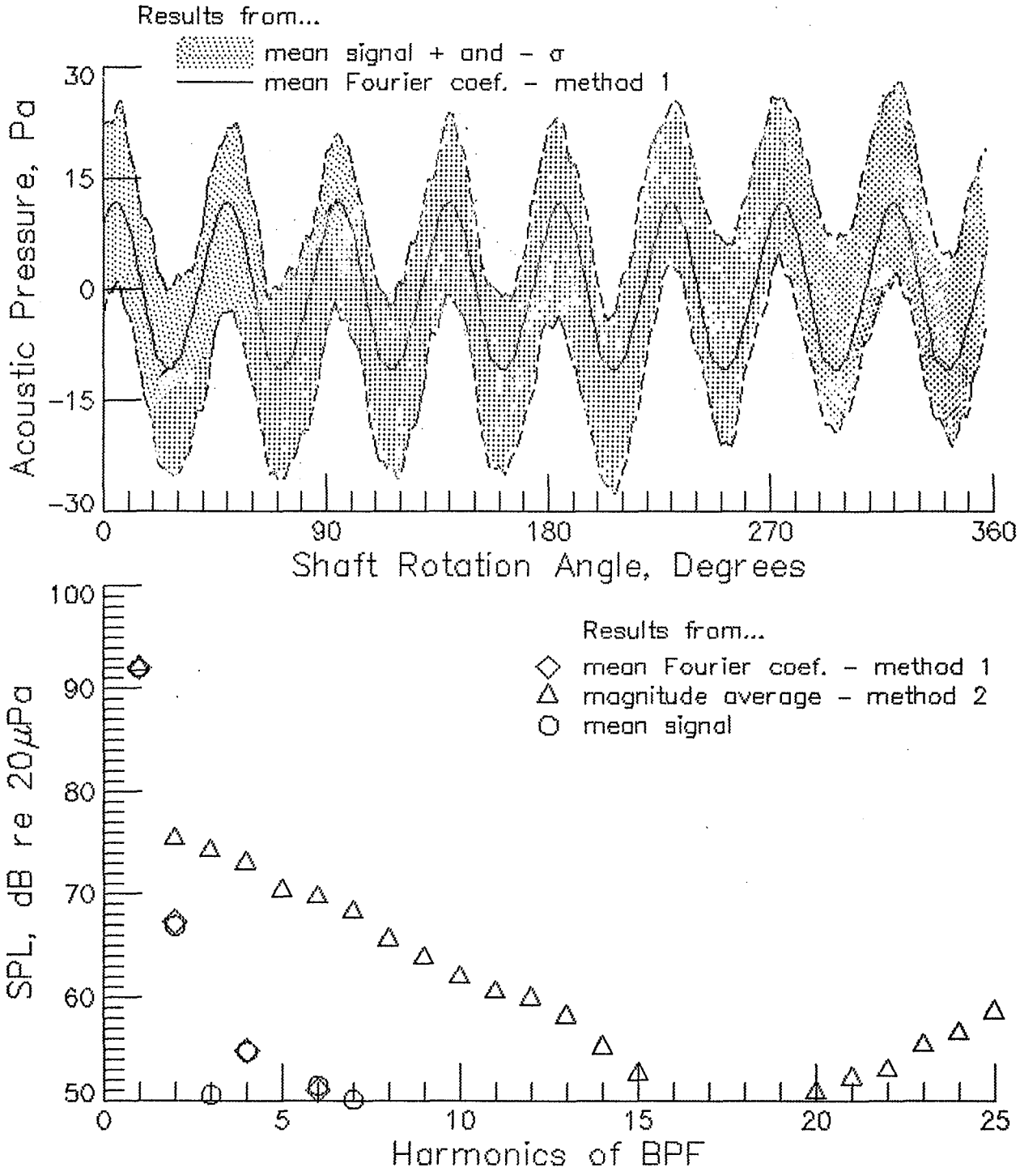

(i) microphone 9

Figure 13 - Continued.

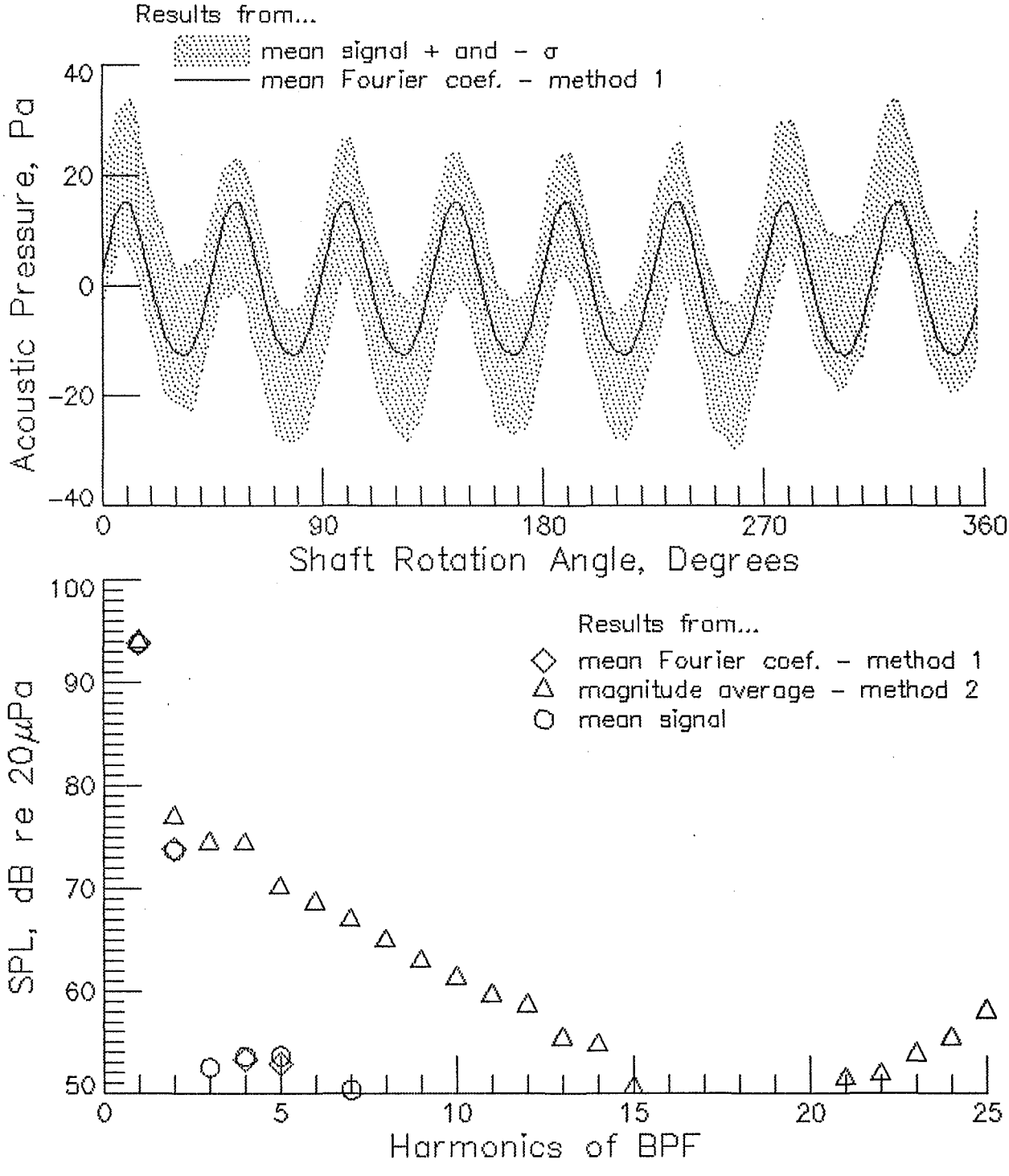

(j) microphone 10

Figure 13 - Continued.

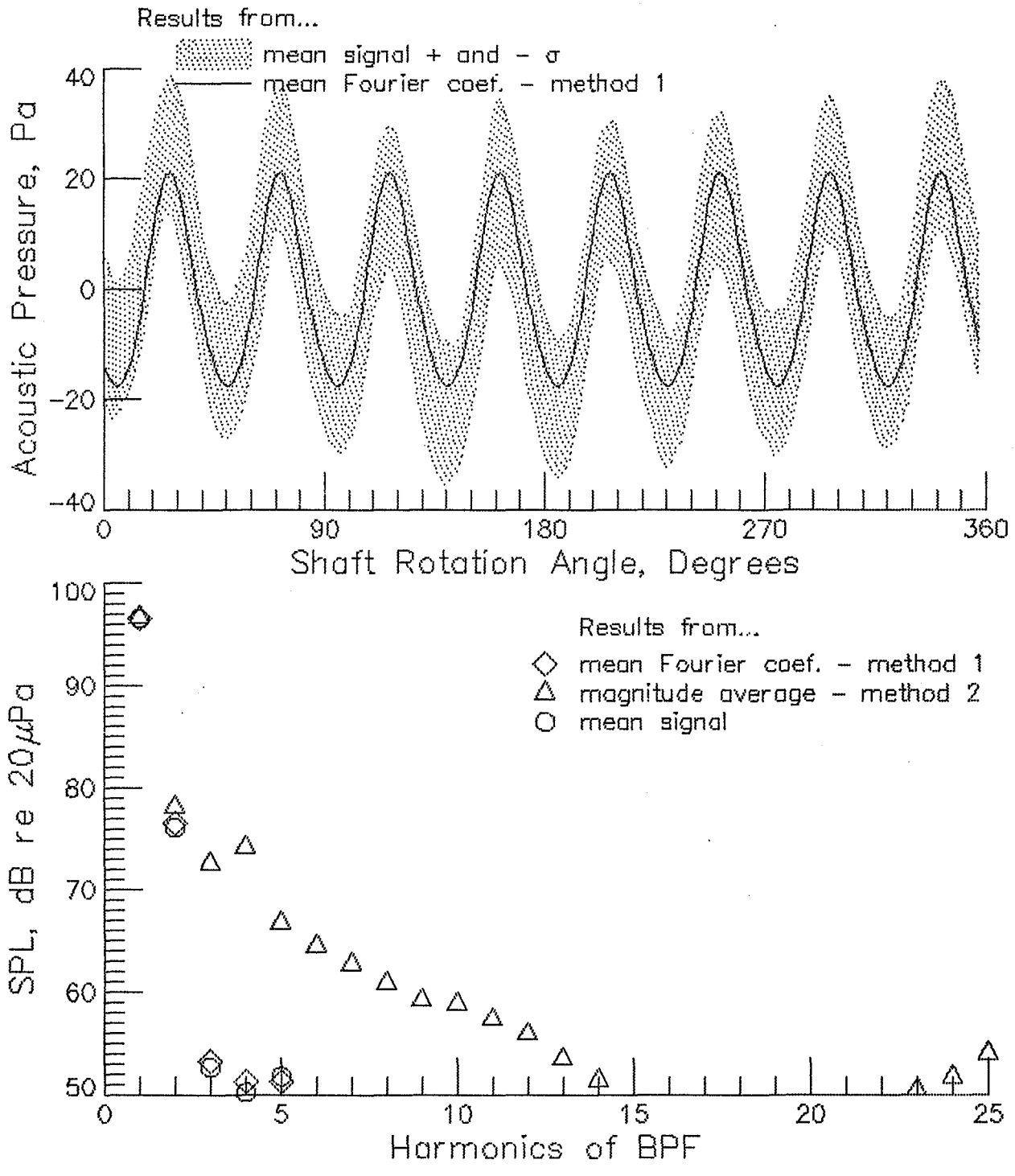

(k) microphone 11

Figure 13. - Continued.

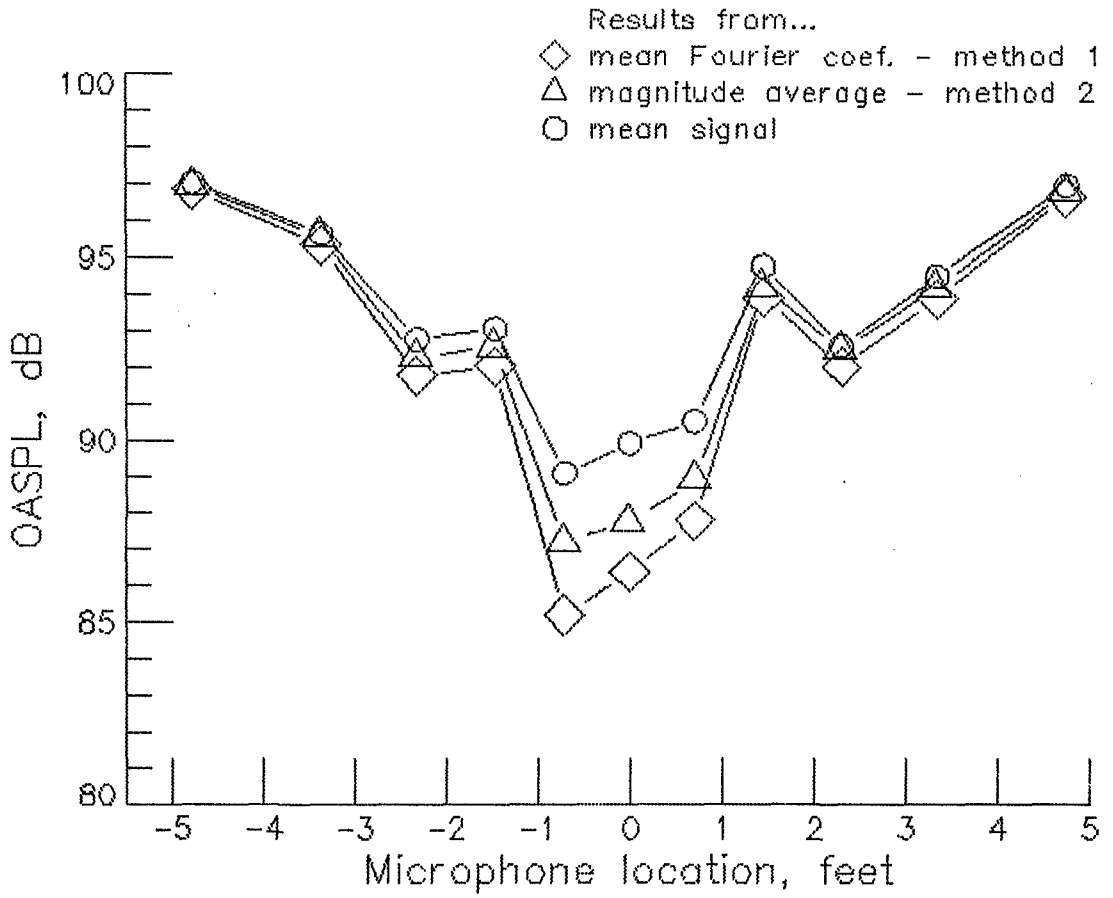

(l) Summary of Stop 3

Figure 13. - Run 141+3. BPF=1348.6 Hz. RPM=10114.6. U_{Tip}=745.9 fps.

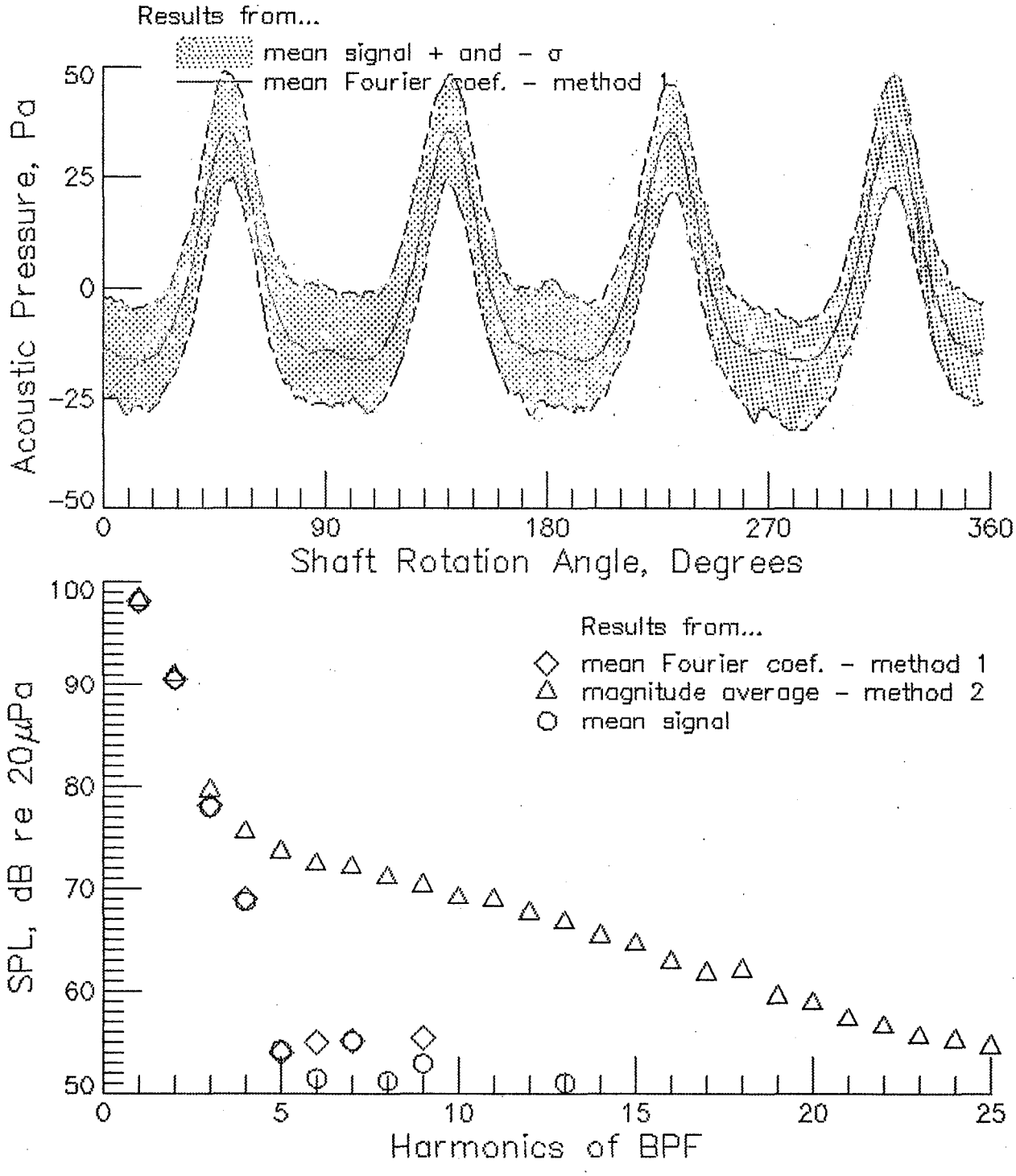

(a) microphone 1

Figure 14. - Run 144+3. BPF= 672.6 Hz. RPM=10088.3. U_{Tip}=743.9 fps.

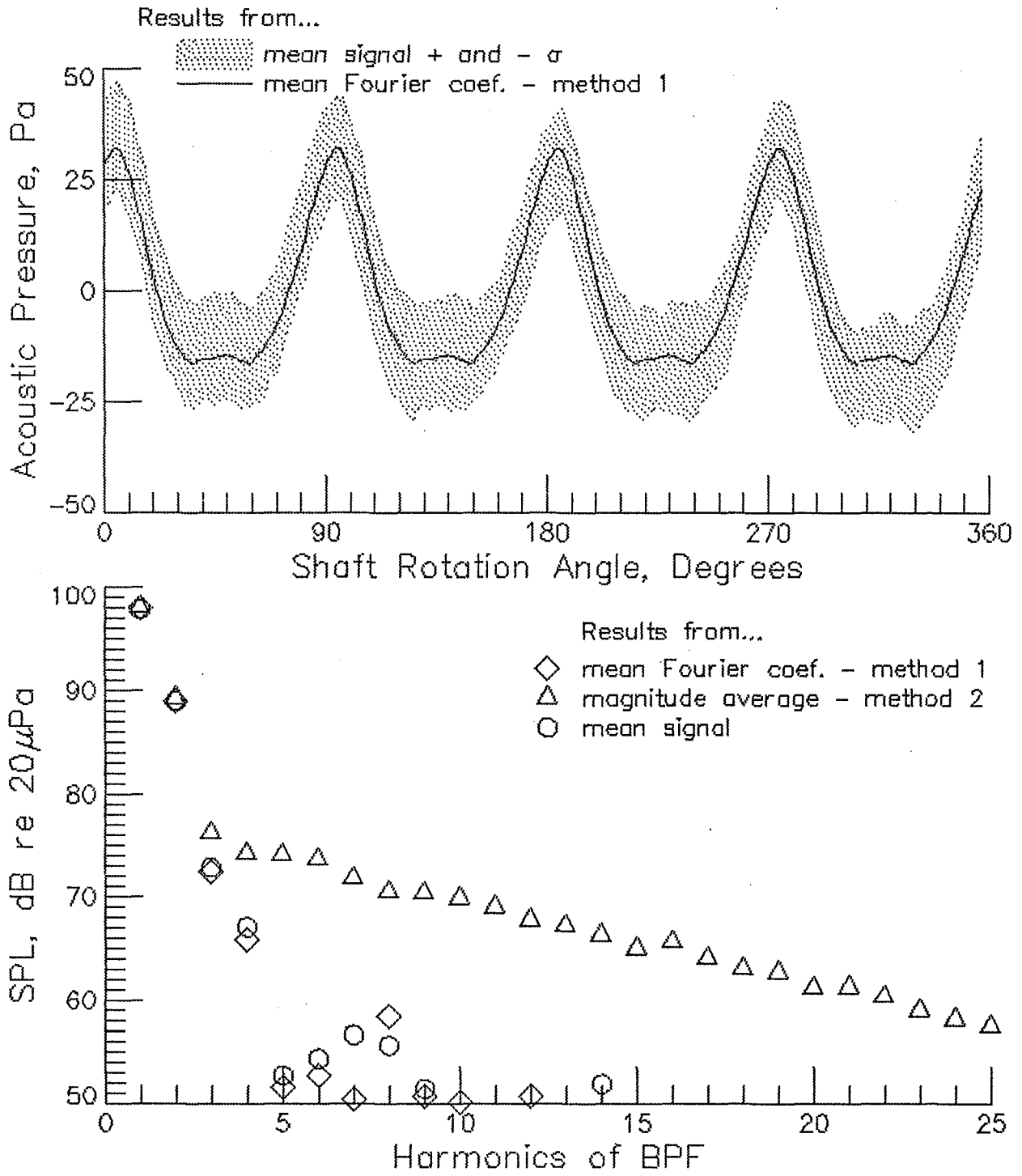

(b) microphone 2

Figure 14 - Continued.

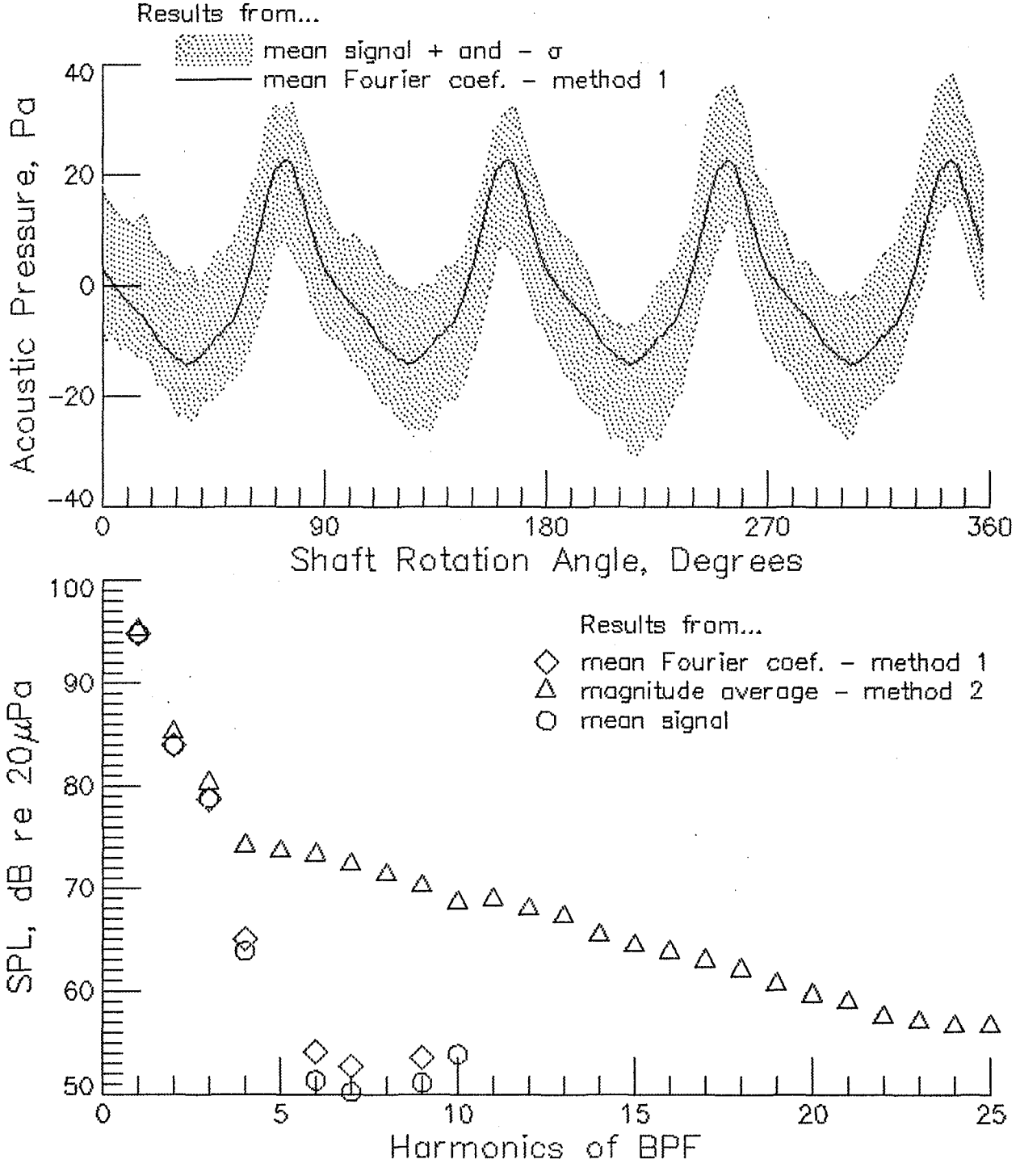

(c) microphone 3

Figure 14 - Continued.

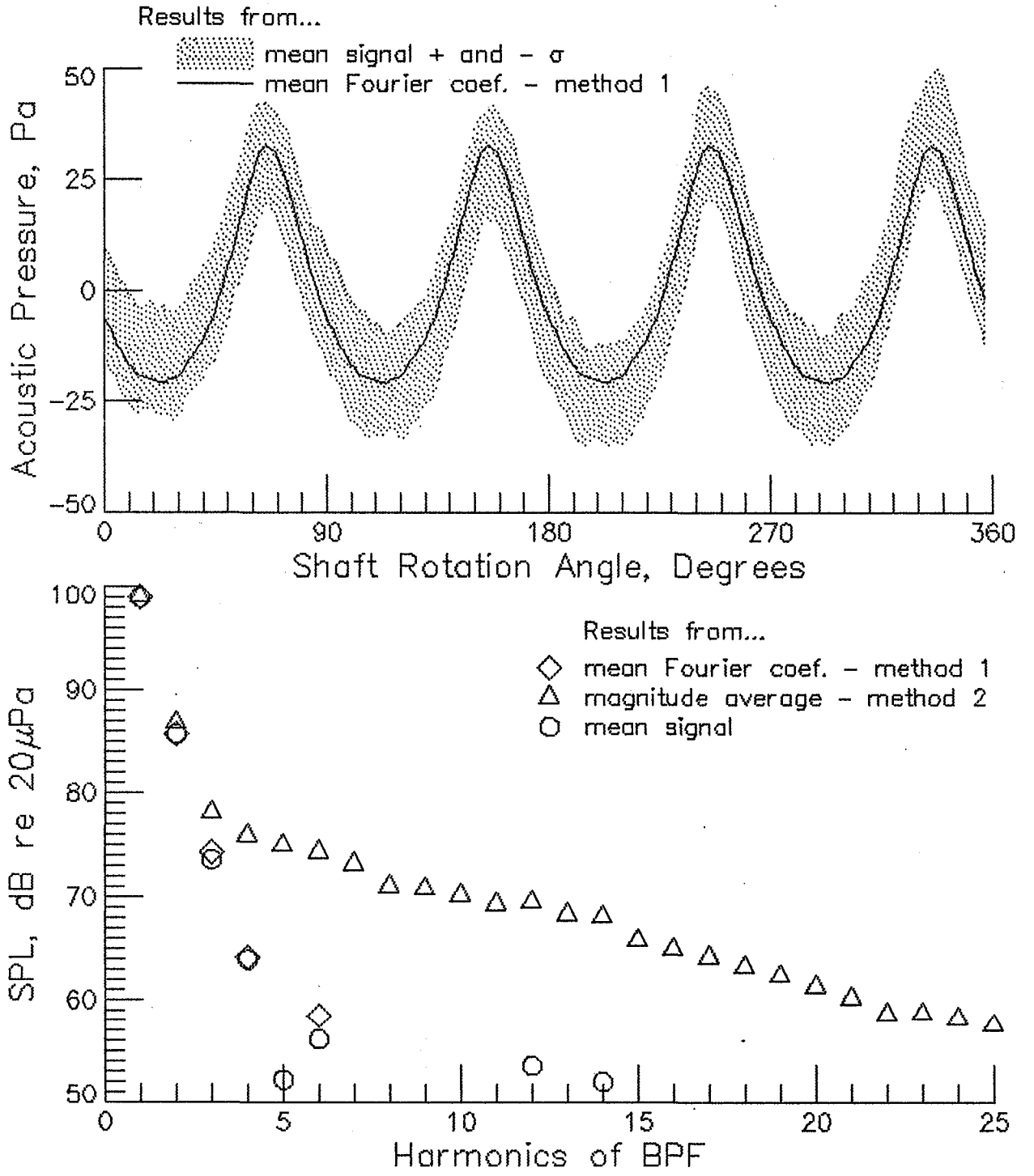

(d) microphone 4

Figure 14. - Continued.

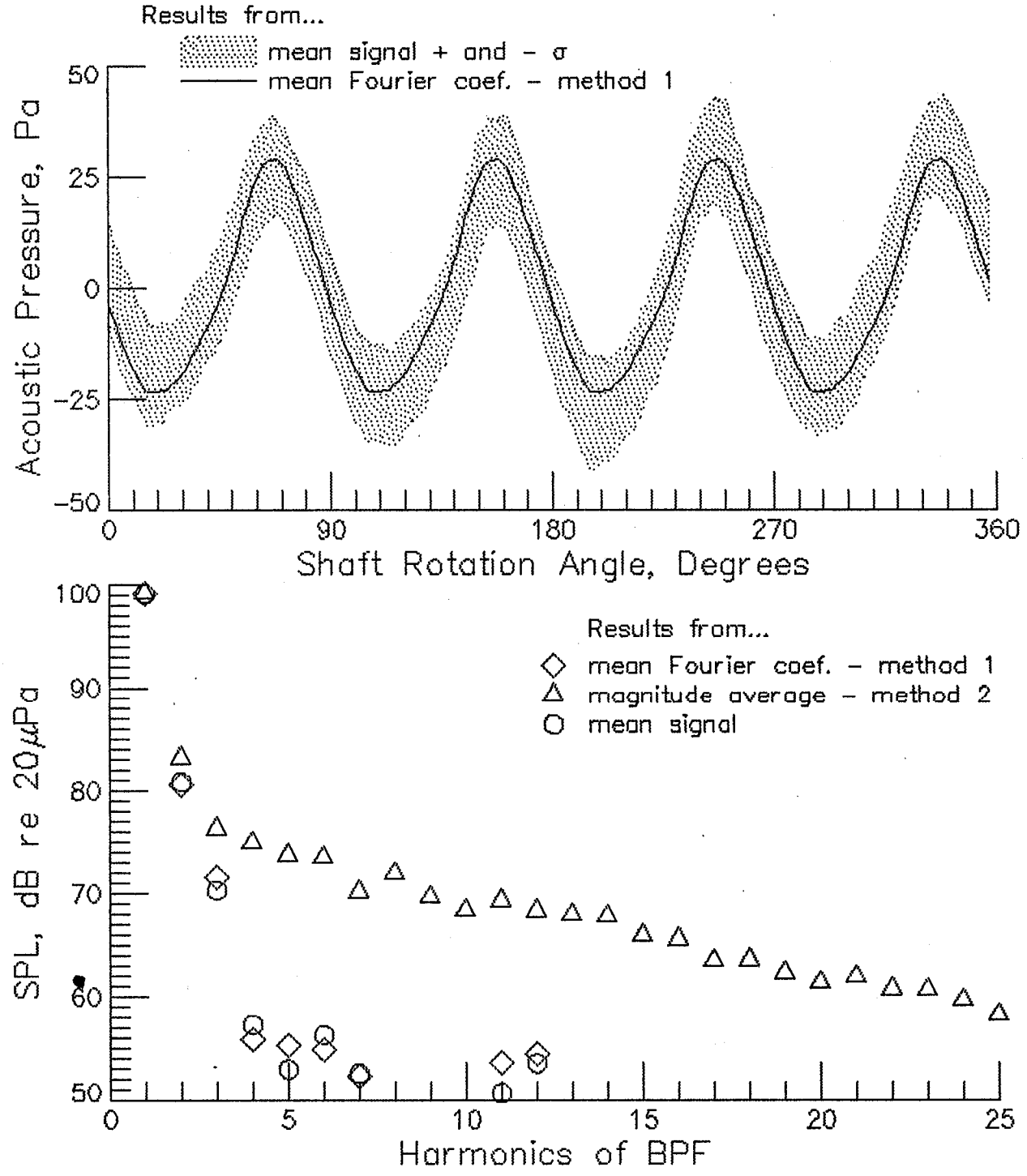

(e) microphone 5

Figure 14. - Continued.

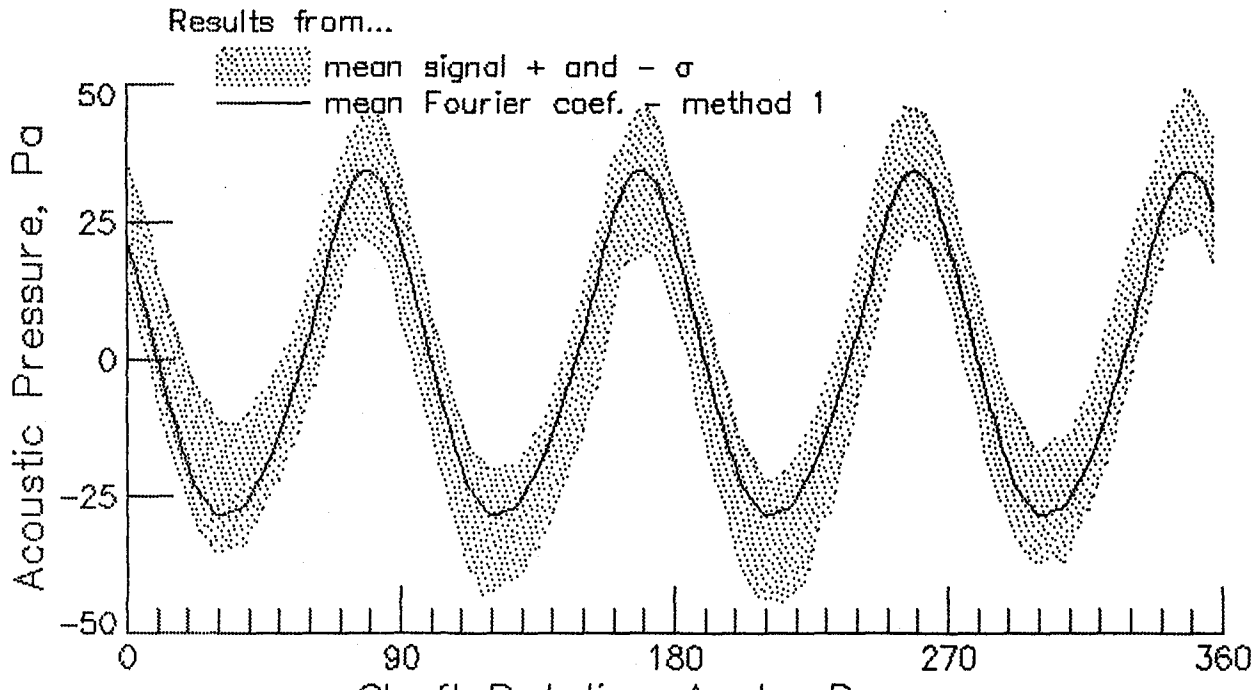

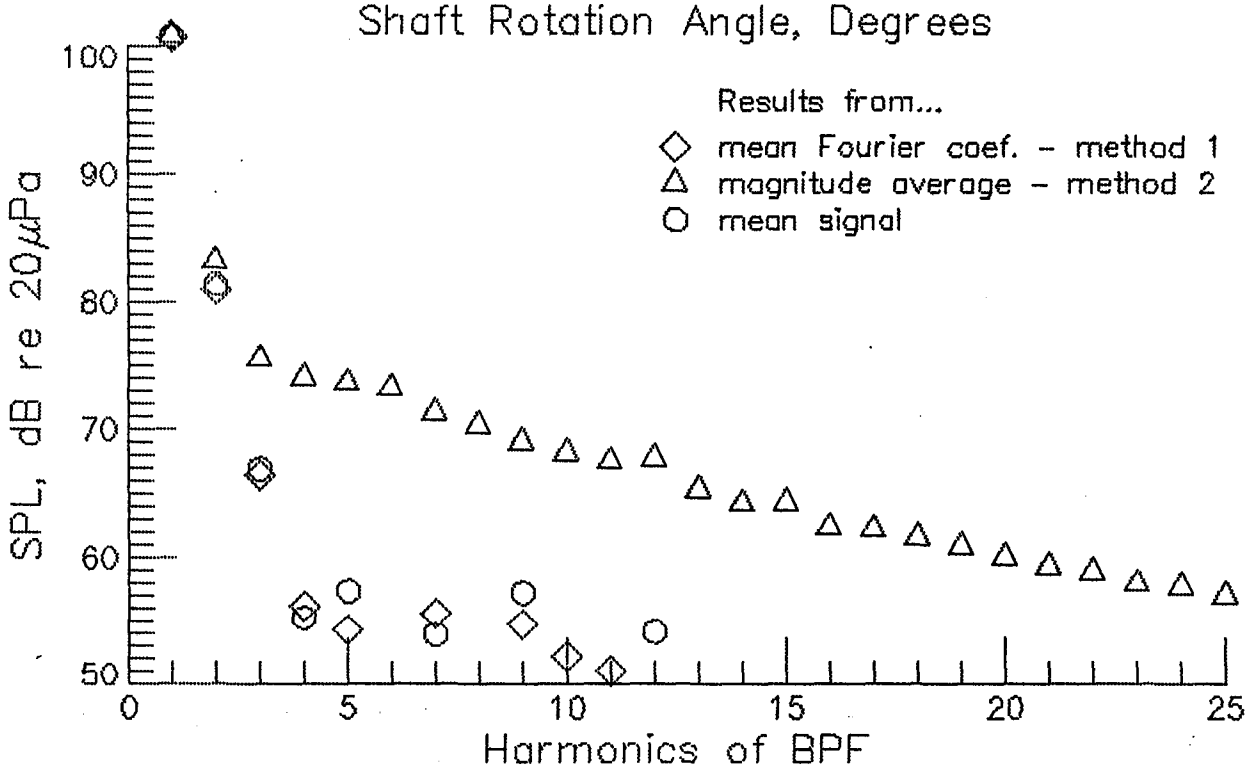

(f) microphone 6

Figure 14. - Continued.

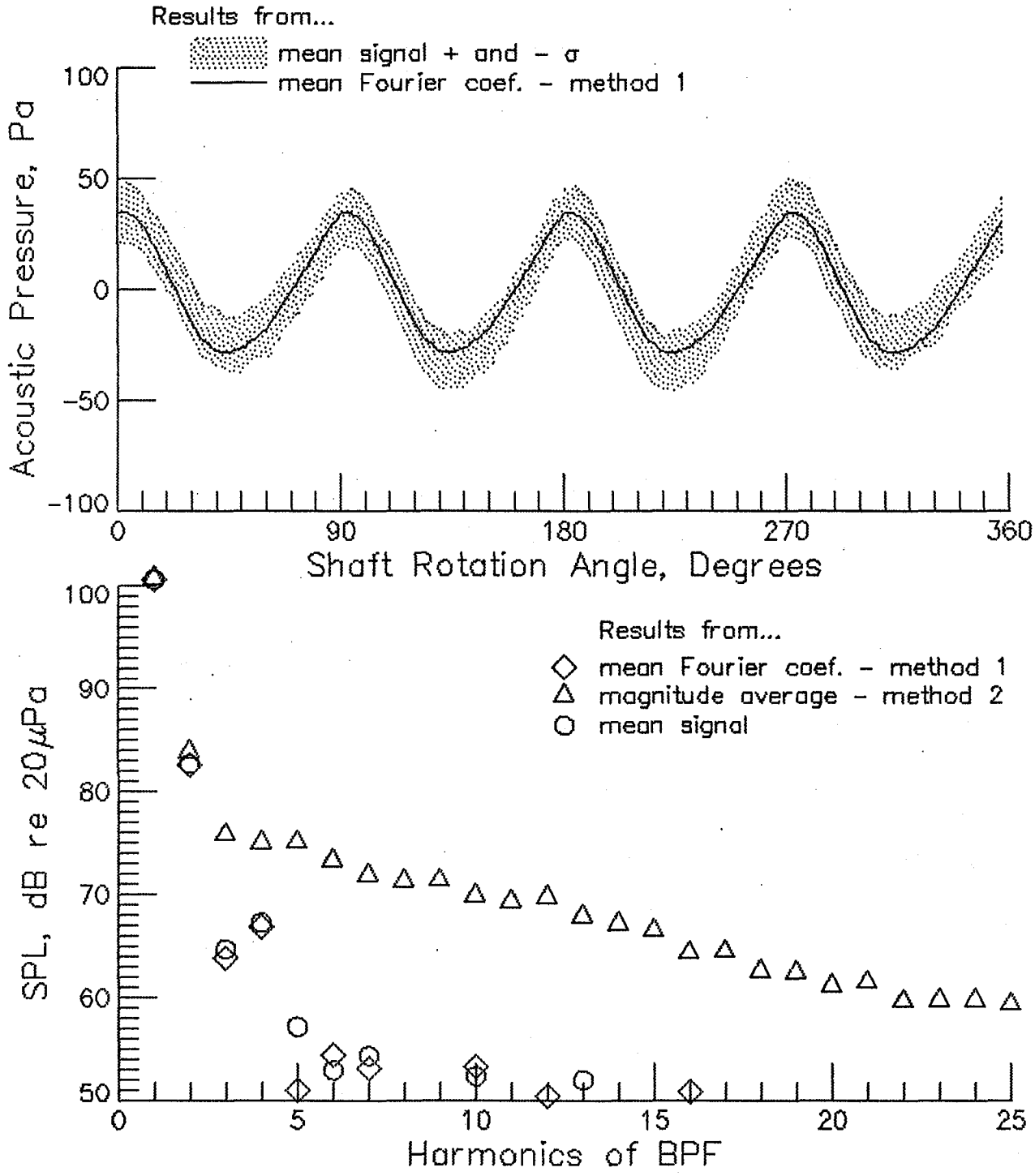

(g) microphone 7

Figure 14 - Continued.

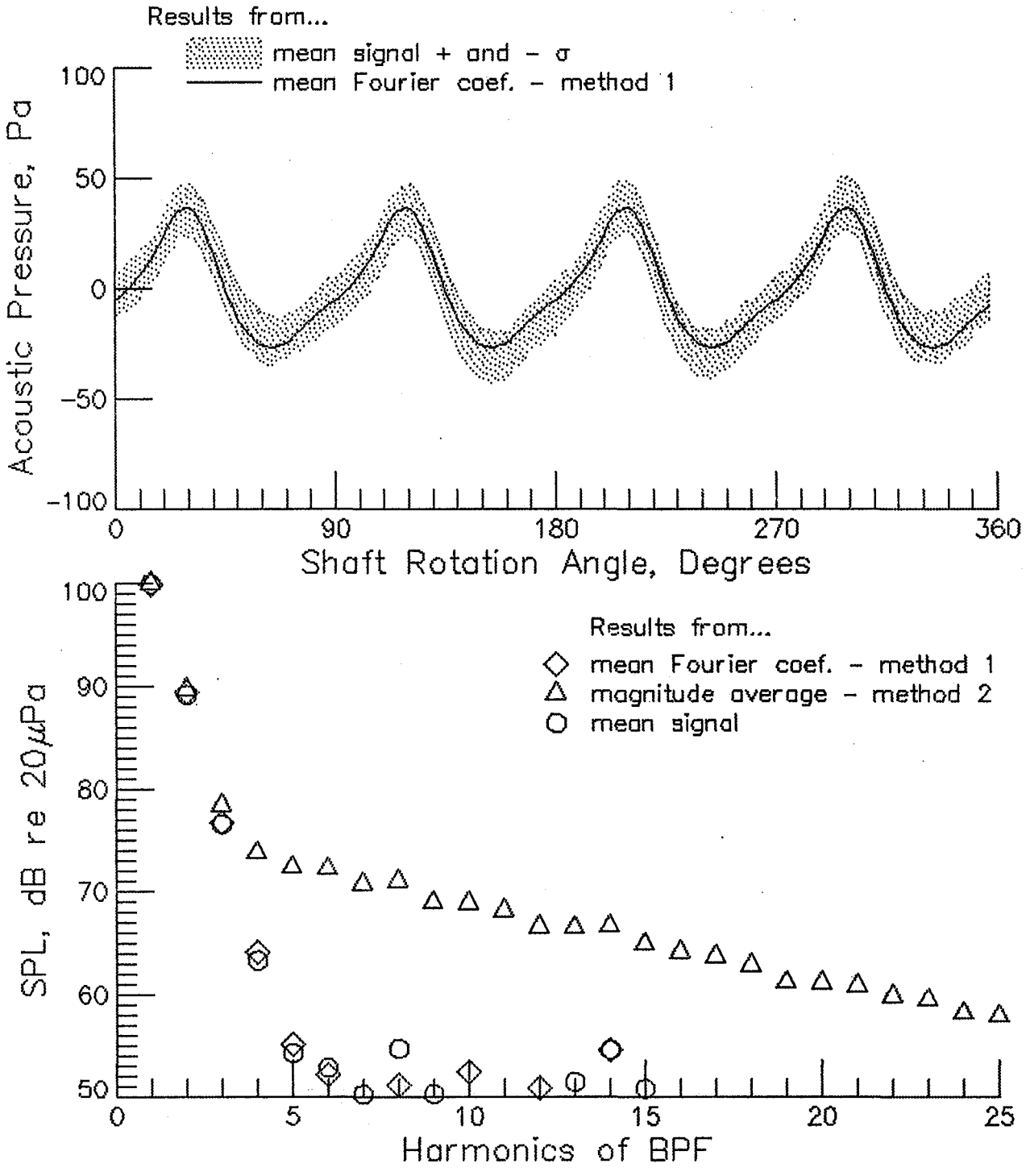

(h) microphone 8

Figure 14 - Continued.

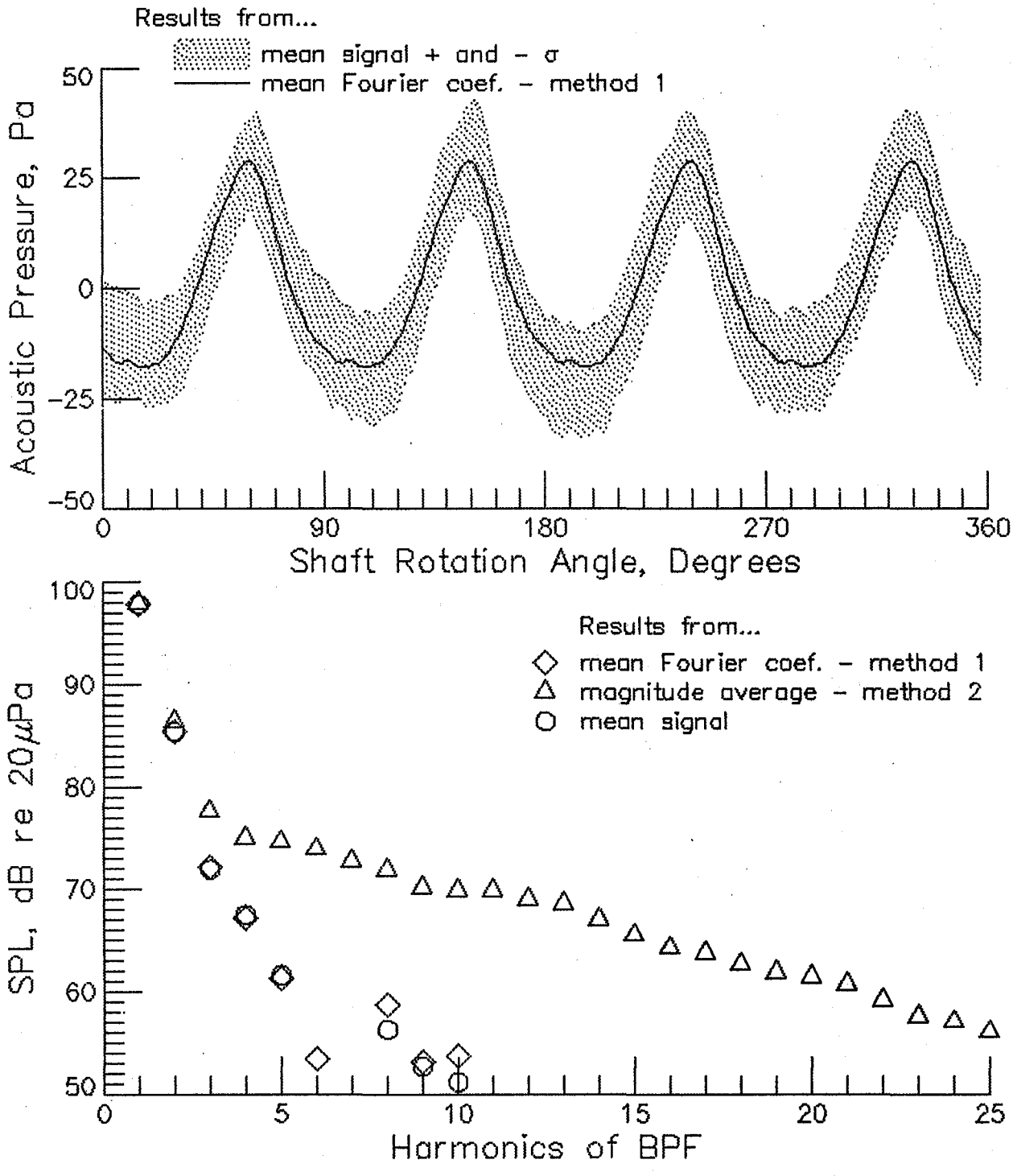

(i) microphone 9

Figure 14 - Continued.

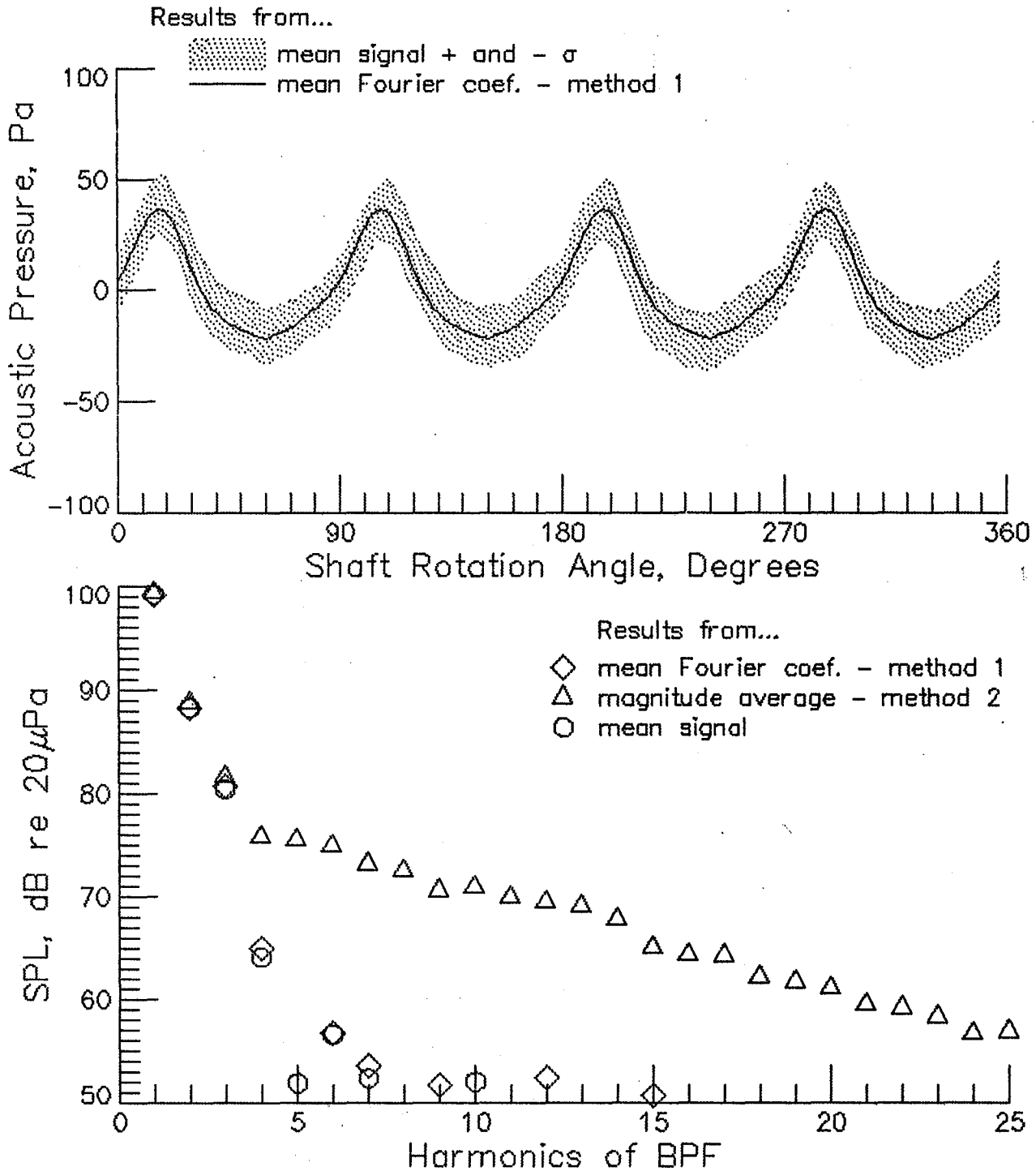

(j) microphone 10

Figure 14. - Continued.

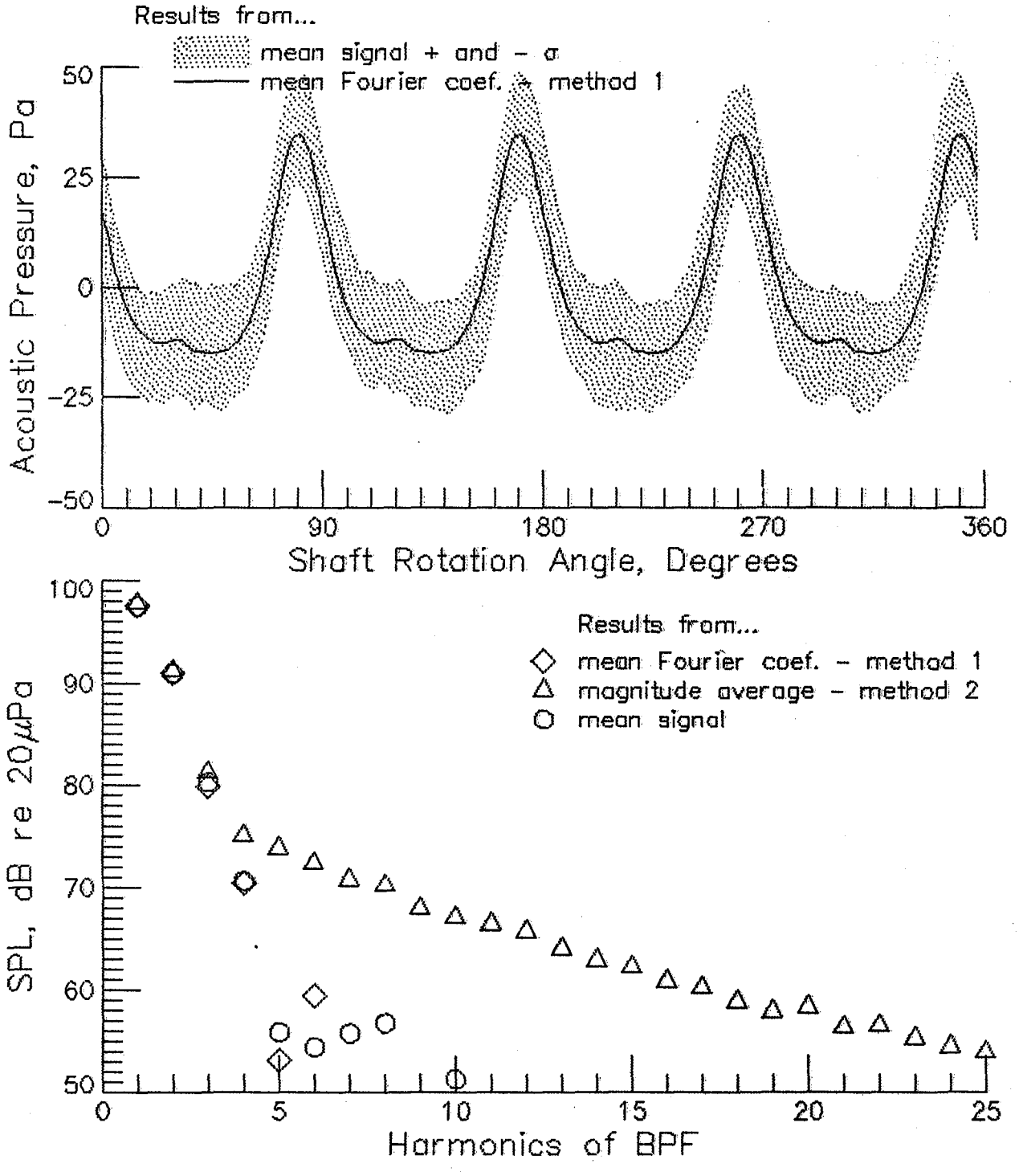

(k) microphone 11

Figure 14. - Continued.

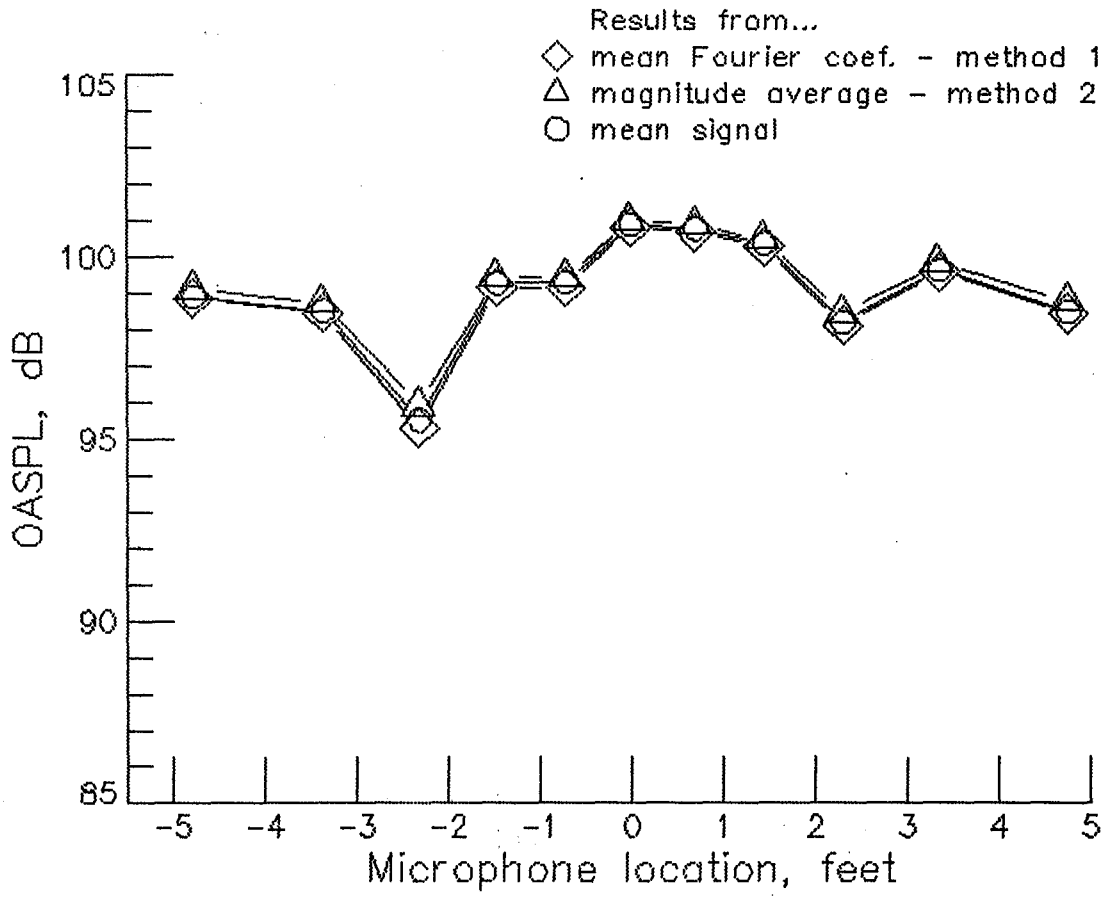

(l) Summary of Stop 3

Figure 14. - Run 144+3. BPF= 672.6 Hz. RPM=10088.3. U_{Tip}=743.9 fps.

1. Report No.	2. Government Accession No.	3. Recipient's Catalog No.
NASA TM-85790		

4. Title and Subtitle	5. Report Date
Installation Noise Measurements of Model SR and CR Propellers	May 1984
	6. Performing Organization Code 535-03-12-08

7. Author(s)	8. Performing Organization Report No.
P. J. W. Block	
	10. Work Unit No.
9. Performing Organization Name and Address NASA Langley Research Center Hampton, Virginia 23665	11. Contract or Grant No.
	13. Type of Report and Period Covered Technical Memorandum
12. Sponsoring Agency Name and Address National Aeronautics and Space Administration Washington, DC 20546	14. Sponsoring Agency Code

15. Supplementary Notes

16. Abstract

This paper summarizes noise measurements on a 0.1 scale SR-2 propeller in a single and counter rotation mode, in a pusher and tractor configuration, and operating at non-zero angles of attack. A measurement scheme which permitted 143 measurements of each of these configurations is also described.

17. Key Words (Suggested by Author(s))	18. Distribution Statement
Aerodynamic Noise, Aircraft Wake, Propellers, Propeller Noise, Acoustic Measurement, Low Speed Wind Tunnels	Unclassified - Unlimited Subject Category 71

19. Security Classif. (of this report)	20. Security Classif. (of this page)	21. No. of Pages	22. Price
Unclassified	Unclassified	102	A06

For sale by the National Technical Information Service, Springfield, Virginia 22161